THIS THESIS IS SUBMITTED FOR THE DEGREE OF DOCTOR OF PHILOSOPHY

A comparative analysis of C_3 and C_4 photosynthesis under dynamic light conditions

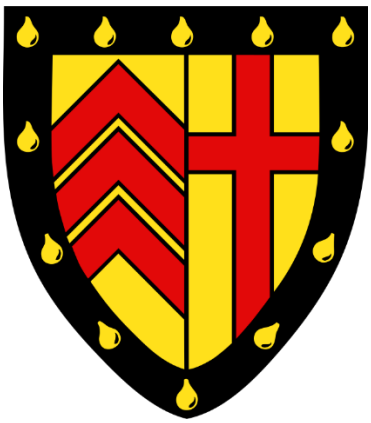

Lucía Arce Cubas

SUPERVISED BY
Dr. Johannes Kromdijk

UNIVERSITY OF CAMBRIDGE
Clare College
Department of Plant Sciences

17th of August 2023

Declaration

This thesis is the result of my own work and includes nothing which is the outcome of work done in collaboration except as specified in the text. It does not exceed the prescribed word limit set out by the Biology Degree Committee. It is not substantially the same as any work that has already been, or is being submitted for any degree, diploma, or other qualification.

Lucía Arce Cubas

Abstract

A COMPARATIVE ANALYSIS OF C_3 AND C_4 PHOTOSYNTHESIS UNDER DYNAMIC LIGHT CONDITIONS

Lucía Arce Cubas

DEPARTMENT OF
Plant Sciences

By 2050, human population growth is predicted to require to a 100-110% rise in global food production, and since traditional targets for crop advancement are falling behind rising demand, improving photosynthesis to increase crop yield has become a major global effort. The response of plants to changes in light intensity has been identified as a source of inefficiency for photosynthesis, as in the dynamic environments of the open field, where crop canopies are subject to constantly changing light intensity, lags in photosynthetic responses can amount to up to a 40% loss in daily carbon assimilation. Although remarkable progress has been made, the vast majority of the work on dynamic light photosynthesis has been conducted in C_3 species, despite the undeniable global importance of C_4 crops to global food supplies. The benefits of the C_4 carbon concentrating mechanism under steady state conditions are well-established, but it is less clear how the C_4 pathway affects the dynamic light response. This thesis employs a comparison between phylogenetically linked C_3 and C_4 species across three different genera to compare C_3 and C_4 photosynthesis under non-steady state conditions. The findings presented in this thesis enhance our understanding of the effects of the biochemical and anatomical features of the C_4 pathway on photosynthetic responses to dynamic light, and on the potential impact of specific engineering strategies for the improvement of photosynthesis in C_4 species.

Acknowledgements

My most important thanks go to the coolest person I know, my supervisor Wanne Kromdijk. Under your guidance I became a better scientist, a better writer, and a true plant physiologist. Thank you for always making time for my work and my research, for putting up with my idiosyncrasies, for your eye for detail and expert craft when reviewing drafts, for teaching me to think like a scientist, improve my result analysis, and push my own boundaries. I couldn't have asked for a more thoughtful, kind, or knowledgeable supervisor, and I cannot put into words how truly lucky I feel to have been your PhD student. Thank you for making me love research and academia, I wish to one day be as cool as you, or know as many things.

I also wish to thank my Masters supervisor Julie Gray, who encouraged me to go for a PhD in the first place, gave me confidence in my ability as a scientist, and probably changed the trajectory of my life when she brought in that one *Arabidopsis* plant to my undergraduate introduction week. Throughout my studies, I have been fortunate to have worked with mentors who imbued me with excitement about science and taught me to work well – special shoutout to Dr. Stuart Casson, the first to give me the chance to work with plants, and Dr. Magdalena Dabrowska, who taught me what proper lab life was like during that internship.

Thank you to Dr. Yuri Munekage, who collaborated with us and tested some of their *F. bidentis* mutants to really exciting results. I really admire the work from the Munekage group, and I hope our collaborative relationship will continue in the future.

My utmost thanks to my funders, the Cambridge Trust and CONACyT, as without their economic patronage I could never have achieved the dream of a PhD. I hope other students will continue to benefit from your support in the future. Thank you also to Clare College for their additional funding through the Graduate Research Fund and for supporting my ongoing efforts to learn Chinese, as well as for a wonderful four years (even with all the building works).

Thank you to all members of the most phenomenal squad of introverts in the Cambridge Department of Plant Sciences, the Kromdijk Group! Special thanks to Richard Vath, master of all things LICOR and DIY for teaching me to tame the machines, helping me through any fixes, and assisting me in setting up my low oxygen experiments. To Cris Sales, without whom I could never have done the fluctuating light experiments and whose input for data interpretation and visualisation was invaluable – I really admire you as a person and as a scientist, and your

work ethic and bright disposition always inspired me in the lab. To Georgia Taylor, for giving me some of her mutants and taking me on an *Arabidopsis* molecular crash course, I hope I was a good student. To Emmanuel Bernardo, the first of us, thank you for all the talks and for sharing the load of taking care of so many species. To Julia Walter, fellow late-night worker, for reminding me to go home occasionally and for helping me with my chemical infiltration protocols. To Jessica Royles, for making the lab liveable and for making all of our research possible. Finally, to everyone, for all the conversations, the brainstorming, and the supportive environment that allowed me to work my best.

The Department of Plant Sciences is filled with incredible, inspiring individuals. I want to thank especially the members of the Hibberd and Griffiths Groups – I am very thankful I got to learn and be inspired by everyone talking about their work on a bi-weekly basis. Thank you to those in the Department who gave me advice (especially Tina, Pallavi, Patrick and Humberto), who were all incredibly helpful on both personal and scientific levels. Thank you to my fellow plant postgraduate students for making sure I still occasionally had fun, and for all the teatime chats.

Onto personal thanks, I want to thank my parents, Estela and Manuel, whose support was integral in my pursuit of a PhD and I can only hope I've made proud; my brother, who is my favourite person in the world; and the rest of my family, my ever-present cheerleaders. Thank you to my friends from home, from debate, and from Clare, for making sure I didn't spend all my time agonising over code or experiments and for making my life glow in a truly special way. Particular thanks to Matt, my forever best friend, with me through everything; to Rachel, queen of Victorian literature and my personal voice of reason; to Charles, my favourite chemist and constant source of weird knowledge, bubble tea and dopamine; and to Oskar, a vitamin pill in any sour day who exponentially increased my productivity by teaching me to navigate the wild storms of ADHD (my academics thank you too).

Finally, I wish to thank the Coca-Cola Company for making my most beloved focus drink, Diet Coke. I couldn't have done it without you.

Table of contents

List of Figures

List of Tables

List of Abbreviations

$[O_2]$ – O_2 concentration

3-PGA – 3-phosphoglyceric acid

A. semialata GMT – Alloteropsis semialata subspecies *semialata GMT*

A. semialata MDG – Alloteropsis semialata subspecies *eckloniana* accession *MDG*

A. thaliana – Arabidopsis thaliana

A_{CO2} – Net photosynthetic CO_2 assimilation

A_{max} – Light-saturated photosynthetic rate

APX – Ascorbate peroxidase

AUC – Area under the curve

BEP – Bambusoideae, Ehrhartoideae, Pooideae

BS – Bundle sheath

CCM – Carbon concentrating mechanism

CEF – Cyclic electron flow

chup1 – A. thaliana chloroplast unusual positioning 1 mutants

C_i – Leaf intracellular CO_2 concentration

$C_{i\,max}$ – Light-saturated C_i

$cytb_6f$ – Cytochrome b_6f

F. bidentis – Flaveria bidentis

F. cronquistii – Flaveria cronquistii

F' – Steady fluorescence

F_m' – Maximal fluorescence

G. gynandra – Gynandropsis gynandra

g_{sw} – Stomatal conductance to water vapour

HYV – High Yield Varieties

IRGA – Infrared Gas Analyzer

L_{abs} – Leaf absorptance

LEF – Linear electron flow

LHCII – Light-harvesting complex II

M – Mesophyll

Ma – Million years ago

MFP – Multiphase Flash Fluorometer

NAD-ME – Nicotinamide adenine dinucleotide-malic enzyme

NADP-ME – Nicotinamide adenine dinucleotide phosphate-malic enzyme

NDH – chloroplast NADH dehydrogenase-like complex

ndho1 – F. bidentis knockdown NDHO1 line

NPQ – Non-Photochemical Quenching

PACMAD – Panicoideae, Aristidoideae, Chloridoideae, Micraioideae, Arundinoideae and Danthonioideae

PEP – Phosphoenolpyruvate

PEPC – Phosphoenolpyruvate carboxylase

PEPCK – Phosphoenolpyruvate carboxykinase

PFD – Photon flux density

PFD_{abs} – Absorbed photon flux density

PGR5 – Proton gradient regulation 5

pgrl1 – F. bidentis knockdown PGRL1 line

PGRL1 – PGR5-like photosynthetic phenotype 1

phot2 – A. thaliana PHOTOTROPIN 2 mutants

P_i – Inorganic phosphate

pI – Photoinhibition

PP – Photosynthetic pathway

PQ – Plastoquinone

PSI – Photosystem I

PSII – Photosystem II

qE – Energy-dependent quenching

qH – Photoinhibition-independent sustained quenching

qM – Apparent quenching due to chloroplast movements

qP_d – Photochemical quenching in the dark

qT – Apparent quenching due to state transitions

qZ – Zeaxanthin-dependent quenching

Rca – Rubisco activase

Rd – Respiration in the light

RH – Relative humidity

ROS – Reactive Oxygen Species

Rubisco – Ribulose 1,5-biphosphate carboxylase/oxygenase

RuBP – Ribulose 1,5-bisphosphate

SOD – Superoxide dismutase

stn7 – *A. thaliana* SNT7 mutants

T – Treatment

T. hassleriana – *Tarenaya hassleriana*

TP -Triose phosphates

TPT – Triose phosphate transporter

TPU – Triose phosphate utilisation

VDE – Violaxanthin De-Epoxidase

WT – Wild Type

A – Quantum yield of assimilation

ΦCO_2 – Quantum yield of CO_2 assimilation

ΦPSII – Quantum yield of Photosystem II

List of Equations

$$\phi CO_2 = \frac{A_{CO2} + Rd}{PFD_{abs}} \quad \textbf{Equation 1A}$$

$$L_{abs} = 1 - T_s - R_s \quad \textbf{Equation 1B}$$

$$Storage\ flux_{H2O} = \frac{\frac{PV}{RT} x \Delta H_2O}{S\ x\ t} \quad \textbf{Equation 2A}$$

$$Storage\ flux_{CO2} = \frac{-\frac{PV}{RT} x \Delta CO_2}{S\ x\ t} \quad \textbf{Equation 2B}$$

$$L_{abs} = 1 - T_s - R_s \quad \textbf{Equation 2C}$$

$$F_0{}'_{calc} = \frac{F_0}{\frac{F_v}{F_m} + \frac{F_0}{F_m{}'}} \quad \textbf{Equation 3A}$$

$$qP_d = \frac{F_m{}' - F_0{}'_{act}}{F_m{}' - F_0{}'_{calc}} \quad \textbf{Equation 3B}$$

$$\Phi PSII_{ideal} = \frac{qP \times \frac{F_v}{F_m}}{1 + (1 - \frac{F_v}{F_m}) \times NPQ} \quad \textbf{Equation 3C}$$

1. Introduction

1.1. Food security and photosynthesis

In 2020 2.3 billion people, nearly one third of the human population, did not have access to adequate food and nutrition and for the first time in five years, undernourishment increased from 8.4% to 9.9% under pressure from the COVID-19 pandemic (FAO, 2021). By 2050, population growth is predicted to lead to 100-110% increase in global food demand (FAO, 2009, Tilman et al., 2011) but with current rates of crop yield improvement already falling behind rising demand (Ray et al., 2013), the threat of an unprecedented food crisis looms large in the horizon. Ineffective land use (Mueller et al., 2012), urbanisation (Satterthwaite et al., 2010), soil erosion (Kopittke et al., 2019), inadequate management of fertilisers (Penuelas et al., 2023), and increasingly unbalanced biogeochemical flows (MacDonald et al., 2011, van der Velde et al., 2014) all increase the challenge of feeding the world. Moreover, recent models suggest the risk of synchronised harvest failure as a consequence of climate change has been underestimated (Kornhuber et al., 2023), adding to the existing unpredictability of changing environmental conditions (Aydinalp and Cresser, 2008, Cogato et al., 2019, Habib-Ur-Rahman et al., 2022, IPCC, 2022). The Green Revolution of the 1960s alleviated emerging food shortages and led to a tripling of cereal crop production with only a 30% increase of cultivated land through the development of High Yield Varieties (HYV) and large public investments into agronomy (Pingali, 2012). Given genetic improvements, be it via conventional breeding or genetic engineering need around 30 years to reach crop fields (Kromdijk and Long, 2016), a global effort to identify, develop and test crop improvement is required.

Improving photosynthesis to increase crop yield has become one of such global efforts (Hibberd et al., 2008, Long et al., 2022, Long et al., 2006, Zhu et al., 2010) and has received significant public and private investment (C4 Rice Project, 2023, CAPITALISE, 2023, RIPE, 2023). Photosynthesis converts absorbed sunlight into plant biomass, yet despite its role as the ultimate origin of yield, photosynthetic efficiency had been relatively neglected in crop improvement efforts due to a theorised lack of correlation between photosynthetic rates and crop yields (Evans, 1997, Evans and Dunstone, 1970, Long et al., 2006). However, this dogmatic viewpoint is being challenged by an increasing body of research. Mounting evidence of photosynthetic rates affecting crop yields comes from hundreds of studies under elevated CO_2 – conditions that enhance photosynthesis – which have shown a positive correlation

between photosynthetic rates and yield (Ainsworth and Long, 2021, Kimball, 1983), and genetic manipulation of photosynthetic processes has been proven to successfully increase yield (De Souza et al., 2022, Ermakova et al., 2023, Kromdijk et al., 2016, Simkin et al., 2019). Given alternative determinants of yield potential like light capture efficiency or distribution of biomass towards harvested products are nearing their theoretical limits, photosynthesis is a natural target for improvement (Long et al., 2006).

1.2. The C_3 and C_4 photosynthetic pathways

1.2.1. C_3 photosynthesis

Photosynthesis converts light into stored chemical energy in the form of carbohydrates and other complex organic molecules, taking up water and atmospheric CO_2, and releasing O_2 (Johnson, 2016). One of the most important biochemical processes on Earth, photosynthesis is the source of the oxygen we breathe and the basis of all global food chains. The majority of plants use C_3 photosynthesis (Still et al., 2003), in which the first stable carbon compound produced contains three carbon atoms. This process involves two essential reactions occurring within distinct compartments of the chloroplast: the light-dependent reactions in the thylakoid membrane; and the carbon reactions in the stroma (Buchanan, 2016, Buchanan et al., 2002).

The light-dependent reactions involve the transfer of electrons from Photosystem II (PSII) to Cytochrome b_6f ($cytb_6f$) and Photosystem I (PSI) via a series of electron carriers, culminating in the reduction of $NADP^+$ into NADPH. Water splitting and the quinone cycle release H^+ into the lumen, forming a proton gradient that powers the thylakoid ATP synthase (Nelson and Ben-Shem, 2004). Electron transfer following the Z-scheme thus leads to production of both NADPH and ATP and is known as linear electron flow (LEF), whereas alternative pathway cyclic electron flow (CEF) contributes only to ATP formation by recycling electrons back from PSI to electron acceptor plastoquinone, which is subsequently oxidised by $cytb_6f$ (Allen, 2003, Arnon et al., 1954). The augmentation of ATP production by CEF has been suggested to adjust the ATP:NADPH ratio in chloroplasts to match demands from downstream metabolism (Yamori and Shikanai, 2016). During the carbon reactions, ATP and NADPH released into the stroma are employed in the C_3 cycle to convert carbon dioxide and water into carbohydrates (Benson and Calvin, 1947, Heineke and Scheibe). Central carbon-fixation enzyme ribulose 1,5-biphosphate carboxylase/oxygenase (Rubisco) starts the cycle by catalysing the carboxylation of Ribulose 1,5-bisphosphate (RuBP) into stable 3-carbon molecules of 3-phosphoglycerate

(Andersson and Backlund, 2008). However, as the name suggests, Rubisco also catalyses an alternative RuBP oxygenation reaction which results in production of 2-phosphoglycolate, which cannot be used in the C_3 cycle and must be recycled via photorespiration, consuming energy and reducing equivalents and releasing ammonia and CO_2. The cost of photorespiration is steep – netting a 25% loss in CO_2 assimilation at 25°C, with higher temperatures correlating with increasing rates of oxygenation (Ludwig and Canvin, 1971).

1.2.2. C_4 photosynthesis

C_4 photosynthesis is a remarkably successful adaptation of the C_3 ancestral form that enhances carbon assimilation by concentrating CO_2 around Rubisco, suppressing photorespiration (Kellogg, 2013, Sage, 2004). The C_4 pathway is thought to have evolved 35 million years ago (Ma) in response to declining CO_2 levels and an increasing ratio of atmospheric O_2 during the Oligocene (Sage et al., 2012). Relative to the C_3 pathway, C_4 photosynthesis typically exhibits faster photosynthetic rates, higher primary productivity, and increased water use efficiency (Kiniry et al., 1989, Sage, 2004), so whilst only 3% of flowering species are C_4, they account for 23% of global carbon fixation (Still et al., 2003). The most common form of the C_4 carbon concentrating mechanism (CCM) constitutes both anatomical and biochemical adaptations, as it operates by spatially separating initial carbon fixation and assimilation between morphologically distinct Mesophyll (M) and Bundle Sheath (BS) cells and transporting metabolic intermediates down a concentration gradient. Almost all C_4 species have leaves with 'Kranz' anatomy, in which leaf veins of higher density are concentrically surrounded by a ring of enlarged BS cells, in turn also bordered by M cells (Sage et al., 2014). In M cells, CO_2 is rapidly converted to bicarbonate and used by phosphoenolpyruvate carboxylase (PEPC) for the carboxylation of PEP to form oxalo-acetate, a 4-carbon molecule that gives C_4 photosynthesis its name. Depending on the C_4 pathway, the molecule is then reduced to malate or transaminated to aspartate before diffusing into the BS cells. As intercellular transport is driven by diffusion, the build-up of metabolite pools is necessary for the cycling of intermediates between M-BS cells (Arrivault et al., 2017, Leegood and Furbank, 1984, Stitt et al., 1985). In the BS, malate or aspartate are decarboxylated to release CO_2 around Rubisco (Leegood, 2002), and the reduced alanine or pyruvate diffuse back to M cells. The regeneration of CCM intermediates comes at an energetic cost, and PEP is regenerated at the cost of ATP, completing the C_4 cycle (Ishikawa et al., 2016, Yin and Struik, 2018). The higher ATP demand of C_4 species is supported by a lower LEF/CEF ratio (Ogawa et al., 2023, Takabayashi et al., 2005, Yamori and Shikanai, 2016).

Aside from the common features of C_4 photosynthesis mentioned above, a range of variations occur, in particular in the transport metabolites and decarboxylating enzymes. C_4 species used to be divided into 'sub-types' based on one of three main decarboxylases: nicotinamide adenine dinucleotide-malic enzyme (NAD-ME), nicotinamide adenine dinucleotide phosphate-malic enzyme (NADP-ME), and phosphoenolpyruvate carboxykinase (PEPCK) (Hatch et al., 1975). However, different decarboxylases have been found to operate in combination (Calsa and Figueira, 2007, Furbank, 2011, Sales et al., 2018), and PEPCK has been suggested to operate only as a supplementary pathway given an inability to meet the energy requirements of the BS cells (Wang et al., 2014a). Combining decarboxylating enzymes could also be advantageous – mixed subtypes can simultaneously use different transfer metabolites, reducing the dependency on intermediate pools and potential time lags during their build-up; and the use of parallel malate and aspartate shuttles can also enhance the regulation of energy balance between ATP:NADPH, as malate transport uniquely contributes redox equivalents into the BS (Morales et al., 2018).

1.2.3. The phenotypic plasticity of C_4 photosynthesis

The physiological advantages that come with C_4 photosynthesis have allowed several C_4 species to dominate the open landscape biomes across warmer regions of the Earth, such as the Great Plains of North America, the African grasslands, and large parts of Australia (Kellogg, 2013). Although C_4 species have a particular competitive advantage in areas with high light and temperature; and low CO_2, nutrient, and water availability, they are underrepresented in cold environments and notably almost absent from certain plant life-forms like trees, or forest understories (Sage and Pearcy, 2000, Young et al., 2020). The energetic cost of C_4 photosynthesis may prove a high trade-off in environments with limited light (Ehleringer, 1978, Kromdijk et al., 2008), but the capacity of C_4 species to adapt to short-term changes in conditions might also be different than that of C_3 species. Some C_4 species have been suggested to lack the capacity to maintain photosynthetic activation following sunflecks (Horton and Neufeld, 1998, Krall and Pearcy, 1993); or when grown in the shade seem unable to maintain the high quantum yields necessary for efficient photosynthesis (Ehleringer and Pearcy, 1983, Ogle, 2003), or fail to reduce carboxylase content resulting in Rubisco and PEPC overcapacity (Winter et al., 1982). Based on these phenomena, it has been postulated that the anatomical and biochemical changes required for C_4 photosynthesis may reduce phenotypic plasticity: the ability of organisms to alter their characteristics to compensate for or acclimate to environmental variation, leaving C_4 plants with a diminished capacity to photosynthetically

acclimate to environmental changes relative to C_3 species (Sage and McKown, 2006). C_4 photosynthesis is more constrained by the intracellular-metabolic coordination between M and BS cells necessary for the C_4 cycle than the C_3 pathway. However, C_4 species also exist in environments where a high degree of phenotypic plasticity is advantageous: several C_4 species form dense canopies where there is extensive self-shading and intermittent light (Christin and Osborne, 2014, Long, 1999, Tang et al., 1988). Although the limitations of C_3 photosynthesis under dynamic light conditions have been amply studied, there is limited data regarding the capacity of C_4 species to adapt to environmental variation, and whether acclimation mechanisms are similar to, or different to those in C_3 species.

1.3. Improving photosynthesis under dynamic light

The vast majority of photosynthesis studies have been conducted under constant light, but steady-state conditions are deeply unrepresentative of conditions on the open field, where light intensity is anything but constant. At the top of the canopy, leaves are subject to changes in sun angle, light intensity and intermittent cloud cover throughout the day; and self-shading from overlying leaves and wind movements make the middle of the canopy even more dynamic (Long et al., 2022, Wang et al., 2020, Zhu et al., 2004). Light intensity can change by several orders of magnitude within seconds but photosynthetic responses are not instantaneous and lag behind, often temporarily operating at an efficiency substantially lower than that achieved under steady state (Slattery et al., 2018). The accumulated losses from fluctuating light in crop canopies have been estimated to, over the course of a day, amount to 10-40% of total carbon assimilation (Taylor and Long, 2017, Wang et al., 2020, Zhu et al., 2004). In recent years there has been increased focus on photosynthesis under non-steady-state conditions (Fu and Walker, 2022, Kaiser et al., 2018, Kaiser et al., 2015, Long et al., 2022, Murchie et al., 2018, Slattery et al., 2018, Zhu et al., 2010), with the dynamic light response becoming a target for improvement of crop productivity, with some approaches already demonstrating success in field trials (De Souza et al., 2022, Kromdijk et al., 2016).

The vast majority of work on dynamic light photosynthesis has been conducted on C_3 species. Although introducing C_4 photosynthesis into C_3 crops is a project of huge global interest (Hibberd et al., 2008), when it comes to photosynthetic improvement research the high yield and photosynthetic rates already achieved by C_4 species mean they are frequently sidelined. The higher efficiency of C_4 photosynthesis is well-established under steady light conditions

(Wang et al., 2012), but C_4 induction responses have consistently been identified as potential points of inefficiency (Sage and McKown, 2006, Sales et al., 2021, Slattery et al., 2018). Given several C_4 species form dense canopies with extensive self-shading and where sunflecks provide up to 90% of light energy (Pearcy, 1990, Slattery et al., 2018, Tang et al., 1988, Way and Pearcy, 2012, Zhu et al., 2004), improvements to photosynthetic efficiency under changing light intensities could be hugely beneficial – maize and sugarcane alone account for over 30% of global agricultural production (FAO, 2020) which coupled with their applications in the biofuel industry makes C_4 species some of the most highly produced commodities (USDA, 2023). Some studies have already begun to characterise the C_4 response (Kromdijk et al., 2010, Kubásek et al., 2013, Lee et al., 2022, Li et al., 2021, Pignon et al., 2021, Wang et al., 2022) and even started targeting strategies that have proven successful in improving C_3 efficiency, such as speeding up relaxation of Non-Photochemical Quenching (NPQ) (Sahay et al., 2023) although evidence of the potential of these strategies in C_4 species is currently lacking.

1.3.1. Limitations to photosynthesis during light induction

Induction refers to the rise in photosynthesis towards steady state upon an increase in light intensity, a common occurrence in plant canopies where periods of shade are interspersed with transient increases in light. In wheat, slow induction rates resulted in 21% decrease in daily carbon assimilation (Taylor and Long, 2017). Since longer lags result in greater losses of potential CO_2 assimilation, speed of induction is an important marker for photosynthetic efficiency under dynamic light (Long et al., 2022, McAusland and Murchie, 2020). Rather than a singular process, speed of induction is determined by a variety of factors: RuBP regeneration, Rubisco activity and stomatal conductance can all limit photosynthesis in C_3 species during a transition to higher light (Mott and Woodrow, 2000, Pearcy, 1990, Pearcy and Seemann, 1990, Sassenrath-Cole and Pearcy, 1992). In some C_3 species, Rubisco carboxylation, and in particular Rubisco activase (Rca) availability have been identified primary limitations to induction (Acevedo-Siaca et al., 2020), with higher presence of Rca correlating with increases in biomass (Carmo-Silva and Salvucci, 2013, Yamori et al., 2012). Given stomatal responses are often slower than photosynthesis to respond to changes in irradiance, induction can also be primarily limited by a constrained CO_2 supply (McAusland et al., 2016).

Some studies have suggested that C_4 species have more impaired carbon assimilation after increases in light intensity than C_3 species (Kubásek et al., 2013, Li et al., 2021, Slattery et al., 2018), and the C_4 CCM could indeed be constrained by specific limitations. C_3 photosynthetic

induction is already affected by mismatches in stomatal and photosynthetic response times (McAusland and Murchie, 2020), and C_4 species have the additional challenge of increasing C_3 and C_4 cycle turnover whilst maintaining synchronous operation (Sage and McKown, 2006). Higher relative photorespiratory rates have been found to occur under low light and during photosynthetic induction in C_4 species (Kromdijk et al., 2010, Medeiros et al., 2022), which could indicate that enzymes of the C_3 cycle are activated faster than the large metabolite gradients necessary for M-BS cell transport of CCM intermediates can be established, resulting in a lower concentration of CO_2 in the BS and incomplete suppression of photorespiration (Slattery et al., 2018). Conversely, significant increases in CO_2 BS leakiness have been found in maize and sorghum (Wang et al., 2022), a potential consequence of the opposite imbalance. Faster activation of the CCM without a corresponding rise in CO_2 demand from the C_3 cycle would result in greater CO_2 diffusion out of the permeable BS and back into M cells, which requires recycling of CO_2 and further raises the energetic cost of carbon assimilation (Kromdijk et al., 2008, Kromdijk et al., 2014). Although there is some variation across species, in general any loss of synchronisation in C_4 plants between the light reactions and the CCM, irrespective of imbalance, would result in a more significant impairment of the light induction response than in C_3 plants. However, despite these considerations, to what extent the induction of photosynthesis in C_4 species is truly impaired relative to C_3 species is still unclear as systematic comparisons are lacking.

1.3.2. The C_4 response to fluctuating light

Fluctuating light conditions lead to both photosynthetic induction responses upon increases in light and assimilation flux adjustments following transitions to lower light. Photosynthetic carbon gain in C_3 species can be determined by Rubisco activation and RuBP regeneration (Mott and Woodrow, 2000, Pearcy and Seemann, 1990, Sassenrath-Cole and Pearcy, 1992), stomatal opening and closing (McAusland et al. 2016) and by the speed of photoprotective responses (Niu et al., 2022, Zhu et al., 2004). The effect of fluctuating light responses on the C_4 pathway is not fully understood (Slattery et al., 2018). Alternative hypotheses have postulated that C_4 photosynthesis either decreases (Kubásek et al., 2013) or increases the efficiency of carbon assimilation under fluctuating light (Stitt and Zhu, 2014). The negative hypothesis suggests that fluctuating light disrupts the establishment of the large metabolic gradients necessary for transfer of intermediates in the C_4 CCM, leading to ineffective suppression of photorespiration and reduced photosynthetic efficiency (Kromdijk et al., 2010, Slattery et al., 2018). BS leakiness could also be a concern if the CCM activates faster than C_3

cycle enzymes during the light induction phase (Wang et al., 2022) or if the CCM is slow to deactivate during transitions to lower light. The positive hypothesis also involves the C_4 metabolic gradients, but it instead suggests these may buffer photosynthesis against rapid changes in light intensity, as the large metabolite pools allow for the storage and release of ATP and reducing equivalents (Leegood and von Caemmerer, 1989, Stitt and Zhu, 2014). Mixed C_4 pathways could also help balance redox equivalents in the BS – temporal upregulation of malate over the aspartate decarboxylation would also increase transport of redox equivalents (Wang et al., 2014a, Yin and Struik, 2021). Paradoxically, there is experimental evidence to support both negative (Kubásek et al., 2013, Li et al., 2021) and positive hypotheses (Laisk and Edwards, 1997, Lee et al., 2022), but there are also indications both can be reconciled: metabolite pools could both slow induction and act as a buffer during transitions to lower light; and given said buffering capacity is likely time-sensitive (Arrivault et al., 2017), differences in fluctuation light protocols across different studies could account for the difference in results (Slattery et al., 2018).

1.3.3. Non-Photochemical Quenching

Leaves in full sunlight regularly absorb more energy that can be used up by photosynthesis. The accumulation of excited chlorophylls and highly reduced electron carriers enhances the probability of formation of reactive oxygen species (ROS) that damage the photosynthetic machinery and cause photoinhibition (Krieger-Liszkay, 2005, Takahashi and Badger, 2011). NPQ refers to a collection of mechanisms that protect against photoinhibition through the release of excess light energy harmlessly as heat (Müller et al., 2001). The fastest and most significant component of NPQ is energy-dependent quenching (qE), activating within seconds (Ruban et al., 2012, Wraight and Crofts, 1970). Other mechanisms that act more slowly (10-15 minutes) include zeaxanthin-dependent quenching (qZ) (Dall'Osto et al., 2005, Demmig-Adams, 1990, Kress and Jahns, 2017, Nilkens et al., 2010), chloroplast movements (qM) (Banaś et al., 2012, Cazzaniga et al., 2013), and state transitions (qT) that change the association of light-harvesting complexes between PSII and PSI (Ruban and Johnson, 2009). Sustained, long-term quenching can come from photodamage, as attributed to photoinhibition (pI) (Ruban, 2017); but there are also photoinhibition-independent quenching processes, like the recently identified qH (Malnoë, 2018).

Although discussed separately here, NPQ is an important determinant of the efficiency of photosynthetic light to dark transitions. The return to the unquenched state takes time, and

model simulations estimate slow rates of NPQ relaxation in crop canopies to cost a 7.5-30% loss in daily carbon assimilation (Wang et al., 2020, Werner et al., 2001, Zhu et al., 2004). Field studies on tobacco and soybean have now shown that engineering NPQ to accelerate shade responses improves crop yield (De Souza et al., 2022). NPQ has also been suggested as a potential area for improvement of C_4 photosynthesis (Sales et al., 2021, Zhu et al., 2004)

Remarkably little is known about the specifics of C_4 NPQ, but functional characteristics of the C_4 pathway can be hypothesised to affect NPQ components (Guidi et al., 2019). CEF-dependent generation of ΔpH has been shown to contribute to qE formation (Takahashi et al., 2009), and the higher CEF found in C_4 species could result in enhanced qE formation (Huang et al., 2015a, Huang et al., 2015b, Miyake et al., 2005). Smaller pools of xanthophyll cycle pigments have been found in maize than in some C_3 species (Romanowska et al., 2017) which could reduce qZ capacity. Higher qE and lower qZ would change the proportional makeup of C_4 NPQ and lead to faster relaxation than in C_3 species. The contribution of qM is also likely different, as chloroplast movement capacity is limited in C_4 species where BS chloroplasts are locked in centrifugal or centripetal positions (Kobayashi et al., 2008, Sage, 2004). Other differences are more speculative: antioxidant localisation in M and BS cells could alter ROS accumulation and qI, while different ratios of PSI/PSII across cell types (Majeran et al., 2010, Meierhoff and Westhoff, 1993) could also lead to differences in state transitions and associated qT. Differences in light induction could in turn also affect NPQ – faster induction means more absorbed light energy is being utilised by photosynthesis, decreasing the need for photoprotection (Long et al., 2022).

1.4. Thesis objectives

Based on the knowledge gaps identified above, this thesis aims to perform a comparative analysis of C_3 and C_4 photosynthesis under dynamic light conditions to A) better understand the effect of the C_4 pathway on photosynthetic performance across diverse light environments, and B) identify whether C_3 and C_4 species have similar limiting factors that can be targets for photosynthesis improvement in the future. Individual chapter objectives are as follows:

1. To compare and contrast C_3 and C_4 photosynthetic pathways during photosynthetic induction (Chapter 2) to test whether C_4 species are more affected by transient decreases in photosynthetic efficiency during light induction than C_3 species.

2. To evaluate the opposing hypotheses regarding C_4 photosynthetic efficiency under fluctuating light (Chapter 3). This chapter analyses the photosynthetic efficiency of C_3 and C_4 species under fluctuating light, looking at both transitions to low and high light. To find out if opposing hypotheses regarding C_4 efficiency under dynamic light can be explained by different fluctuating light protocols between different studies, repeat fluctuations of different lengths are also evaluated.

3. To characterise the induction and relaxation responses of NPQ in C_3 and C_4 photosynthesis (Chapter 4) to test if the NPQ kinetics in C_4 species reflect different proportional contributions of different NPQ components. Observed differences are further studied to identify the underpinning mechanisms.

1.5. Use of phylogenetically controlled comparisons to study differences between C_3 and C_4 photosynthetic pathways

C_4 photosynthesis is a striking example of convergent evolution, having independently evolved at least 66 times in angiosperms in both monocots and dicots, and appeared in 19 unrelated plant families (Kellogg, 2013, Sage, 2004). The huge phylogenetic diversity that underlies the common physiological and biochemical features of the C_4 pathway complicates comparisons between C_3 and C_4 photosynthesis, as species-specific responses could be erroneously attributed to photosynthetic pathway (Taylor et al., 2010). Indeed, certain physiological and ecological characteristics originally linked to either C_3 or C_4 photosynthesis in grasses have been found to instead relate to phylogenetic differences between C_3 *BEP* (*Bambusoideae*, *Ehrhartoideae*, *Pooideae*) grasses, and C_4 *PACMAD* (*Panicoideae, Aristidoideae, Chloridoideae, Micrairoideae, Arundinoideae* and *Danthonioideae*) grasses (Edwards and Still, 2008, Edwards et al., 2007). Comparing C_3 and C_4 species from within a monophyletic clade has been shown to be successful in controlling for phylogenetic variation and separating the effects of photosynthetic pathway from evolutionary variation on ecophysiological traits in grasses (Taylor et al., 2010). Since controlling for phylogenetic bias is crucial when attempting to understand the functional consequences of C_3 and C_4 photosynthesis this thesis conducted experimental comparisons on phylogenetically linked C_3 and C_4 species from three independent lineages representative of monocots and dicots, and of all three C_4 decarboxylation enzymes: *Alloteropsis, Flaveria*, and *Cleome*.

The approximate age of the C_4 origins differ between these three genera. Evolution of C_4 photosynthesis dates back ~17 Ma in *Cleome*, ~2 Ma in *Flaveria*, and <2 Ma for *Alloteropsis* (Christin et al., 2011, Lundgren et al., 2015). Studying pairs of C_3 and C_4 species evolved from a relatively recent common ancestor, subspecies C_3 *Alloteropsis semialata* accession *GMT* and C_4 *Alloteropsis semialata* accession *MDG*, C_3 *Flaveria cronquistii* and C_4 *Flaveria bidentis,* and C_3 *Tarenaya hassleriana* and C_4 *Gynandropsis gynandra* (shown in **Table 1.1**, phylogenetic tree in **Figure 1.1**) provides a means to separate phylogenetic differences from differences between C_3 and C_4 photosynthetic pathways. While there is reduced phylogenetic distance between each C_3 and C_4 pair, significant evolutionary distance separates the three genera.

Table 1.1: Phylogenetically linked C_3 and C_4 *Alloteropsis*, *Flaveria*, and *Cleome* species used in this thesis with their photosynthetic pathway, main C_4 subtype where applicable, and class. (Published in Arce Cubas et al., 2023a.)

Genus	Species and accession	Photosynthetic pathway	C4 subtype	Class
Alloteropsis	*Alloteropsis semialata* subspecies *semialata* accession GMT	C_3	---	Monocot
	Alloteropsis semialata subspecies *eckloniana* accession MDG	C_4	NADP-ME/PEPCK	
Flaveria	*Flaveria cronquistii*	C_3	---	Dicot
	Flaveria bidentis	C_4	NADP-ME	
Cleome	*Tarenaya hassleriana*	C_3	---	
	Gynandropsis gynandra	C_4	NAD-ME	

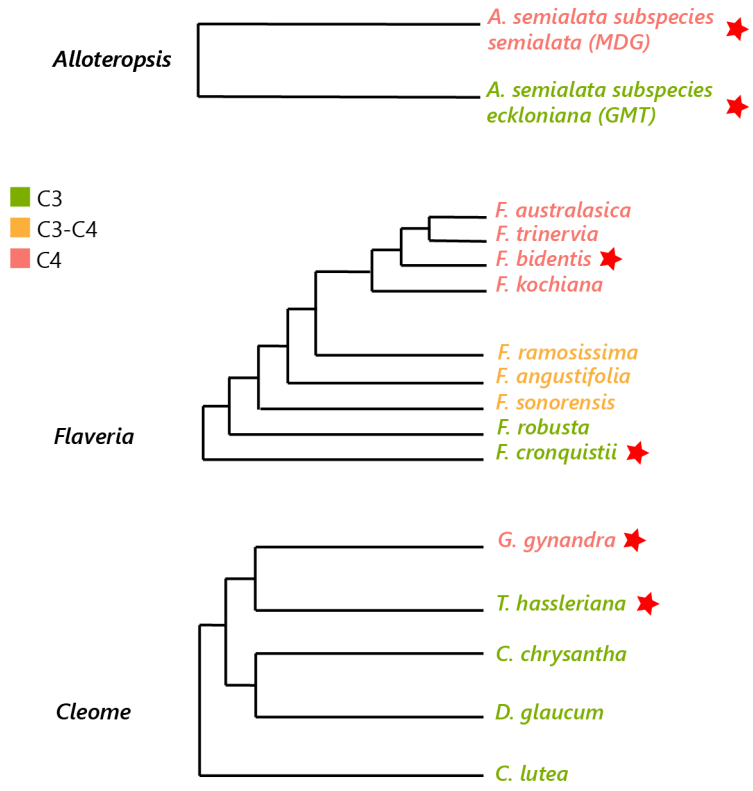

Figure 1.1: Phylogenetic tree of *Alloteropsis*, *Flaveria* and *Cleome* genera. Species used in this thesis are marked with a red star (based on Ibrahim et al. 2009, Lyu et al., 2015, and Shi et al., 2021; published in Arce Cubas et al., 2023b).

Alloteropsis semialata remains the only known grass species with C_3, C_3-C_4 and C_4 subspecies (Ellis, 1974) and is further unique in that the C_3 subspecies may represent a reversion from a C_3-C_4 intermediate (Ibrahim et al., 2009), contrasting with the usual determinism of C_4 evolution. Both of these features make *Alloteropsis* a valuable model for study of C_4 photosynthesis and evolution, and particularly C_3 and C_4 comparisons (Dunning et al., 2019, Ellis, 1974, Lundgren et al., 2016, Ueno and Sentoku, 2006). The *Alloteropsis* genus belongs to the Panicoideae grass subfamily, which also includes crop species of high commercial importance like maize and sugarcane (Sutherland, 1987). *Alloteropsis* plants are distributed amongst tropical and subtropical parts of Africa, Asia, and Australia, as well as Papuasia, but the specific *GMT* and *MDG* accessions originated from South Africa (Lundgren et al., 2015, Lundgren et al., 2016).

The *Flaveria* genus has also been used for studying the C_4 evolutionary trajectory as it includes species with C_3, C_3-C_4 intermediates and C_4 pathways, and has provided key insights into PEPC regulation and C_4 metabolic activity and physiology (Adachi et al., 2023, Gowik et al., 2011,

Sage et al., 2013, Svensson et al., 2003). Naturalized globally, C_3 *F. cronquistii* originates from tropical and subtropical areas of Mexico, and C_4 *F. bidentis* from South America (Sudderth et al., 2009). C_3 *F. cronquistii* does not yield seed under experimental conditions, so it is propagated via cuttings in research (Drincovich et al., 1998, Ku et al., 1991).

The final genus, *Cleome*, has been called 'the future of C_4 research' (Brown et al., 2005) as it is the most closely related genus containing C_4 species to *Arabidopsis*. As a result, C_4 *Gynandropsis gynandra* often shows high similarity in gene sequence to C_3 model species *Arabidopsis thaliana* (Bräutigam et al., 2010). As such, C_3 *T. hassleriana* and C_4 *Gynandropsis gynandra* have been extensively used as systems to study the C_3 to C_4 evolutionary transition (Hoang et al., 2023, Marshall et al., 2007, Parma et al., 2022, Singh et al., 2023). Both *Cleome* species are distributed worldwide. C_3 *T. hassleriana* is native to the temperate regions of South America, and C_4 *G. gynandra* to tropical or sub-tropical areas of Africa (Feodorova et al., 2010, Iltis and Cochrane, 2007). Overall, *Alloteropsis*, *Flaveria* and *Cleome* represent excellent model genera for the study of C_3 and C_4 photosynthetic traits (Brown et al., 2005, Ueno and Sentoku, 2006). The combined use of these three phylogenetically controlled comparisons in the experimental chapters of this thesis has provided a powerful means to identify true differences between C_3 and C_4 photosynthetic pathways, i.e. which persist across all three genera.

2. Comparing C_3 and C_4 photosynthetic induction responses

This chapter has been published as Arce Cubas et al. (2023b).

2.1. Introduction

Photosynthesis is the foundation of life on earth, the source of food, oxygen, and most of our energy. A particularly successful adaptation to the ancestral form is C_4 photosynthesis, which despite its complexity has independently arisen in at least 66 lineages of angiosperms and appeared in 19 unrelated plant families (Kellogg, 2013, Sage, 2004). Although only 3% of flowering species use the C_4 pathway, C_4 species represent 23% of global carbon fixation (Still et al., 2003), and maize and sugar cane are two of the four crops that account for half of the world's crop production (FAO, 2020). Despite the undeniable importance of C_4 species, there is comparatively less focus on improving C_4 performance – photosynthetic induction has consistently been flagged as a source of inefficiency in C_4 species relative to C_3 ones (Sage and McKown, 2006, Sales et al., 2021, Slattery et al., 2018), yet a lack of knowledge on the specifics of the C_4 induction response persists due to limited understanding of variation in photosynthetic induction between C_3 and C_4 photosynthesis, as well as across different C_4 species.

Most C_4 species display 'Kranz' anatomy, in which mesophyll (M) and bundle sheath (BS) cells are arranged concentrically around the leaf veins. Unlike in C_3 species, where initial CO_2 fixation and assimilation processes occur within the same cell, in C_4 species these activities are typically partitioned between M and BS cells. In the cytosol of M cells, equilibrium between CO_2 and bicarbonate is rapidly established by carbonic anhydrase. Bicarbonate is then fixed by phosphoenolpyruvate carboxylase (PEPC) into 4-carbon molecules that are further reduced before diffusing into the BS, where they are decarboxylated to release CO_2 around ribulose 1,5-biphosphate carboxylase/oxygenase (Rubisco), the central enzyme in carbon fixation (Leegood, 2002). The C_4 carbon concentrating mechanism (CCM) thus enhances photosynthesis and suppresses Rubisco's oxygenase activity and resulting photorespiration – the phospho-glycolate salvaging pathway that consumes energy and reducing equivalents, and releases CO_2. However, the operation of the CCM has an energetic cost, and C_4 species require additional ATP for PEP regeneration on top of the energetic demands of the C_3 cycle (Yin and Struik, 2018).

The increased efficiency of the C_4 pathway relative to the C_3 ancestral state is especially apparent under constant high light (Wang et al., 2012). However, during changes in light intensity, some C_4 species display impaired carbon assimilation in comparison to C_3 species (Kubásek et al., 2013, Li et al., 2021, Slattery et al., 2018). Decreases in photosynthetic efficiency during light induction (in response to an increase in light intensity) occur irrespective of photosynthetic pathway and are often explained by lags in regeneration of ribulose-1,5-biphosphate (RuBP) within the C_3 cycle, Rubisco activation, and stomatal opening (Mott and Woodrow, 2000, Pearcy, 1990, Pearcy and Seemann, 1990, Sassenrath-Cole and Pearcy, 1992). In addition, C_4 photosynthesis requires synchronous operation of C_3 and C_4 cycles and any loss of coordination during induction could lead to reduced efficiency of carbon fixation in C_4 species. Faster activation of the CCM relative to C_3 cycle activation in the BS may result in diffusional leakage of highly concentrated CO_2 out of the permeable BS back into M cells and a raised energetic cost for CO_2 assimilation, as recently suggested by Wang et al. (2022) and Lee et al. (2022). A 30-60% increase in BS leakiness of CO_2 during photosynthetic induction relative to steady state photosynthesis has been identified in maize and sorghum (Wang et al., 2022). This suggest that the C_3 cycle in some C_4 species is slower to activate than the C_4 CCM. Alternatively, the C_4 cycle could be the limiting factor during induction due to the need to build up metabolite gradients for the shuttling of CCM intermediates between M and BS cells. If so, the reduced supply of CO_2 to the BS would lead to weaker suppression of photorespiration, and a temporary disconnect between photosynthetic electron transport and CO_2 fixation (Kromdijk et al., 2010, Sage and McKown, 2006, Slattery et al., 2018). Although incomplete suppression of photorespiration can reduce photosynthetic efficiency, photorespiratory metabolite pools have also been suggested to help prime the C_4 cycle (Kromdijk et al., 2014, Medeiros et al., 2022, Schlüter and Weber, 2020, Stitt and Zhu, 2014). Higher relative photorespiratory rates appear to occur under low light and during photosynthetic induction (Kromdijk et al., 2010, Medeiros et al., 2022); the resulting photorespiratory intermediates could act as a carbon reservoir from which to build C_3 and C_4 metabolite pools (Fu and Walker, 2022). The presence of an endogenous source of carbon is supported by the inability to account for the net increase in C_3 and C_4 cycle intermediates during light induction based on rates of CO_2 assimilation alone (Leegood and Furbank, 1984, Usuda, 1985).

Whilst the experimental evidence and putative mechanisms detailed above may indeed suggest that C_4 species could be more affected by transient decreases in photosynthetic efficiency

during induction relative to steady state than C_3 species, most of the work does not directly compare C_3 and C_4 species in a common experiment, but instead often focuses on a single species, such as maize (Kromdijk et al., 2010, Medeiros et al., 2022, Zelitch et al., 2009). Some direct comparisons between C_3 and C_4 photosynthesis have been made in sets of contrasting grass species (Lee et al., 2022) and species within the same genus (Kubásek et al., 2013), but so far the only C_3 and C_4 species studied that share a relatively recent common ancestor are *Flaveria* (Li et al., 2021). Phylogenetic distance can strongly confound the apparent photosynthetic differences observed (Taylor et al., 2010) and to confirm whether observed differences are due to photosynthetic pathway or evolutionary variation, studies conducted on phylogenetically linked C_3 and C_4 species are necessary. Furthermore, despite striking similarities in the anatomy and biochemistry of C_4 species from diverse evolutionary origins, there is still great diversity amongst species. Some common variations are the main decarboxylases utilised to release CO_2 in BS cells: nicotinamide adenine dinucleotide-malic enzyme (NAD-ME), nicotinamide adenine dinucleotide phosphate-malic enzyme (NADP-ME), and phosphoenolpyruvate carboxykinase (PEPCK). Although C_4 subtypes had initially been defined by these main decarboxylases (Hatch et al., 1975), more recent work suggests there is a greater degree of nuance than traditional C_4 classifications connote, as NADP-ME and NAD-ME often operate alongside a PEPCK auxiliary pathway, and the energetic requirements of C_4 photosynthesis render a pure PEPCK subtype unlikely (Wang et al., 2014a). Variations across C_4 species and phylogenetic distance are thus important considerations when trying to derive generic differences between C_3 and C_4 photosynthesis.

In this chapter we analysed steady state photosynthesis and photosynthetic induction in three phylogenetically linked pairs of C_3 and C_4 species from *Alloteropsis*, *Flaveria*, and *Cleome* genera, representative of monocots and dicots, and all three C_4 decarboxylation enzymes. Photosynthetic gas exchange was measured in response to a step-change to moderate and strongly saturating light intensities to characterise differences in photosynthetic induction rates. Experiments were conducted at both 21% and 2% O_2 concentration to evaluate the role of photorespiration during induction. Activation of CO_2 assimilation at the start of light induction was slower in all C_4 species compared to their C_3 counterparts although the mechanism of impairment varied across genera. Furthermore, although both C_3 and C_4 *Flaveria* had greater CO_2 assimilation under 2% O_2, assimilation in C_3 and C_4 *Alloteropsis* species as well as C_3 *T. hassleriana* was negatively impacted by low O_2. The variation in responses highlights the

natural diversity of C_4 species, and the importance of controlling for phylogenetic distance in comparisons between C_3 and C_4 photosynthesis.

2.2. Materials and methods

2.2.1. Plant materials

Three pairs of phylogenetically linked *Alloteropsis*, *Flaveria* and *Cleome* C_3 and C_4 species were selected to decrease evolutionary variation within each pair (see **Table 1.1, Figure 1.1**) but maintain significant evolutionary distance between the three genera, as C_4 origins arose ~ 17 million years ago (Ma) in *Cleome*, ~ 2 Ma in *Flaveria*, and even earlier in *Alloteropsis* (Christin et al., 2011, Lundgren et al., 2015). The selected species include monocots (C_3 *Alloteropsis semialata* subspecies *semialata* accession GMT and C_4 *Alloteropsis semialata* subspecies *eckloniana* accession MDG), dicots (C_3 *Flaveria cronquistii*, C_4 *Flaveria bidentis*, C_3 *Tarenaya hassleriana* and C_4 *Gynandropsis gynandra*), and the three major decarboxylase enzymes of the C_4 pathway, which have been suggested to be dominant in different C_4 species: PEPCK in mixed NADP-ME/PEPCK pathway in *A. semialata* MDG (Ueno and Sentoku, 2006), NADP-ME in *F. bidentis* (Gowik et al., 2011), and NAD-ME in *G. gynandra* (Bräutigam et al., 2010).

2.2.2. Plant growth and propagation

All plants were measured during the vegetative growth phase. Plants were grown in Levington Advance M3 compost (Scotts, Ipswich, UK) mixed with Miracle-Gro All Purpose Continuous Release Osmocote (Scotts Miracle-Gro Company, Marysville, OH, USA; 4 L compost : 25g Osmocote). Medium vermiculite was added to the *Alloteropsis* soil mix (4 L compost : 1 L vermiculite : 25g Osmocote) to prevent waterlogging.

The *Alloteropsis* GMT and MDG accessions were vegetatively propagated and grown on 2 L pots under well-watered conditions in a glasshouse at 18-25ºC, 40-60% relative humidity (RH), with supplemental lightning provided to ensure at least 140-160 μmol m^{-2} s^{-1} photon flux density (PFD) across a 16-hour photoperiod. Plants were measured two weeks after propagation.

The *Flaveria* and *Cleome* species were grown under well-watered conditions in a Conviron growth room (Conviron Ltd., Winnipeg, MB, CA) at 20ºC temperature, 60% RH, and 150 μmol m^{-2} s^{-1} PFD over a 16-hour photoperiod. Because *F. cronquistii* requires vegetative propagation, plants from both *Flaveria* species were propagated from lateral shoot cuttings –

F. bidentis plants were initially grown from seed and then propagated. Cuttings were dipped in Doff Hormone Rooting Powder (Doff Portland Ltd., Hucknall, UK) to induce root development, and *Flaveria* cuttings were grown on 0.25 L pots and measured after 8-10 weeks.

Cleome germination was induced under sterile conditions at 30ºC/20ºC day/night cycle for *T. hassleriana*, and at 30ºC for *G. gynandra*. Germinated seeds were initially sown in 24-cell seed trays before transfer to 0.25 L pots. As *G. gynandra* has a lower development rate than *T. hassleriana*, germination was staggered so both species could be measured at approximately the same developmental stage, after 8-10 weeks for *G. gynandra* and 4-6 weeks for *T. hassleriana*.

2.2.3. Gas exchange and chlorophyll fluorescence

Gas exchange and chlorophyll fluorescence were measured simultaneously using an open gas exchange system (LI-6400XT, LI-COR, Lincoln, NE, USA) with an integrated leaf chamber fluorometer (6400-40 LCF). Leaves were measured in a 2 cm^2 chamber at 25ºC block temperature, 410 ppm sample CO_2 concentration, and 50-65% RH with flow of 300 µmol s^{-1}. Average leaf VPD was 1.1 ± 0.1 kPa at the start and 1.35 ± 0.1 kPa at the end of the light treatment. Actinic light was provided by the LCF and composed of 10% blue (470 nm) and 90% red light (630 nm).

The LCF used a 0.25 Hz modulated measuring light and a multiphase flash (Loriaux et al., 2013) to measure steady (*F'*) and maximal (F_m') fluorescence to derive the quantum yield of Photosystem II (ΦPSII) (Genty et al., 1989).

For experiments using 2% O_2, a pre-mixed 2% O_2 and 98% N_2 gas mixture was supplied to the LI-6400XT through the air inlet, using a mass flow controller (EL-FLOW, Bronkhorst High-tech BV, Ruurlo, NL) and an open T-junction to regulate constant surplus flow. Infrared Gas Analyzer (IRGA) calibration was adjusted to the O_2 gaseous composition in the instrument settings prior to measurement.

2.2.4. Leaf absorptance

Light absorptance of the plants used in experiments was measured with an integrating sphere (LI1800-12, LI-COR) optically connected to a miniature spectrometer (STS-VIS, Ocean Insight, Orlando, FL, USA) according to manufacturer instructions (LI-COR, 1988). Leaf absorptance (L_{abs}) was calculated using **Equation 1B**, where T_s and R_s are transmittance and reflectance of a diffuse sample.

$$L_{abs} = 1 - T_s - R_s \quad \textbf{Equation 1B}$$

Incident PFD was converted to absorbed photon flux density (PFD_{abs}) using the measured leaf absorptance of the emission wavelengths of the 6400-40 LCF light source. The specific absorptance values can be found in **Supplementary table 2.1.**

2.2.5. Steady state light response curves

Steady state light response curves of photosynthetic gas exchange were measured for all species at both 21% and 2% O_2. Leaves were light-adapted at 1000 µmol m^{-2} s^{-1} and once CO_2 assimilation and stomatal conductance reached steady state, gas exchange and chlorophyll fluorescence parameters were measured in a descending gradient of light intensity: 2000, 1700, 1500, 1200, 1000, 800, 600, 400, 300, 200, 100, 75, 30, and 0 µmol m^{-2} s^{-1}. Gas exchange and chlorophyll fluorescence parameters were logged after 120 – 240 s, when leaf intracellular CO_2 concentration (C_i) and CO_2 assimilation were stable.

To analyse steady state responses, a non-rectangular hyperbola was fitted to the light response curves (Stinziano et al., 2021). The quantum yield of assimilation (α) was derived from the initial slope, and the light-saturated photosynthetic rate (A_{max}) from the asymptote of the curve. C_i values obtained above 600 µmol m^{-2} s^{-1} were averaged to estimate light-saturated C_i ($C_{i\,max}$).

Approximate light intensities at the inflection point (600 µmol m^{-2} s^{-1}) and in the saturating part of the response (1500 µmol m^{-2} s^{-1}) were used in the light induction experiments. Respiration in the light (*Rd*) was estimated for all species at each O_2 concentration as the y-intercept using a linear regression of the initial light response curve slope. To account for the Kok effect, measurements in darkness and at 30 µmol m^{-2} s^{-1} light intensity were not included in the regression (Kok, 1949).

2.2.6. Light induction experiments and analysis of lag in carbon assimilation

Leaves were dark-adapted until stomatal conductance reached constant levels (between 30-60 minutes depending on the species), illuminated with 600 µmol m^{-2} s^{-1} or 1500 µmol m^{-2} s^{-1} PFD for 1 hour, and then returned to darkness for another half hour. Starting from the last 5 minutes of initial dark adaption, gas exchange parameters were logged every minute, and chlorophyll fluorescence parameters at 5, 15, 25, 35, 45, and 60 minutes after starting light exposure. Light induction experiments at both light intensities were conducted at 21% and 2% O_2. Carbon assimilation was corrected for respiration to determine net photosynthetic CO_2 assimilation (A_{CO2}) using the *Rd* obtained from light response curves.

To analyse photosynthetic responses across the induction period, the trapezoidal rule (Jawień, 2014) was used to integrate the area under the curve (AUC) (Makowski et al., 2019) of A_{CO2} during the 0 – 5, 5 – 10, and 10 – 60 minute phases of light exposure.

2.2.7. Alternative electron sinks

The electron cost of assimilation can be approximated by the ΦPSII/ΦCO_2 ratio (Genty et al., 1989, Oberhuber and Edwards, 1993), with ΦCO_2 being the quantum yield of CO_2 assimilation (**Equation 1A**). Lower ratios are associated with greater coupling as more electrons captured by PSII go towards CO_2 assimilation (Krall and Edwards, 1990). For light response curves the ΦPSII/ΦCO_2 ratio was calculated for the values obtained at 600 µmol m^{-2} s^{-1} (*600* ΦPSII/ΦCO_2) and 1500 µmol m^{-2} s^{-1} (*1500* ΦPSII/ΦCO_2). During light induction ΦPSII/ΦCO_2 values were taken from across the light period at each intensity. Data points were excluded if calculated ΦCO_2 showed negative values.

$$\phi CO_2 = \frac{A_{CO2} + Rd}{PFD_{abs}} \quad \textbf{Equation 1A}$$

2.2.8. Statistical analysis

All statistical analyses were conducted separately on paired *Alloteropsis, Flaveria,* and *Cleome* light response curves, light induction at 600 µmol m^{-2} s^{-1} PFD, and light induction at 1500 µmol m^{-2} s^{-1} PFD. Mean and standard error of the mean of light response curve parameters (A_{max}, α, $C_{i\ max}$, *600* ΦPSII/ΦCO_2 and *1500* ΦPSII/ΦCO_2), A_{CO2} AUC at different phases of induction, and ΦPSII/ΦCO_2 across light induction were calculated. Linear mixed models (LMMs) were fitted to the light response curve parameters and A_{CO2} AUC at different phases of induction using photosynthetic pathway, O_2 concentration and their interaction as fixed effects; and to ΦPSII/ΦCO_2 across light induction using photosynthetic pathway, O_2 concentration, time, and their interactions as fixed effects. Time of day and measured plant were included as random effects in all models. Two and three-way ANOVA tables for the fixed effects were generated from the LMMs using the Satterthwaite's approximation method (Kuznetsova et al., 2017). The data was independent and assumptions of normality, homogeneity of variance and sphericity were satisfied.

All data analysis and plot generation was done on RStudio 1.3 (Posit Team, 2022) with R 4.1.1 (R Core Team, 2021) using the tidyverse (Wickham et al., 2019), RColorBrewer (Neuwirth, 2014), lme4 (Bates et al., 2015), lmerTest (Kuznetsova et al., 2017) and bayestestR libraries (Makowski et al., 2019).

2.3. Results

2.3.1. Steady state measurements confirm canonical differences in CO_2 assimilation between C_3 and C_4 species

Light response curves were used to first characterise C_3 and C_4 responses under steady state at 21% (**Figure 2.1 A-C, Figure 2.2 A-C, Table 2.1**). The responses of C_4 species in comparison to their C_3 phylogenetic pairs were genus specific – C_4 *F. bidentis* had higher maximum rates of net carbon assimilation (A_{max}) than C_3 *F. cronquistii* ($P = 0.03$; C_3 12.5 ± 1.3 vs C_4 16.7 ± 1.0 μmol m^{-2} s^{-1}), but A_{max} values in C_4 *G. gynandra* were similar to those found in C_3 *T. hassleriana* ($P = 0.24$; C_3 15.5 ± 2.0 vs C_4 16.7 ± 0.7 μmol m^{-2} s^{-1}), and A_{max} values in C_4 *A. semialata MDG* also were similar to C_3 *A. semialata GMT* ($P = 0.02$; C_3 11.8 ± 1.1 vs C_4 10.2 ± 2.7 μmol m^{-2} s^{-1}). A two-way ANOVA (**Table 2.2**) showed photosynthetic pathway had a significant effect on C_i during light saturation in all genera. However, whilst the C_4 pathway was associated with lower $C_{i\,max}$ in *Flaveria* ($P \leq 0.001$; C_3 238 ± 19 vs C_4 86 ± 27 μmol mol^{-1}) and *Cleome* ($P \leq 0.001$; C_3 310 ± 8 vs C_4 125 ± 27 μmol mol^{-1}), in *Alloteropsis* the C_4 association was instead with higher $C_{i\,max}$ ($P \leq 0.01$; C_3 242 ± 9 vs C_4 285 ± 21 μmol mol^{-1}). **Figure 2.1 C** shows that the lower C_i of C_4 species corresponded to lower stomatal conductance, excepting C_4 *A. semialata MDG*, where stomatal conductance to water vapour (g_{sw}) was similar to C_3 *A. semialata GMT* across the light response.

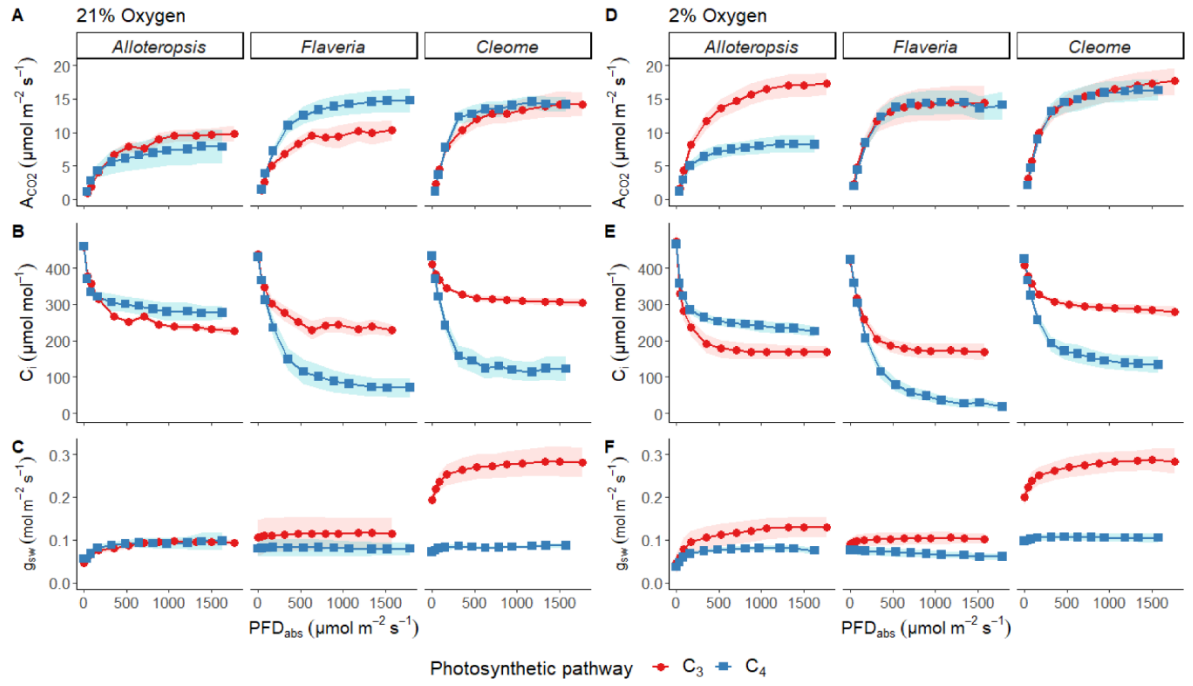

Figure 2.1: Measurements of gas exchange traits during light response curves for phylogenetically linked C_3 and C_4 *Alloteropsis*, *Flaveria* and *Cleome* species under 21% and 2% O_2. Plots show net CO_2 assimilation (A_{CO2}, **A, D**), intercellular CO_2 concentration (C_i, **B, E**), and stomatal conductance to water vapour (g_{sw}, **C, F**)as a function of absorbed light intensity. Ribbons represent standard error of the mean (n=5).

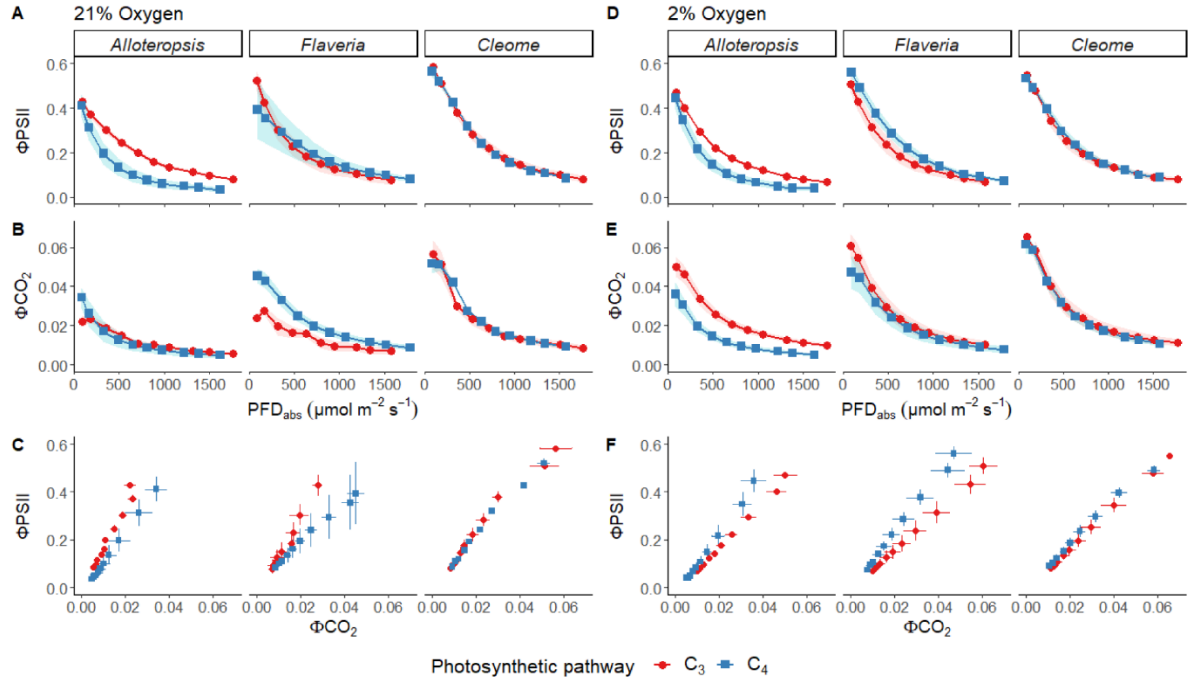

Figure 2.2: Measurements of gas exchange and chlorophyll fluorescence traits during light response curves for phylogenetically linked C_3 and C_4 *Alloteropsis*, *Flaveria* and *Cleome* species under 21% and 2% O_2. Plots show quantum yield of PSII (ΦPSII, **A, D**), and quantum yield of CO_2 assimilation (ΦCO_2, **B, E**) as a function of absorbed light intensity. Ribbons represent standard error of the mean (n=5). Plots **C** and **F** display the relationship between ΦPSII and ΦCO_2. Error bars represent standard error of the mean for both parameters.

Table 2.1: Light response curve parameters estimated from steady state light response curves under 21% and 2% O_2 on phylogenetically linked C_3 and C_4 *Alloteropsis*, *Flaveria* and *Cleome* species. The light-saturated photosynthetic rate (A_{max}) and the quantum yield of assimilation (α) were calculated by fitting the light response curves with a non-rectangular hyperbola. The C_i at light saturation point ($C_{i\ max}$) is the average C_i at PFD ≥ 600 µmol m^{-2} s^{-1}. Values for *600* ΦPSII/ΦCO_2 and *1500* ΦPSII/ΦCO_2 were taken at PFD = 600 µmol m^{-2} s^{-1} and PFD =1500 µmol m^{-2} s^{-1}. Means and standard error of the mean are shown (n = 5).

		21% Oxygen		**2% Oxygen**	
Genus	**Parameter**	**C_3**	**C_4**	**C_3**	**C_4**
Alloteropsis	A_{max} (µmol m^{-2} s^{-1})	11.8±1.1	10.2±2.7	20.9±2.4	10.3±1.4
	α	0.04±0.00	0.10±0.02	0.08±0.01	0.09±0.01
	$C_{i\ max}$ (µmol mol^{-1})	242±9	285±21	171±19	240±14
	600 ΦPSII/ΦCO_2	16.7±1.8	11.3±2.4	8.9±1.7	10.0±2.4
	1500 ΦPSII/ΦCO_2	16.2±1.6	8.6±2.1	7.5±1.2	6.8±2.6
	Rd	0.9±0.2	1.4±0.6	1.5±0.3	1.5±0.1
Flaveria	A_{max} (µmol m^{-2} s^{-1})	12.5±1.3	16.7±1.0	15.6±1.7	15.3±1.8
	α	0.07±0.02	0.06±0.01	0.07±0.01	0.06±0.01
	$C_{i\ max}$ (µmol mol^{-1})	238±19	86±27	174±18	43±15
	600 ΦPSII/ΦCO_2	14.0±0.3	9.0±5.2	7.6±0.3	12.6±3.2
	1500 ΦPSII/ΦCO_2	12.2±0.6	9.5±2.2	8.1±0.6	11.1±3.2
	Rd	0.9±0.3	1.0±0.4	0.6±0.2	0.4±0.2
Cleome	A_{max}	15.5±2.0	16.7±0.7	20.9±2.5	17.7±1.5
	α	0.07±0.01	0.09±0.02	0.15±0.03	0.08±0.01
	$C_{i\ max}$ (µmol mol^{-1})	310±8	125±27	290±11	149±21
	600 ΦPSII/ΦCO_2	12.3±0.8	11.7±1.1	7.7±1.0	9.4±0.5
	1500 ΦPSII/ΦCO_2	10.5±0.5	9.8±1.0	8.7±0.7	8.8±0.3
	Rd	0.3±0.2	1.8±0.7	2.1±0.7	0.8±0.5

Table 2.2: ANOVA table of modelled light response curve parameters for phylogenetically linked C_3 and C_4 *Alloteropsis*, *Flaveria* and *Cleome* species. Photosynthetic pathway, PP. O_2 concentration, [O_2]. Interaction effect, PP:[O_2]. Table shows degrees of freedom; *F*-value; and *P*-value. Significant ($a < 0.05$) *P*-values are shown in bold.

	Alloteropsis			***Flaveria***			***Cleome***		
Parameter	**PP**	**[O_2]**	**PP:[O_2]**	**PP**	**[O_2]**	**PP:[O_2]**	**PP**	**[O_2]**	**PP:[O_2]**
A_{max}	1,15; 7.40; **0.02**	1,15; 4.47; 0.06	1,15; 5.90; **0.03**	1,15; 5.81; **0.03**	1,15; 1.40; 0.26	1,15; 7.73; **0.01**	1,15; 0.29; 0.59	1,15; 3.19; 0.09	1,15; 1.51; 0.24
α	1,15; 3.89; 0.06	1,15; 1.85; 0.20	1,15; 3.69; 0.07	1,15; 1.38; 0.26	1,15; 0.03; 0.87	1,15; 0.26; 0.62	1,15; 1.45; 0.24	1,15; 3.77; 0.07	1,15; 5.58; **0.03**
Ci_{max}	1, 16; 11.06; **≤0.01**	1, 16; 12.00; **≤0.01**	1, 16; 0.54; 0.45	1, 16; 49.07; **≤0.001**	1, 16; 6.75; **0.02**	1, 16; 0.27; 0.61	1, 16; 70.23; **≤0.001**	1, 16; 0.00; 0.93	1, 16; 1.27; 0.27
600 ΦPSII/ΦCO_2	1,16; 6.05; **0.03**	1,16; 24.29; **≤0.001**	1,16; 12.28; **≤0.01**	1,16; 2.01; 0.16	1,16; 5.31; **0.05**	1,16; 5.95; **0.03**	1,16; 0.05; 0.84	1,16; 30.01; **≤0.01**	1,16; 5.39; **0.05**
1500 ΦPSII/ΦCO_2	1,16; 22.75; **≤0.001**	1,16; 35.56; **≤0.001**	1,16; 15.67; **≤0.01**	1,16; 0.37; 0.56	1,16; 1.55; 0.26	1,16; 6.68; **0.05**	1,16; 0.08; 0.78	1,16; 15.61; **0.01**	1,16; 5.57; **0.05**

ΦPSII decreased exponentially with higher light intensities. Although ΦPSII values were very similar across C_3 and C_4 pairs in *Flaveria* and *Cleome*, more pronounced decreases were observed in C_4 *A. semialata MDG* than in C_3 *A. semialata GMT* (**Figure 2.2 A**). ΦCO_2 was also lower at higher light intensities, following a similar pattern to A_{max} across the light response, as ΦCO_2 was similar between C_3 and C_4 species in *Alloteropsis* and *Cleome*, but higher in C_4 *F. bidentis* compared to C_3 *F. cronquistii* (**Figure 2.2 B**). These differences across genera were also apparent for the observed ΦPSII and ΦCO_2 ratios, but not always significantly so. C_4 *F. bidentis* had lower ΦPSII/ΦCO_2 than C_3 *F. cronquistii* ($P = 0.16$; C_3 14.0 ± 0.3 vs C_4 9.0 ± 2.4 at PFD = 600 µmol m^{-2} s^{-1}, and $P = 0.56$; C_3 12.2 ± 0.6, C_4 9.5 ± 2.2 at PFD = 1500 µmol m^{-2} s^{-1}) and the same was observed for C_4 *A. semialata MDG* compared to C_3 *A. semialata GMT* ($P = 0.03$; C_3 16.7 ± 1.8 vs C_4 11.3 ± 2.4 at PFD = 600 µmol m^{-2} s^{-1}, and $P \leq 0.001$; C_3 16.2 ± 1.6 vs C_4 8.6 ± 2.1 at PFD = 1500 µmol m^{-2} s^{-1}), suggesting that in these C_4 species less electron transfer through PSII is needed per CO_2 fixed. **Figure 2.2 C** shows that the lower ratio of ΦPSII to ΦCO_2 in C_4 *Flaveria* and *Alloteropsis* in relation to their C_3 counterparts was observed across most light intensities, although the difference appeared to be marginal at higher light intensities. At 21% O_2, both C_3 and C_4 *Cleome* species had very similar ΦPSII/ΦCO_2 ($P = 0.84$; C_3 12.3 ± 0.8 vs C_4 11.7 ± 1.1 at PFD = 600 µmol m^{-2} s^{-1}, and $P = 0.78$; C_3 10.5 ± 0.5 vs C_4 9.8 ± 1.0 at PFD = 1500 µmol m^{-2} s^{-1}).

Light response curves were also performed at 2% O_2 to minimize photorespiration (**Figure 2.1 D-F, Figure 2.2 D-F, Table 2.1**). All three C_3 species had substantially higher CO_2 assimilation rates under low O_2 – A_{max} was around 75% higher in C_3 *A. semialata MDG*, 25% higher in C_3 *F. cronquistii*, and 35% higher in C_3 *T. hassleriana* than under 21% O_2. 2% O_2 also led to a decrease in $C_{i\ max}$ in *Alloteropsis* ($P \leq 0.01$ in C_3 171 ± 19 vs C_4 240 ± 14 µmol mol^{-1}) and *Flaveria* ($P = 0.02$; C_3 174 ± 18 vs C_4 43 ± 15 µmol mol^{-1}) but no significant change in either *Cleome* species ($P = 0.93$; C_3 290 ± 11 vs C_4 149 ± 21 µmol mol^{-1}), where A_{CO2} and g_{sw} appeared tightly coordinated. The increase in A_{max} was not mirrored in C_4 species, as evidenced by significant interactions (**Table 2.2**) between photosynthetic pathway and oxygen in *Alloteropsis* ($P = 0.03$) and *Flaveria* ($P = 0.01$), where low O_2 concentrations were associated with higher A_{max} on C_3 but not C_4 species. (**Table 2.2**). Similar patterns were observed for the two *Cleome* species, however the increase in A_{max} at 2% O_2 for C_3 *T. hassleriana* was less pronounced than for the other C_3 species and instead the initial slope α appeared to be subject to a significant interaction between effects of photosynthetic pathway and O_2 ($P = 0.03$). The

different effects on assimilation at low O_2 between C_3 and C_4 species were also reflected in the changing relationship between ΦPSII and ΦCO_2 (**Figure 2.2 C&F**) – photosynthetic pathway and O_2 concentration were found to have significant interactions on $\Phi PSII/\Phi CO_2$ in all three genera (**Table 2.2**, $P = 0.05$ in *Flaveria* and *Cleome*, $P \leq 0.01$ in *Alloteropsis*), due to decreases in $\Phi PSII/\Phi CO_2$ in C_3 species at 2% O_2 not observed in C_4 species. This data confirms that photorespiration is a significant electron sink under steady state for all three C_3 species, whereas the steady state suppression of photorespiration at 21% O_2 in the C_4 species is sufficient to prevent any significant further decreases in $\Phi PSII/\Phi CO_2$ under 2% O_2.

2.3.2. Substantial differences in photosynthetic traits exist between C_3 and C_4 species during light induction

Photosynthetic induction rates were measured in leaves exposed to 600 µmol m^{-2} s^{-1} or 1500 µmol m^{-2} s^{-1} PFD from darkness (**Figure 2.3 A-C** and **G-I**). The light induction response across all species and light intensities generally consisted of gradual stomatal opening in line with a rise in A_{CO2} towards steady state, and a sharp drop in C_i at the start of induction, followed by a gradual recovery.

In addition to these general patterns, several differences were observed across genera and between paired species. Stomata tended to open more quickly in the C_3 species than in their respective C_4 counterparts. Furthermore, the speed of A_{CO2} induction appeared to vary between some C_3 and C_4 pairs; where carbon assimilation was notably slower to induce in C_4 *G. gynandra* compared to C_3 *T. hassleriana* under both light intensities, with more subtle differences observed in the *Alloteropsis* and *Flaveria* C_3 and C_4 pairs.

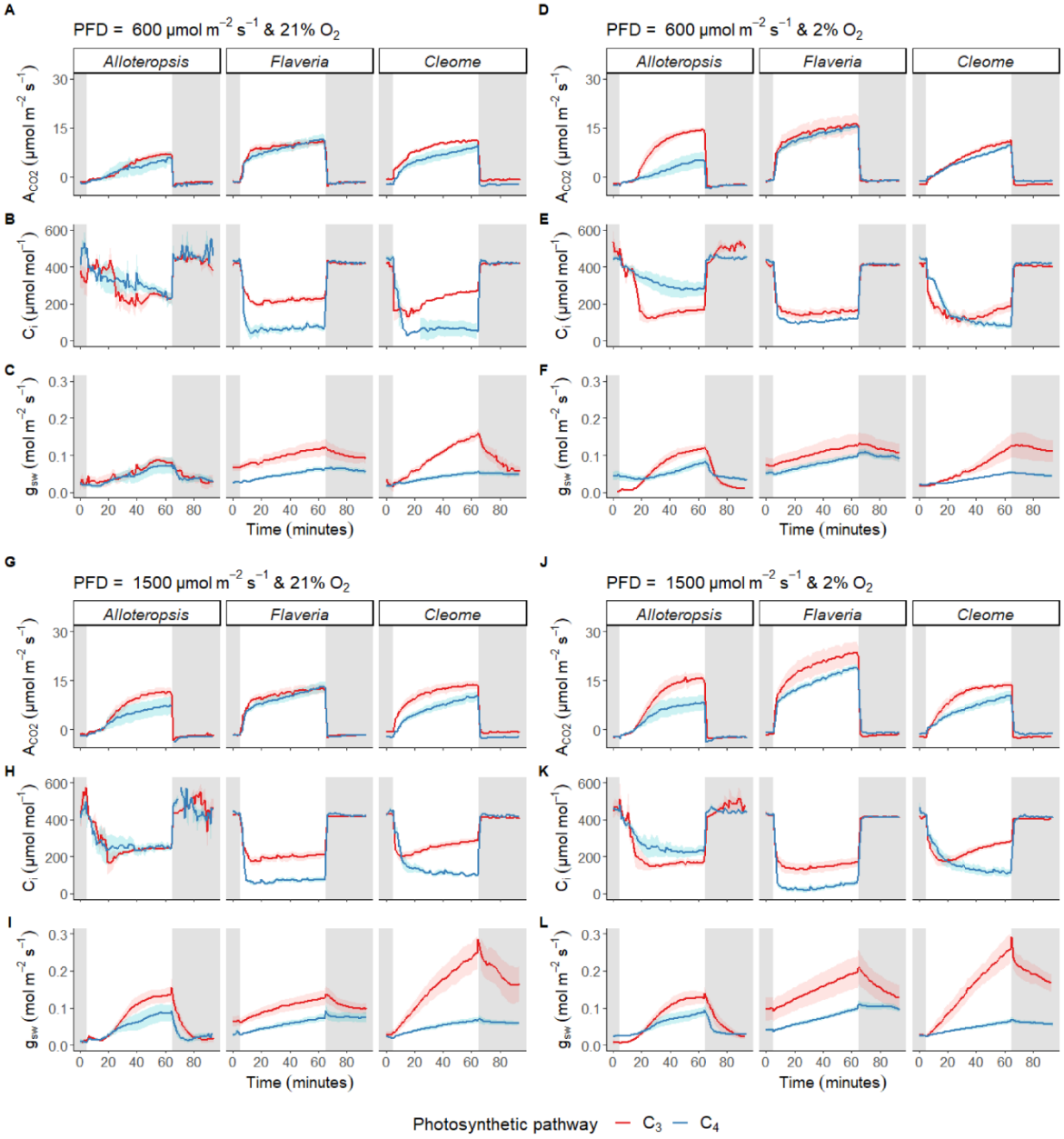

Figure 2.3: Measurements of gas exchange during light induction in phylogenetically linked C_3 and C_4 *Alloteropsis*, *Flaveria* and *Cleome* species. Leaves were acclimated to darkness, exposed to 1 hour of light, and returned to darkness for another half hour. Plots show net CO_2 assimilation (A_{CO2}, A, D, G, J), intercellular CO_2 concentration (C_i, B, E, H, K) and stomatal conductance to water vapour (g_{sw}, C, F, I, L) across the light induction experiment, at PFD = 600 µmol m^{-2} s^{-1} and PFD =1500 µmol m^{-2} s^{-1}, in 21% and 2% O_2. Ribbons represent standard error of the mean (n = 5).

2.3.3. Reductions in assimilation of CO_2 at the start of induction in C_3 and C_4 species vary across genera

In order to systematically explore C_3 and C_4 differences in the activation of CO_2 assimilation, the induction time-series were subdivided into three periods, 0 – 5 min, 5 – 10 min, and the remaining 10 – 60 min, and integrated carbon assimilation (AUC) was calculated for each

period (**Figure 2.4**). During the 0 – 5 min period, C_4 *F. bidentis* had lower AUC than C_3 *F. cronquistii* under both PFD = 600 µmol m^{-2} s^{-1} (P = 0.09; C_3 12.4 ± 1.7 vs C_4 5.8 ± 2.0 µmol m^{-2}) and PFD = 1500 µmol m^{-2} s^{-1} (P = 0.02; C_3 14.8 ± 1.8 vs C_4 8.0 ± 1.8 µmol m^{-2}), with the difference becoming significant under higher light (**Table 2.3**). The difference in assimilated CO_2 between C_3 and C_4 at the start of induction was even more pronounced in *Cleome*, where the AUC of C_4 *G. gynandra* was significantly lower than that of C_3 *T. hassleriana* under both light intensities ($P \leq 0.01$; C_3 12.6 ± 2.0 vs C_4 -1.4 ± 1.9 µmol m^{-2} at PFD = 600 µmol m^{-2} s^{-1}, and $P \leq 0.01$; C_3 13.8 ± 3.2 vs C_4 -3.1 ± 1.8 µmol m^{-2} at PFD = 1500 µmol m^{-2} s^{-1}). The AUC in C_4 *G. gynandra* continued to be significantly lower than in C_3 *T. hassleriana* under both light intensities during the following two periods of induction analysed (**Table 2.3**). In contrast, the significant difference in cumulative CO_2 uptake between *Flaveria* species was only significant during the first five minutes of induction (**Figure 2.4 A**). Thus, there was a more pronounced lag in CO_2 assimilation during induction in C_4 photosynthesis in *Flaveria* and *Cleome* than in C_3 photosynthesis in the same genera. This was especially apparent in relation to the steady state comparison between both species-pairs (**Figure 2.1 A**). In *Alloteropsis*, the C_4 *A. semialata MDG* also started at lower AUC than C_3 *A. semialata GMT* during the 0 – 5 min period under both light intensities (P = 0.36; C_3 -4.4 ± 0.5 vs C_4 -6.22 ± 0.39 at PFD = 600 µmol m^{-2} s^{-1}, and P = 0.07; C_3 -4.2 ± 0.2, vs C_4 -6.8 ± 0.6 at PFD = 1500 µmol m^{-2} s^{-1}), but the difference in AUC between pathways was only found to be significant for the final 10 – 60 min ($P \leq 0.01$; C_3 194.8 ± 34.3 vs C_4 142.2 ± 101.0 at PFD = 600 µmol m^{-2} s^{-1}, and P = 0.03; C_3 403.3 ± 59.5 vs C_4 241.5 ± 115.6 at PFD = 1500 µmol m^{-2} s^{-1}).

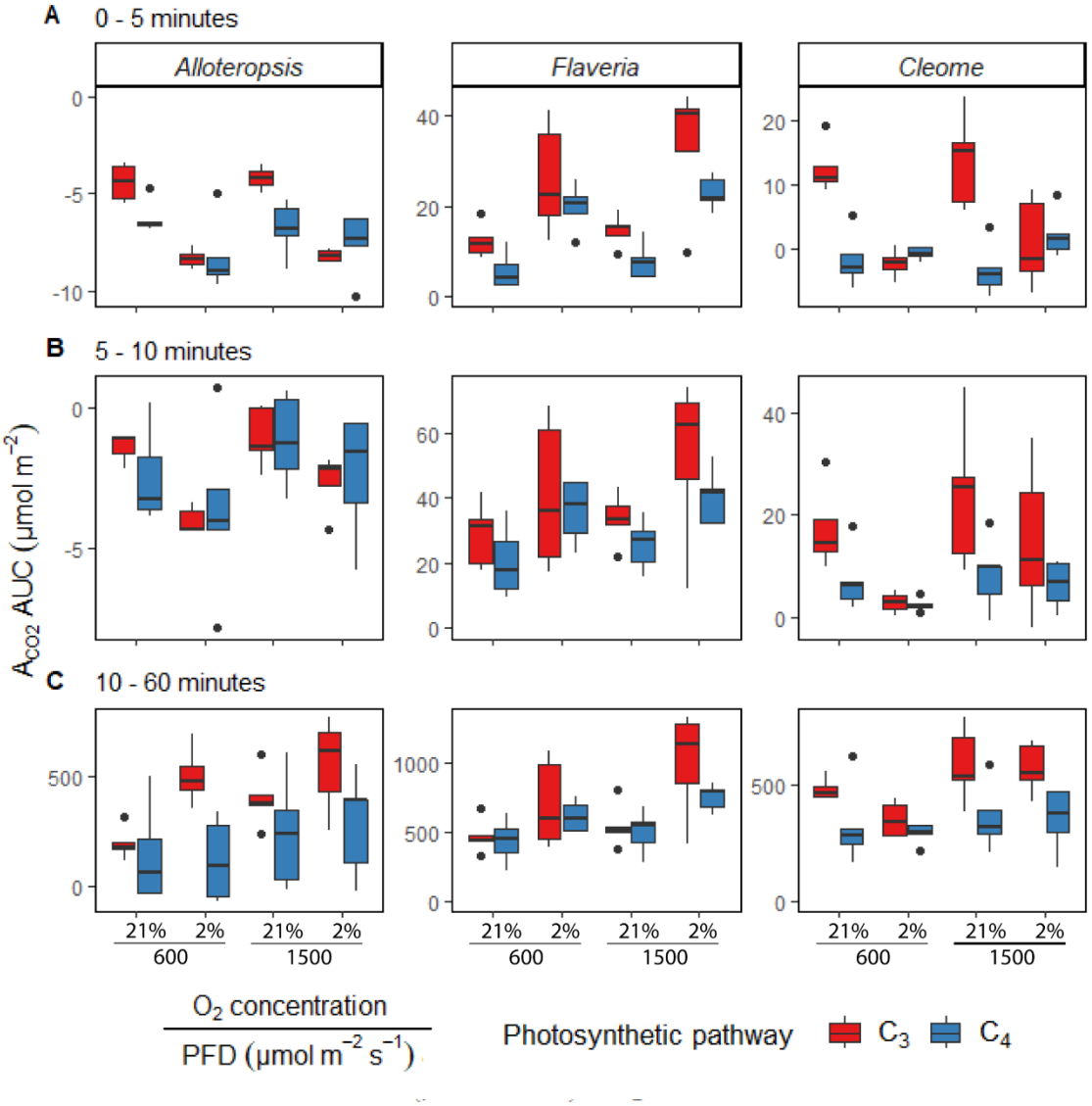

Figure 2.4: Boxplots of cumulative CO_2 assimilation over different phases of light induction in phylogenetically linked C_3 and C_4 *Alloteropsis*, *Flaveria* and *Cleome* species, under different light and O_2 treatments (n = 5 for each combination of species/measurement condition). Box edges represent first and third quartiles, the solid line indicates the median, and points represent outliers beyond 1.5 times the interquartile range. The area under the curve (AUC) was calculated from the A_{CO2} of light induction experiments where plants at 21% or 2% O_2 concentrations were dark-adapted and exposed to PFD = 600 µmol m^{-2} s^{-1} or PFD =1500 µmol m^{-2} s^{-1} for 1 hour. Plots show the AUC of induction during 0 – 5 minutes (**A**), 5 – 10 minutes (**B**), and 10 – 60 minutes (**C**). Two-way ANOVAs (**Table 2.3**) were used to test the effect of photosynthetic pathway, O_2 concentration and their interaction on A_{CO2} AUC at different phases of light induction in *Alloteropsis, Flaveria,* and *Cleome.*

Table 2.3: ANOVA table of the carbon assimilation AUC of different phases of light induction for phylogenetically linked C_3 and C_4 *Alloteropsis*, *Flaveria* and *Cleome* species. Photosynthetic pathway, PP. O_2 concentration, [O_2]. Interaction effect, PP:[O_2]. Table shows degrees of freedom, *F*-value, and *P*-value. Significant ($a < 0.05$) *P*-values are shown in bold.

		Alloteropsis			***Flaveria***			***Cleome***		
Light intensity (µmol m^{-2} s^{-1})	**Induction phase (minutes)**	**PP**	**[O_2]**	**PP:[O_2]**	**PP**	**[O_2]**	**PP:[O_2]**	**PP**	**[O_2]**	**PP:[O_2]**
600	0 – 5	1,16; 1.34; 0.26	1,16; 27.85; **≤0.001**	1,16; 3.13; 0.10	1,16; 3.18; 0.09	1,16; 15.08; **≤0.01**	1,16; 0.00; 0.95	1,16; 15.56; **≤0.01**	1,16; 15.12; **≤0.01**	1,16; 25.03; **≤0.001**
	5 – 10	1,16; 0.20; 0.66	1,16; 5.81; **0.02**	1,16; 0.80; 0.38	1,16; 0.86; 0.36	1,16; 3.60; 0.08	1,16; 0.05; 0.83	1,16; 5.01; **0.04**	1,16; 10.06; **≤0.01**	1,16; 2.95; 0.11
	10 – 60	1,16; 8.87; **≤0.01**	1,16; 3.68; 0.07	1,16; 5.14; **0.03**	1,16; 0.39; 0.54	1,16; 4.46; **0.05**	1,16; 0.08; 0.78	1,16; 4.58; **0.05**	1,16; 2.41; 0.14	1,16; 0.89; 0.36
1500	0 – 5	1,16; 3.81; 0.07	1,16; 22.30; **≤0.001**	1,16; 10.14; **≤0.01**	1,16; 6.39; **0.02**	1,16; 24.21; **≤0.001**	1,16; 0.33; 0.57	1,16; 9.48; **≤0.01**	1,16; 2.07; 0.17	1,16; 12.85; **≤0.01**
	5 – 10	1,16; 0.00; 0.99	1,16; 3.40; 0.08	1,16; 0.07; 0.78	1,16; 2.54; 0.13	1,16; 7.06; **0.01**	1,16; 0.12; 0.73	1,16; 5.90; **0.02**	1,16; 1.18; 0.29	1,16; 0.49; 0.49
	10 – 60	1,16; 5.09; **0.03**	1,16; 1.06; 0.31	1,16; 0.33; 0.57	1,16; 2.16; 0.16	1,16; 12.59; **≤0.01**	1,16; 1.01; 0.33	1,16; 12.96; **≤0.01**	1,16; 0.03; 0.86	1,16; 0.00; 0.95

2.3.4. CO_2 assimilation during induction is enhanced under 2% O_2 in some species but suppressed in others

In order to test whether the presence or absence of photorespiration affected the activation of CO_2 assimilation, both light treatments were also conducted under 2% O_2 (**Figure 2.3 D-F** and **J-L**). In *Flaveria*, the decrease in O_2 concentration significantly increased the AUC of both C_3 *F. cronquistii* and C_4 *F. bidentis* during the first five minutes of induction (**Table 2.3**, **Figure 2.4 A**), under both light intensities ($P \leq 0.01$; C_3 26.1 ± 5.4 vs C_4 19.9 ± 2.6 µmol m^{-2} at PFD = 600 µmol m^{-2} s^{-1} and $P \leq 0.001$; C_3 33.8 ± 6.3 vs C_4 23.1 ± 1.6 at PFD = 1500 µmol m^{-2} s^{-1}). Interestingly, although the stimulating effect of 2% O_2 on C_4 *F. bidentis* was less pronounced for 5 – 10 min and 10 – 60 min, the effect was still significant across both periods under both light intensities, except for 5 – 10 min at PFD = 600 µmol m^{-2} s^{-1} ($P = 0.08$, **Table 2.3**). This suggests that photorespiration is insufficiently suppressed during induction in C_4 *F. bidentis,* whereas in contrast, no change was observed for CO_2 assimilation in steady state C_4 *F. bidentis* under 2% O_2 (**Figure 2.1 A&D**). In *Cleome* no such enhancement of the photosynthetic response was observed in C_4 *G. gynandra*. Instead, the significant interaction between photosynthetic pathway and O_2 concentration from 0 – 5 min was primarily associated with a

decrease in assimilated CO_2 in C_3 *T. hassleriana* and only a marginal increase in C_4 *G. gynandra* AUC under 2% O_2 compared to under 21% O_2 ($P \leq 0.001$). The negative effect of 2% O_2 on AUC in C_3 *T. hassleriana* was transiently observed from 0 – 10 min at PFD = 600 µmol m^{-2} s^{-1} and only from 0 – 5 min at PFD = 1500 µmol m^{-2} s^{-1}. From 10 – 60 min AUC at 2% O_2 in C_3 *T. hassleriana* was similar to the AUC at 21% O_2 under both light intensities. Thus, the stimulation of steady state CO_2 assimilation by 2% O_2 in this species was not observed under any of the transient conditions (**Table 2.3, Figure 2.4**). Suppression of carbon assimilation by low O_2 was also observed during the start of induction in both C_3 and C_4 *Alloteropsis* species. The AUC from 0 – 5 min was reduced in C_3 *A. semialata GMT* and C_4 *A. semialata MDG* compared to AUC in 21% O_2 under both light intensities, a significant effect ($P \leq 0.001$) that persisted well into the 5 – 10 min period for PPFD = 600 µmol m^{-2} s^{-1} ($P \leq 0.02$). However, by 10 – 60 min the effect of O_2 was reversed in C_3 *A. semialata GMT*, with AUC for this period being significantly higher than for 21% O_2 ($P = 0.03$). For this period C_3 *A. semialata GMT* also had a significantly higher AUC in 2% O_2 than C_4 *A. semialata MDG* ($P \leq 0.01$; C_3 504.4 ± 57.5 vs C_4 116.4 ± 84.7 µmol m^{-2} at PFD = 600 µmol m^{-2} s^{-1}, and $P = 0.03$; C_3 558.71 ± 94.6 vs C_4 285.2 ± 108.7 µmol m^{-2} at PFD = 1500 µmol m^{-2} s^{-1}). Whereas the stimulating effect of 2% O_2 on transient CO_2 assimilation may be indicative of photorespiration as a negative factor during photosynthetic induction, the suppression of carbon assimilation found under 2% O_2 for both *Alloteropsis* species as well as the *Cleome* C_3 *T. hassleriana* could indicate photorespiration is not always detrimental to photosynthetic efficiency and may indeed support the activation of CO_2 assimilation in some C_3 and C_4 species.

2.3.5. Transient decoupling between electron transport and carbon fixation during induction is more pronounced in C_4 species and ameliorated by 2% O_2

During activation of CO_2 assimilation, a temporary decoupling between the electron transport chain and photosynthetic carbon fixation in C_4 species could occur due to the time needed to activate the C_3 cycle, incomplete suppression of photorespiration due to an inactive CCM, or because of an increase in the energetic cost of carbon fixation via BS CO_2 leakage. To look for evidence of transient decoupling during induction, ΦPSII/ΦCO_2 ratios across the light induction period under each light and O_2 condition were further analysed within each genus (**Figure 2.5**, **Table 2.4**).

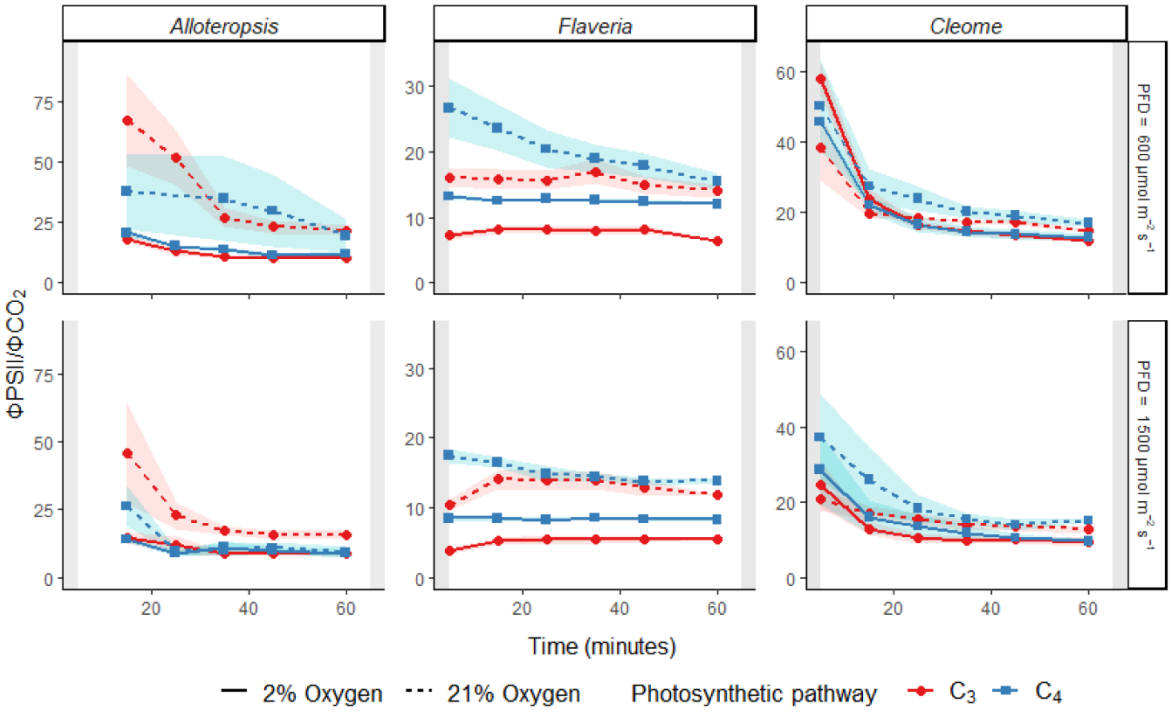

Figure 2.5: Line plots of the ΦPSII/ΦCO$_2$ ratio during light induction at PFD = 600 µmol m^{-2} s^{-1} (**A**) and PFD =1500 µmol m^{-2} s^{-1} (**B**) in phylogenetically linked C$_3$ and C$_4$ *Alloteropsis*, *Flaveria* and *Cleome* species. Plots show ΦPSII/ΦCO$_2$ under 21% (dashed line) and 2% O$_2$ (solid line). Values of ΦPSII/ΦCO$_2$ were excluded if ΦCO$_2$ values were negative, resulting in the 5 minute *Alloteropsis* values being excluded. Ribbons show standard error of the mean (n = 5).

Table 2.4: ANOVA table of the ΦPSII/ΦCO$_2$ ratio during light induction for phylogenetically linked C$_3$ and C$_4$ *Alloteropsis*, *Flaveria* and *Cleome* species. Photosynthetic pathway, PP. Time, t. O$_2$ concentration, [O$_2$]. Interaction effects, PP:[O$_2$], PP:t, and PP:[O$_2$]:t. Table shows degrees of freedom, *F*-value, and *P*-value. Significant (a < 0.05) *P*-values are shown in bold.

Light intensity (µmol m^{-2} s^{-1})	**Genus**	**PP**	**t**	**[O$_2$]**	**PP:[O$_2$]**	**PP:t**	**O$_2$:t**	**PP:[O$_2$]:t**
600	*Alloteropsis*	1,63; 0.11; 0.74	1,63; 28.69; **≤0.001**	1,63; 13.07; **≤0.001**	1,63; 0.71; 0.40	1,63; 0.62; 0.43	1,63; 5.98; **0.02**	1,63; 0.93; 0.34
	Flaveria	1,100; 52.64; **≤0.001**	1,100; 146.83; **≤0.001**	1,100; 6.96; **≤0.01**	1,100; 0.13; 0.73	1,100; 4.23; **0.04**	1,100; 6.60; **0.01**	1,100; 4.43; **0.04**
	Cleome	1,98; 0.69; 0.41	1,98; 7.71; **≤0.01**	1,98; 53.53; **≤0.001**	1,98; 1.57; 0.21	1,98; 0.00; 0.95	1,98; 0.04; 0.83	1,98; 0.30; 0.58
1500	*Alloteropsis*	1,70; 3.30; 0.07	1,70; 11.82; **≤0.001**	1,70; 12.50; **≤0.001**	1,70; 3.90; **0.05**	1,70; 0.60; 0.44	1,70; 4.20; **0.04**	1,70; 0.46; 0.49
	Flaveria	1,101; 67.884; **≤0.001**	1,101; 478.57; **≤0.001**	1,101; 0.60; 0.44	1,101; 2.06; 0.15	1,101; 9.33; **≤0.01**	1,101; 4.51; **0.03**	1,101; 2.91; 0.09
	Cleome	1,101; 4.14; **0.04**	1,101; 6.44; **0.01**	1,101; 27.65; **≤0.001**	1,101; 0.52; 0.47	1,101; 3.06; 0.08	1,101; 00.00; 0.96	1,101; 0.64; 0.42

The effect of time was significant for all genera. All the C_4 species showed higher ΦPSII/ΦCO_2 at the start of induction under 21% O_2, with values gradually decreasing as the leaves became more acclimated to the light conditions. The average ΦPSII/ΦCO_2 ratio during induction was also noticeably higher than the steady state ΦPSII/ΦCO_2 for all species, which ranged between 8-12 e^-/CO_2 depending on the species, indicating a significant transient decoupling during induction compared to steady state. In *Flaveria*, C_4 *F. bidentis* had higher ΦPSII/ΦCO_2 ratio than C_3 *F. cronquistii* under all light and oxygen conditions, the complete opposite of steady state. This suggests the C_4 pathway in *Flaveria* does have some features that make the activation of photosynthesis more energetically demanding at the onset of light induction. Notably, the interaction of O_2 concentration and time also had a significant effect on ΦPSII/ΦCO_2 ($P = 0.01$ at PFD = 600 µmol m^{-2} s^{-1}, $P = 0.01$ at PFD = 1500 µmol m^{-2} s^{-1}), since in 2% O_2 the ratio decreased at an earlier point of induction than in 21% O_2. During induction at PFD = 600 µmol m^{-2} s^{-1}, the three-way interaction was significant ($P = 0.04$), reflecting the strong decrease in ΦPSII/ΦCO_2 over time observed at 21% O_2 in C_4 *F. bidentis*. This decrease may reflect the progressive suppression of photorespiration by activation of the C_4 CCM, since the same trend in ΦPSII/ΦCO_2 was not present in C_3 *F. cronquistii,* nor under 2% O_2 when photorespiration would have been negligible.

In *Cleome*, C_3 *T. hassleriana* also had a lower ΦPSII/ΦCO_2 ratio than C_4 *G. gynandra,* in another reversal of differences observed during steady state conditions. ΦPSII/ΦCO_2 was significantly affected by time ($P \leq 0.01$ at PFD = 600 µmol m^{-2} s^{-1}, $P = 0.01$ at PFD = 1500 µmol m^{-2} s^{-1}) as well as O_2 concentration ($P \leq 0.001$ at both light intensities), but in contrast to *Flaveria* no significant interaction was found between O_2 and time ($P = 0.21$ at PFD = 600 µmol m^{-2} s^{-1}, $P = 0.47$ at PFD = 1500 µmol m^{-2} s^{-1}). Instead, in *Cleome* ΦPSII/ΦCO_2 was marginally lower at 2% O_2 than at 21% O_2 across the induction period. The temporal decrease in ΦPSII/ΦCO_2 was similar under both O_2 concentrations, suggesting that the transient decoupling between electron transport and CO_2 fixation was relatively insensitive to O_2 in both *Cleome* species.

Finally, ΦPSII/ΦCO_2 ratios in *Alloteropsis* were not significantly affected by a main effect of photosynthetic pathway ($P = 0.74$ at PFD = 600 µmol m^{-2} s^{-1}, $P = 0.07$ at PFD = 1500 µmol m^{-2} s^{-1}), again in contrast to steady state where C_4 *A. semialata MDG* had lower ratios than C_3 *A. semialata GMT*. However, the interaction between photosynthetic pathway and O_2 was significant ($P \leq 0.001$ at both light intensities), due to the fact that the O_2 effect on ΦPSII/ΦCO_2

was much less pronounced in C_4 *A. semialata MDG* than in C_3 *A. semialata GMT*. Similar to the *Flaveria* and *Cleome* results, a significant interaction between O_2 concentration and time ($P \leq 0.001$ at both light intensities) was also observed in *Alloteropsis*, with 2% O_2 more significantly reducing ΦPSII/ΦCO_2 during the start of induction than towards the end.

2.4. Discussion

The presented experiments investigated the efficiency of photosynthesis during light induction in phylogenetically linked *Alloteropsis, Flaveria*, and *Cleome* C_3 and C_4 species. Steady state and photosynthetic induction responses to light were measured to evaluate relative differences between paired species – controlling for evolutionary distance allowed for better differentiation between the effects of photosynthetic pathway and species-specific variation. At the start of light induction C_4 species had greater lag in CO_2 assimilation than C_3 species in all three comparisons (**Figure 2.4 A**), confirming that the activation of CO_2 assimilation is generally slower in C_4 photosynthesis within the studied genera. However, the underlying reasons for this difference appeared to be genus specific. In C_4 *Flaveria*, slower induction appeared to be explained at least in part by less efficient suppression of photorespiration, since 2% O_2 resulted in increased CO_2 assimilation and fewer transferred electrons per fixed CO_2 (**Figure 2.5**). Although decreased photorespiratory electron sinks were also observable in C_4 *Alloteropsis* and *Cleome* induction under 2% O_2, there were no concurrent increases in CO_2 assimilation (**Figure 2.4 A**), implying alternative limiting factors were at play, such as C_3 cycle activation. In C_3 *Cleome* and both *Alloteropsis* species, 2% O_2 actually suppressed activation of CO_2 assimilation, suggesting that photorespiration may support the induction of photosynthesis in these species.

2.4.1. Slower activation of CO_2 assimilation during light induction in C_4 versus C_3 photosynthesis

In line with previously observed photosynthetic induction responses (Mott and Woodrow, 2000, Pearcy, 1990, Pearcy and Seemann, 1990, Sassenrath-Cole and Pearcy, 1992) a transient reduction in CO_2 assimilation relative to steady state was observed in all species during light induction, with a more pronounced effect found in C_4 species (**Figure 2.4**). Greater losses of photosynthetic efficiency have previously been observed in C_4 grown under dynamic light in comparison to C_3 species and linked to mechanisms involving photosynthetic induction (Kubásek et al., 2013). Further fluctuating light on plants grown under constant light (including

C_4 *F. bidentis*) has also shown an increased lag in CO_2 assimilation in C_4 compared to C_3 species following step-increases in light intensity (Li et al., 2021). Similarly, in a study comparing a selection of C_3 and C_4 grasses (Lee et al., 2022), a biphasic increase in assimilation during the low to high light transition was the most significant limitation in maize and big bluestem, again emphasizing the C_4 lag in CO_2 assimilation. However, both Li et al. (2021) and Lee et al. (2022) studies examined the efficiency of fully induced photosynthesis subsequently exposed to stepwise decreases and increases in light intensity, whereas the C_4 lag-time when activation starts from darkness or from prolonged periods of low light may be even more pronounced.

During darkness or low light periods, stomatal closure could subsequently restrict photosynthetic assimilation during light induction due to a lack of coordination between CO_2 influx and assimilation. However, g_{sw} appears to increase in tandem with decreases in C_i, so stomatal opening does not seem to be the major source of limitation (**Figure 2.3 C&F, I&L**). The lower g_{sw} found in C_4 species during light induction is consistent with studies that show C_4 species to have lower stomatal conductance and greater water use efficiency (McAusland et al., 2016, Way et al., 2014). It is worth noting that C_4 monocots under dynamic light have been reported to have faster stomatal opening and closing than C_3 monocots and dicots (Ozeki et al., 2022) yet stomatal kinetics in C_4 *A. semialata MDG* instead appear to be slower, again emphasizing the importance to account for species or genus-specific phenomena. However, although CO_2 availability can affect CO_2 assimilation during induction, other biochemical limitations appeared to dominate the responses observed here, as discussed in more detail below. The different C_4 decarboxylase pathways found across the three C_4 species studied have distinct energetic demands per cell type. The NADP-ME subtype found in C_4 *F. bidentis* and NAD-ME subtype in C_4 *G. gynandra* require substantial transfer of reductant between M and BS cells (Ishikawa et al., 2016) and steeper metabolite gradients for CCM operation, whilst mixed NADP-ME/PEPCK CCM found in C_4 *A. semialata MDG* can meet ATP and NADPH requirements more cell autonomously (Yin and Struik, 2021). Modelling simulations indicate that reduced metabolite concentrations may be required to sustain this C_4 pathway (Wang et al., 2014a). The greater cell autonomy regarding energetic supply and demand found in C_4 *A. semialata MDG* could suggest a capacity for faster activation of photosynthetic assimilation, yet in the light induction experiments CO_2 assimilation in C_4 *A. semialata MDG* lagged behind the other C_4 species during the first ten minutes after starting light exposure (**Figure 2.4 A&B**).

In the following paragraphs we explore the different mechanisms underlying the slow activation of C_4 photosynthesis across the three genera.

2.4.2. Photorespiration during C_4 photosynthetic induction, disadvantageous or beneficial?

Reduced CO_2 assimilation during induction in C_4 species has been hypothesised to derive from the need to build up C_4 cycle intermediates leading to a lag in the efficient suppression of photorespiration (Sage and McKown, 2006). If so, induction in C_4 species when the photorespiratory pathway is suppressed by low O_2 should result in an increase in photosynthetic carbon assimilation. This appeared to be confirmed in C4 *F. bidentis,* where CO_2 assimilation during induction was higher under 2% O_2 than under 21% O_2 (**Figure 2.4**), in contrast to CO_2 assimilation in C_4 *F. bidentis* under steady state which showed no difference in A_{CO2} between O_2 concentrations (**Figure 2.1 A&D, Table 2.1**). Comparatively, the lack of an equivalent improvement in CO_2 assimilation under 2% O_2 in C_4 *A. semialata GMT* and C_4 *G. gynandra* suggests that in these species the activation of the C_3 cycle (Mott and Woodrow, 2000, Sassenrath-Cole and Pearcy, 1992) could instead be the limiting factor.

Surprisingly, despite the stimulating effect of 2% O_2 on steady state CO_2 assimilation in C_3 *A. semialata GMT* and C_3 *T. hassleriana*, and lack of O_2 sensitivity in C_4 *A. semialata GMT* (**Figure 2.1 A&D**, **Table 2.1**), CO_2 assimilation in all three species during the first 10 min of light induction was lower in 2% O_2 than in 21% O_2 (**Figure 2.4 A&B**). Reverse sensitivity to O_2 in C_3 species has been linked to limitation by the rate of triose phosphate utilisation (TPU) (Sharkey, 1985). Low O_2 suppresses the net export of photorespiratory intermediates serine or glycine and limits endogenous pools of inorganic phosphate (P_i), as the amino acids come from phosphorylated plastidic metabolites that when used up in the cytosol liberate P_i otherwise used in the glycerate-PGA conversion (McClain and Sharkey, 2019). Additionally, reduced rates of starch biosynthesis from triose phosphates, and phosphoglucose isomerase inhibition have been found in low O_2 conditions (Dietz, 1985). The lower CO_2 assimilation observed in 2% O_2 compared to 21% O_2 during induction in C_3 *A. semialata GMT* and C_3 *T. hassleriana* could thus be due to 2% O_2 causing suboptimal stromal phosphate levels, thereby transiently exacerbating TPU limitation. It remains unclear whether C_4 species suffer from TPU limitation (Zhou et al., 2019), or whether alternative mechanisms may be involved.

The photorespiratory pathway has previously been suggested to help prime the C_4 cycle by providing a carbon source from which to build C_3 and C_4 metabolite pools (Fu and Walker, 2022, Kromdijk et al., 2014, Medeiros et al., 2022, Schlüter and Weber, 2020, Stitt and Zhu,

2014). In C_4 species, photorespiration could help establish CCM metabolic gradients through interconversion of 3-phosphoglyceric acid (3-PGA) and PEP (Arrivault et al., 2016), and in plants with NADP-ME decarboxylase, such as mixed subtype NADP-ME PEPCK C_4 *A. semialata GMT,* models suggest photorespiration could support the activation of redox-regulated C_3 enzymes and contribute to the formation of C_3 cycle intermediates in the BS through the triose phosphate transporter (TPT) (Wang et al., 2014b, Weber and von Caemmerer, 2010). In C_3 photosynthesis, beyond its photoprotective role (Kozaki and Takeba, 1996), photorespiration has been shown to enhance CO_2 fixation through the assimilation of nitrogen (Busch et al., 2018). A recent metabolomic analysis in maize suggested that photorespiratory intermediates may also provide this supporting role in C_4 species (Medeiros et al., 2022).

2.4.3. Decoupling between electron transport and photosynthesis: alternative electron sinks and BS leakiness

Particularly at the start of light induction, C_3 and C_4 species had significantly higher $\Phi PSII/\Phi CO_2$ ratios (**Figure 2.5**) than during steady state measurements (**Table 2.1**), indicating less of the reducing power of the electron transport chain was going towards photosynthetic carbon fixation. This was particularly prominent in the C_4 species, both in absolute values and relative to steady state, where C_4 plants had either lower (C_4 *Alloteropsis* and *Flaveria*) or equal (C_4 *Cleome*) $\Phi PSII/\Phi CO_2$ values compared to their C_3 counterparts. The build-up of metabolite pools to establish sufficient concentration gradients between M and BS cells required for the efficient operation of C_4 photosynthesis seems a likely contributing factor increasing $\Phi PSII/\Phi CO_2$ ratios in C_4 photosynthesis. However, the change in ratio could also be due to a variety of alternative electron sinks having greater presence during induction and drawing electrons away from the C_3 cycle.

Not surprisingly, reductions in $\Phi PSII/\Phi CO_2$ ratio under 2% O_2 were observed in all C_3 species as well as in C_4 *F. bidentis*, showing the importance of photorespiration as an electron sink. Although a gradual decrease in $\Phi PSII/\Phi CO_2$ across time was observed during induction in both *Alloteropsis* and *Cleome* C_4 species (**Figure 2.4**), in contrast to C_4 *F. bidentis* the temporal changes were not O_2 sensitive. An alternative electron sink to photorespiration could be the Mehler reaction, which reduces O_2 in the chloroplast to hydrogen peroxide and has been suggested to play a role in C_3 and C_4 photosynthesis (Sagun et al., 2021). Suppression of the Mehler reaction under 2% O_2 could be consistent with the small reductions in CO_2 assimilation observed in both *Alloteropsis* species and C3 *T. hassleriana*, as the Mehler reaction supports ATP formation and the activity of related enzymes has been found to increase when

photosynthesis is impaired (Fryer et al., 1998). However, evidence to support a significant contribution of the Mehler reaction to high rates of photosynthesis in both C_3 and C_4 species is generally lacking (Driever and Baker, 2011).

A transient increase in BS leakiness could be an alternative contributing factor to the elevated energetic cost of CO_2 assimilation during induction in C_4 *A. semialata* and C_4 *G. gynandra* that accounts for the lack of O_2 sensitivity. A lag in activation of the C_3 cycle following light exposure would result in an imbalance between the C_3 and C_4 cycles and greater leakage of CO_2 from the BS due to the CCM over-pumping, reducing quantum efficiency by requiring more ATP per CO_2 fixed (Kromdijk et al., 2014, Sage and McKown, 2006). Transient isotope discrimination measurements on sorghum and maize during the first 10 min following a step-increase in light intensity suggested that bundle sheath leakiness could be 60% higher than steady state (Kubásek et al., 2013, Wang et al., 2022) and remain elevated for up to 30 min. This seems consistent with the timing of the decrease in $\Phi PSII/\Phi CO_2$ during induction in the *Alloteropsis* and *Cleome* C_4 species. Thus, activation of CO_2 assimilation in these species may be limited by activation of the C_3 cycle, whereas the stable $\Phi PSII/\Phi CO_2$ values in C_4 *F. bidentis* under 2% O_2 suggest C_3 cycle activation is faster than the CCM in this species.

2.5. Conclusion

This chapter confirms C_4 photosynthesis experiences greater lag than C_3 photosynthesis during light induction – the greater depression of CO_2 assimilation in C_4 species was independently found in three evolutionary divergent comparisons of phylogenetically linked C_3 and C_4 species, providing experimental support for previous hypotheses and observations of less efficient photosynthetic induction in C_4 photosynthesis (Kubásek et al., 2013, Li et al., 2021, Sage and McKown, 2006, Sales et al., 2021, Slattery et al., 2018). Despite the generally slower induction of CO_2 assimilation found in all C_4 species in comparison to their C_3 pairs, the underlying mechanisms to explain these differences were distinctly different – less effective suppression of photorespiration seemed to underlie the reduction in CO_2 assimilation in C_4 *Flaveria* whereas delayed activation of the C_3 cycle appeared to be the limiting factor in C_4 species in *Alloteropsis* and *Cleome*, where a potential supporting role for photorespiration in photosynthetic induction was also identified. The substantial variation observed between and across phylogenetic pairs during both steady state and light induction measurements underscore

the crucial importance of controlling for evolutionary distance when studying differences between photosynthetic pathways.

2.6. Supplementary material

Supplementary table 2.1: Leaf absorptance values of phylogenetically linked C_3 and C_4 *Alloteropsis*, *Flaveria* and *Cleome* species from the blue (470 nm) and red (630 nm) wavelengths of the actinic light source used in Chapter 2 experiments (6400-40 Leaf Chamber Fluorometer, LI-COR), measured with an integrating sphere. Means and standard error of the mean are shown (n = 5).

Genus	Species	Abs_470	Abs_630
Alloteropsis	C3 *A. semialata GMT*	0.90±0.02	0.88±0.02
	C4 *A. semialata MDG*	0.87±0.02	0.81±0.02
Flaveria	C3 *F. cronquistii*	0.87±0.04	0.79±0.05
	C4 *F. bidentis*	0.94±0.00	0.89±0.01
Cleome	C3 *T. hassleriana*	0.94±0.00	0.88±0.01
	C4 *G. gynandra*	0.85±0.03	0.78±0.03

3. Evaluating C_4 photosynthetic efficiency under fluctuating light

This chapter has been published as Arce Cubas et al. (2023a).

3.1. Introduction

Plants exhibiting C_4 photosynthesis are mostly found in warm, high light environments (Sage, 2000). Although these environments have high light intensity at the top of the canopy, the light conditions experienced by leaves within the canopy can be extremely dynamic. Indeed, sun angle and cloud cover can alter light intensity by orders of magnitude on a second to minute scale, and shading by higher leaves can further modify the temporal fluctuations experienced by individual leaves. Several C_4 species form dense canopies with extensive self-shading where sunflecks can provide up to 90% of the energy for photochemistry (Pearcy, 1990, Slattery et al., 2018, Tang et al., 1988, Way and Pearcy, 2012, Zhu et al., 2004). Since photosynthetic responses to changes in light are not instantaneous, fluctuating light has been identified as an area of improvement for crop productivity (Acevedo-Siaca et al., 2020, Kaiser et al., 2018, Kromdijk et al., 2016, Lawson et al., 2012, Long et al., 2006, Pearcy, 1990, Taylor and Long, 2017). Although recent studies have begun to characterise the C_4 response (Kubásek et al., 2013, Lee et al., 2022, Li et al., 2021, Pignon et al., 2021), most of our understanding of the limitations of photosynthesis under fluctuating light still comes from C_3 species (Kaiser et al., 2018, Pearcy, 1990, Pearcy et al., 1997). Despite the undeniable global importance of C_4 crops, with maize (*Zea mays*) and sugarcane (*Saccharum officinarum*) alone accounting for over 30% of global agricultural production (FAO, 2020), the impact of the CO_2 concentrating C_4 acid shuttle on photosynthetic performance in dynamic light remains understudied (Sales et al., 2021, Slattery et al., 2018)

C_4 photosynthesis is a remarkably ubiquitous adaptation that has evolved independently at least 66 times in angiosperms (Kellogg, 2013) and typically leads to faster photosynthetic rates, higher yields, and greater water use efficiency than the ancestral C_3 pathway (Kiniry et al., 1989, Sage, 2004). Most C_4 species operate their carbon concentrating mechanism (CCM) by compartmentalising initial carbon fixation and assimilation between the morphologically distinct mesophyll (M) and bundle sheath (BS) cells, arranged concentrically around the leaf vasculature in 'Kranz' anatomy. In the cytosol of M cells, CO_2 is rapidly converted to

bicarbonate by carbonic anhydrase and fixed by phosphoenolpyruvate carboxylase (PEPC) into a 4-carbon oxaloacetate molecule that is further reduced into more stable metabolites malate or aspartate for transport into the BS. The 4-carbon molecules are decarboxylated in the BS to concentrate CO_2 around the carbon-fixing enzyme ribulose 1,5-biphosphate carboxylase/oxygenase (Rubisco) and thus enhance photosynthesis by suppressing Rubisco's alternative oxygenation reaction and resulting photorespiration, which consumes energy and reducing equivalents and re-releases CO_2 (Leegood, 2002). Reduced carbon in the form of alanine (Ala) or pyruvate is then transported back to the M cells, where phosphoenolpyruvate (PEP) is regenerated at the cost of ATP, imposing an additional cost to C_4 metabolism. The specific transport metabolites and enzymes of the C_4 pathway vary, and whilst species have been traditionally classified based on predominant decarboxylases nicotinamide adenine dinucleotide-malic enzyme (NAD-ME), nicotinamide adenine dinucleotide phosphate-malic enzyme (NADP-ME), and phosphoenolpyruvate carboxykinase (PEPCK) (Hatch et al., 1975), there is a growing consensus that different decarboxylating enzymes often operate in conjunction, with PEPCK likely acting predominantly as a supplementary pathway (Calsa and Figueira, 2007, Furbank, 2011, Pick et al., 2013, Sales et al., 2018). Crucially, intercellular transport of C_4 intermediates is driven by diffusion, making the establishment of high metabolic gradients a requirement for the operation of the CCM (Arrivault et al., 2017, Leegood and Furbank, 1984, Lilley et al., 1977, Stitt et al., 1985), although model simulations suggest mixed C_4 pathways could be less reliant on large metabolite pools (Wang et al., 2014a).

Studies conducted on C_3 species show that photosynthetic response to fluctuating light is restricted by several factors: slow stomatal opening reduces CO_2 diffusive transfer into the leaf and slow stomatal closing decreases water use efficiency (McAusland et al., 2016), Rubisco activation and the regeneration of ribulose-1,5-biphosphate (RuBP) delay C_3 cycle activity (Mott and Woodrow, 2000, Pearcy and Seemann, 1990, Sassenrath-Cole and Pearcy, 1992), and the speed of up- and down-regulation of photoprotection lowers light use efficiency (Niu et al., 2022, Zhu et al., 2004). Although said limitations exist irrespective of photosynthetic pathway, C_4 species have the additional challenge of coordinating the C_3 and C_4 cycles (Kromdijk et al., 2014), and the specifics of the C_4 response to fluctuating light are not yet fully understood (Kaiser et al., 2018, Slattery et al., 2018). Two apparently contradictory hypotheses can be found in the literature – where C_4 photosynthesis is suggested to be either less (Kubásek

et al., 2013), or more efficient (Stitt and Zhu, 2014) under fluctuating light than the ancestral C_3 form.

The first hypothesis suggests that C_4 species are more negatively impacted by sudden changes in light intensity due to the C_3 and C_4 cycles temporarily operating asynchronously (Sage and McKown, 2006). Fluctuations in light could disrupt the build-up of metabolic gradients necessary for the effective operation of the CCM, leading to impaired suppression of photorespiration and reduced photosynthetic efficiency (Kromdijk et al., 2010, Slattery et al., 2018). Alternatively, if the CCM is faster to activate during light induction than the C_3 cycle there could be transient over-pumping of CO_2 and an increase in BS leakiness – where CO_2 diffuses out of BS cells back into M cells, raising the energetic cost of carbon fixation due to the futile cycling of PEP. Greater BS leakiness during induction relative to steady state has been previously observed in maize and sorghum (*Sorghum bicolor*) (Wang et al., 2022). Lags in CCM deactivation during transitions to lower light could also increase leakiness and reduce quantum yields if malate/aspartate accumulated in the BS is decarboxylated despite insufficient C_3 cycle activity. In further support for the "negative effect" hypothesis, previous studies have found assimilation rates under fluctuating light relative to steady state to be almost four times lower in C_4 compared to C_3 species due to slower photosynthetic induction (Li et al., 2021), as well as a more pronounced reduction of biomass in C_4 than C_3 plants grown under fluctuating compared to steady light conditions (Kubásek et al., 2013).

The second hypothesis instead posits that C_4 species are better able to buffer against sudden changes in light intensity because the large metabolite pools required to drive the CCM can store and release ATP and reducing equivalents (Stitt and Zhu, 2014). The reversible reactions linking the exchange of 3-phosphoglyceric acid (3-PGA) and triose phosphates (TP) between M and BS cells could provide or consume ATP and NADPH to support the C_3 cycle (Leegood and von Caemmerer, 1989); and mixed C_4 pathways could transiently enhance Mal over Asp decarboxylation to temporarily increase transport of redox equivalents into the BS (Wang et al., 2014a). In favour of the "positive effect" hypothesis, some of the highest post-illumination CO_2 fixation rates have been found in C_4 species (Laisk and Edwards, 1997), and a recent study on grasses recorded higher rates of carbon assimilation in C_4 over C_3 species under fluctuating light due to slower decreases in photosynthetic capacity during high-to-low light transitions compared to steady state values (Lee et al., 2022).

Although seemingly opposing, there are indications that both hypotheses may coexist. Features of C_4 biochemistry could have mixed effects – the need to establish large metabolite pools could slow photosynthetic induction but enable higher rates of assimilation upon transitioning to a lower light intensity. Slattery et al. (2018) estimated the buffering capacity of C_4 photosynthesis to be limited to 10-15 seconds based on maize metabolite pool sampling (Arrivault et al., 2017) and suggested that the specific C_4 response could thus depend on the length of light fluctuations. A time-sensitive response could account for the different responses observed between sunflecks (Laisk and Edwards, 1997) and longer fluctuations (Kubásek et al., 2013, Li et al., 2021). However, the different light treatments and species used across studies makes it difficult to draw clear conclusions. This is further complicated by C_4 subtype-specific responses like the post-illumination CO_2 burst observed in NAD-ME species (Krall and Pearcy, 1993, Lee et al., 2022), as well as phylogenetic distance, which can strongly confound comparisons between photosynthetic pathways (Taylor et al., 2010), leading to the inappropriate association of species-specific phenomena with the presence or absence of the C_4 pathway.

In this chapter, we compared the photosynthetic response to fluctuating light in relation to steady state across three phylogenetically linked pairs of C_3 and C_4 species from *Alloteropsis* (C_3 *Alloteropsis semialata GMT* & C_4 *Alloteropsis semialata MDG*), *Flaveria* (C_3 *Flaveria cronquistii* & C_4 *Flaveria bidentis*), and *Cleome* (C_3 *Tarenaya hassleriana* & C_4 *Gynandropsis gynandra*) genera representative of monocots and dicots, and of all three C_4 decarboxylase subgroups. Leaves were subjected to a 1-hour fluctuating light treatment consisting of repetitive stepwise changes in light intensity from 800 to 100 µmol m^{-2} s^{-1} photon flux density (PFD), with three different times between fluctuations being tested: 6, 30, and 300 seconds. To evaluate the impact of photorespiration on the responses to fluctuating light, experiments were conducted under both 2% and 21% oxygen concentration. We hypothesised that 1) after a transition to low light, C_4 species will be better able to sustain photosynthetic rates than C_3 species, even when photorespiration is suppressed, 2) C_4 species will incur a higher penalty during transitions to high light; and 3) the impact of both effects will be inversely associated with fluctuation length.

3.2. Materials and methods

3.2.1. Plant materials

To control for evolutionary distance, three pairs of phylogenetically linked *Alloteropsis*, *Flaveria*, and *Cleome* C_3 and C_4 species (shown in **Table 1.1. Figure 1.1**) were selected. Substantial evolutionary distance exists between the selected genera and C_4 photosynthesis evolved independently in each. The C_4 origin dates back approximately 17 million years (Ma) in *Cleome*, ~ 2 Ma in *Flaveria*, and is even more recent in *Alloteropsis* (Christin et al., 2011, Lundgren et al., 2015). In addition, the selected species include both monocots (*Alloteropsis*) and dicots (*Flaveria* and *Cleome*), and all three major decarboxylase enzymes of the C_4 pathway: NADP-ME/PEPCK (C_4 *Alloteropsis semialata MDG*), NAD-ME (C_4 *Flaveria bidentis*), and NAD-ME (C_4 *Gynandropsis gynandra*) (Bräutigam et al., 2008, Gowik et al., 2011, Ueno and Sentoku, 2006).

3.2.2. Plant growth and propagation

Flaveria and *Cleome* species were grown in a Conviron walk-in growth room (Conviron Ltd., Winnipeg, MB, CA) at 20 ºC, 60% relative humidity (RH), and 150 µmol m^{-2} s^{-1} PFD over a 16-hour photoperiod; and the *Alloteropsis* accessions in a glasshouse in Cambridge, England, at 18-25 ºC, 40-60% RH, with supplemental lightning to provide a minimum of 140-160 µmol m^{-2} s^{-1} PFD over a 16-hour photoperiod in addition to incoming irradiance. All plants were well-watered and grown in Levington Advance M3 compost (Scotts, Ipswich, UK) mixed with Miracle-Gro All Purpose Continuous Release Osmocote (Scotts Miracle-Gro Company, Marysville, OH, USA; 4 L compost : 25 g Osmocote), with vermiculite being added to the *Alloteropsis* soil mix to prevent waterlogging (1 L vermiculite : 4 L compost : 25 g Osmocote).

Alloteropsis and *Flaveria* species were vegetatively propagated whilst *Cleome* species were grown from seed. *Alloteropsis* MDG and GMT accession tillers were grown in 2 L pots and all gas exchange measurements taken after 2 weeks. For *Flaveria* propagation, lateral shoot cuttings were dipped in Doff Hormone Rooting Powder (Doff Portland Ltd., Hucknall, UK) to induce root development, grown on 0.25 L pots, and measured after 8-10 weeks. *Flaveria cronquistii* requires vegetative propagation, so *F. bidentis* plants were first grown from seed and subsequently propagated via cuttings. *Cleome* germination was induced with a 30 ºC/20 ºC day/night cycle for *Tarenaya hassleriana*, and at 30 ºC for *G. gynandra*. The germinated seeds were sown in 24-cell trays before transfer to 0.25 L pots. Due to the different developmental rates of the *Cleome* species, germination was staggered so both species could

be measured at approximately the same developmental stage, after 8-10 weeks for *G. gynandra* and 4-6 weeks for *T. hassleriana*. All plants were measured during vegetative state.

3.2.3. Gas exchange measurements at 21% and 2% O_2

Gas exchange under steady and fluctuating light conditions was measured on young, fully expanded leaves using an open gas exchange system (LI-6800, LI-COR, Lincoln, NE, USA) with a Multiphase Flash Fluorometer (MPF) chamber (6800-01A, LI-COR). Chamber conditions were controlled at 410 ppm sample CO_2 concentration, 60% relative humidity with average leaf VPD of 1.3 ± 0.1 kPa, 25 ºC heat exchanger temperature, and flow rate of 600 µmol s^{-1}. Actinic light was provided by the MPF and composed of 90% red (625 nm) and 10% blue light (475 nm).

For experiments in 2% O_2, a pre-mixed 2% O_2 and 98% N_2 gas mixture (BOC Ltd., Woking, UK) was supplied to the LI-6800 through the air inlet using a mass flow controller (EL-FLOW, Bronkhorst Hight-tech BV, Ruurlo, NL) and an open T-junction to regulate constant surplus flow according to manufacturer instructions. The LI-6800 Infrared Gas Analyser (IRGA) calibration was adjusted to the O_2 concentration in the instrument constants prior to measurement.

3.2.4. Steady state light response curves

Photosynthetic responses to steady light were measured for all species at both 21% and 2% O_2. Leaves were illuminated with 1000 µmol m^{-2} s^{-1} PFD for 20-40 minutes to allow CO_2 assimilation and stomatal conductance to reach steady state, and gas exchange was subsequently measured in a descending gradient of light intensity: 2000, 1700, 1500, 1200, 1000, 800, 600, 400, 300, 200, 100, 75, 30 and 0 µmol m^{-2} s^{-1} PFD. Gas exchange parameters were logged between 120 – 240 seconds at a given light intensity, when leaf intracellular CO_2 concentration (C_i) and CO_2 assimilation (A_{CO2}) were stable.

Respiration in the light (*Rd*) was estimated from the y-intercept of a linear regression of the slope before the inflection point. Measurements at 0 and 30 µmol m^{-2} s^{-1} PFD were not included in the regression to account for the Kok effect (Kok, 1949). Photosynthetic rates and C_i at 100 and 800 µmol m^{-2} s^{-1} PFD were taken as the steady state values for comparison with fluctuating light measurements. The quantum yield of CO_2 assimilation (ΦCO_2) was calculated from net CO_2 assimilation (A_{CO2}), absorbed PFD (PFD_{abs}) and *Rd* using **Equation 1A**.

3.2.5. Fluctuating light experiments, correction for dynamic conditions, and analysis

To measure photosynthetic responses to fluctuating light, leaves were first acclimated at 150 µmol m^{-2} s^{-1} PFD, the minimum growth light intensity of all species, for 30-60 minutes until stomatal conductance and photosynthetic rates reached constant levels. Using a custom program, leaves were then exposed to repetitive stepwise fluctuations in light intensity from 800 to 100 µmol m^{-2} s^{-1} PFD for 1 hour, with gas exchange parameters recorded every 2 seconds. Three different light treatments were tested, with each light step lasting 6, 30, or 300 seconds. To avoid interference with the shorter fluctuations and the data sampling interval, the averaging time of the LI-6800 logging was kept minimal (averaging time was set to 0), meaning that each log should represent an average of the preceding 0.5 s, the inverse of the instrument digital update frequency of 2 Hz. The IRGAs were only matched prior to the program starting. Experiments were conducted at both 21% and 2% O_2 and the light treatments and oxygen concentration were randomised within each phylogenetic pair.

As measurements during light fluctuations violate the steady state assumption underlying default rate equations, a storage flux correction was applied that follows the same principle as the dynamic assimilation technique previously developed for fast CO_2 and light response curves (Saathoff and Welles, 2021). Saathoff and Welles (2021) show that based on mass balance of the instrument cuvette, the derivative of the cuvette concentration over time can be used to adjust carbon assimilation and transpiration rates. Accordingly, here **Equation 2A and 2B** were used to compute derivatives from the time-series data and adjust the steady state *E* and A_{CO2} rates– and other instrument calculations derived from these.

$$Storage\ flux_{H2O} = \frac{\frac{PV}{RT} x \Delta H_2O}{S\ x\ t} \quad \textbf{Equation 2A}$$

$$Storage\ flux_{CO2} = \frac{-\frac{PV}{RT} x \Delta CO_2}{S\ x\ t} \quad \textbf{Equation 2B}$$

The equations use the ideal gas law, where *P* represents pressure (Pa, from instrument recordings), *V* represents cuvette volume (8.67e^{-5} m^3), *R* represents the molar gas constant, and *T* represents temperature to calculate the change in moles of gas of CO_2 or H_2O using instrument recordings of current and previous gas concentration. *S* represents leaf area (m^{-2}) and *t* represents time since last log (s) and are used to convert the molar concentrations to flux per area. The signum reconciles CO_2 flux with scientific convention for assimilation.

3.2.6. Leaf absorptance

After gas exchange measurements, the spectral qualities of the leaves were measured with an integrating sphere (LI-1800-12, LI-COR) optically connected to a miniature spectrometer (STS-VIS, Ocean Insight, Orlando, FL, USA) following manufacturer instructions (LI-COR, 1988). Leaf absorptance (L_{abs}) was calculated using **Equation 1B**, where T_s and R_s are transmittance and reflectance of a diffuse sample. For the light response curves, incident PFD was converted to absorbed PFD using L_{abs} of the red and blue emission wavelengths of the 6800-01A MPF light source. For the specific absorptance values, see **Supplementary table 3.1**.

3.2.7. Data processing

Data from the last 10 minutes of the fluctuating light treatment were used for analysis to ensure the effects observed were due to fluctuations and not induction, which was apparent during the first 30 min of the timeseries (**Supplementary figure 3.1**). To analyse the relative performance of each species, net photosynthesis (A_{CO2}) under fluctuating light was expressed as a percentage of the steady state rates achieved at the corresponding light intensity. Additionally, ΦCO_2 under fluctuating light was calculated using **Equation 1A**.

The area under the curve (AUC) (Makowski et al., 2019) of A_{CO2} relative to steady state and ΦCO2 during the 100 and 800 µmol m^{-2} s^{-1} PFD periods of the light treatment was integrated using the trapezoidal rule (Jawień, 2014) and divided by the duration to obtain an average value for each light level which was used to compare between fluctuations of different length and, in the case of Φ_{CO2}, directly to steady state values. To compare differences in PIB between 21% and 2% oxygen, the analysis of A_{CO2} relative to steady state was also performed specifically during the time of the 100 µmol m^{-2} s^{-1} PFD periods where the PIB was evident: 10-30 s in the 30 s fluctuations, and 10-70 s in the 300 s fluctuations. The PIB was not observed during the initial 10 s, hence the 6 s fluctuations were not included for this analysis.

3.2.8. Statistical analysis

Each phylogenetically controlled comparison was run as an independent experiment, thus statistical analyses were conducted separately on paired *Alloteropsis*, *Flaveria,* and *Cleome* light response curves (*800* A_{CO2}, *100* A_{CO2}, $C_{i\ 800}$, $C_{i\ 100}$, *800* ΦCO_2, *100* ΦCO_2, *Rd*), and fluctuating light measurements (A_{CO2} relative to steady state, ΦCO_2). Two-way ANOVA was used to test for the effects of photosynthetic pathway, oxygen concentration, and their interactions on steady state photosynthesis parameters; and three-way ANOVA to test for the

effects of photosynthetic pathway, fluctuation length, oxygen concentration, and their interactions on A_{CO2} relative to steady state and ΦCO_2. Specifically for the ΦCO_2 analysis, the quantum yields obtained under steady state at 800 and 100 µmol m^{-2} s^{-1} PFD were included in the dataset as an additional fluctuation length. For each ANOVA, assumptions of normality, homogeneity of variance and sphericity were satisfied. Mean and standard error of the mean for steady state photosynthesis parameters, A_{CO2} relative to steady state, and ΦCO_2 across the light fluctuation regimes were calculated for reporting.

All data analysis and plot generation was done with R 4.1.1 (R Core Team, 2021) on RStudio 2022.12.0+353 (Posit Team, 2022) using the tidyverse (Wickham et al., 2019), RColorBrewer (Neuwirth, 2014), lme4 (Bates et al., 2015) , and bayestestR libraries (Makowski et al., 2019).

3.3. Results

3.3.1. Steady state responses of CO_2 assimilation in paired C_3 and C_4 species are consistent with well-established differences between photosynthetic pathways.

To provide a baseline for comparing CO_2 assimilation rates between three pairs of closely related C_3 and C_4 species under fluctuating light, first the steady state light response of photosynthetic gas exchange was measured under 21% and 2% O_2 to minimize photorespiration (**Figure 3.1**). We focus here on photosynthetic parameters at the light intensities that were used in subsequent fluctuating light treatments, 800 and 100 µmol m^{-2} s^{-1} PFD (**Table 3.1**). Two-way ANOVA was used to assess the effects of photosynthetic pathway, oxygen concentration, and their interactions within each genus (**Table 3.2**). At both light intensities C_3 species trended towards higher assimilation values and quantum yields under photorespiration-suppressing conditions than C_4 species.

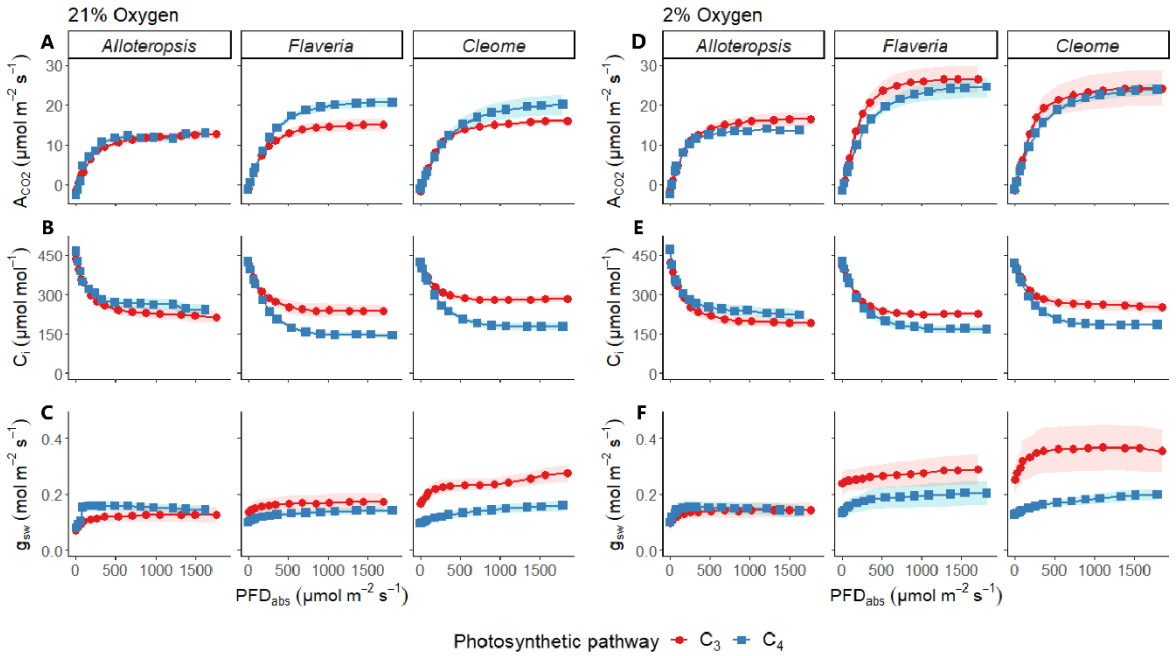

Figure 3.1: Light response curves of phylogenetically linked C_3 and C_4 *Alloteropsis*, *Flaveria* and *Cleome* species at 21% and 2% O_2. As a function of absorbed light intensity, plots show net CO_2 assimilation (A_{CO2}, **A, D**), intercellular CO_2 concentration (C_i, **B, E**), and stomatal conductance to water vapour (g_{sw}, **C, F**). Ribbons represent standard error of the mean (n=5).

At 800 µmol m^{-2} s^{-1} PFD, net CO_2 assimilation (A_{CO2}) values in C_4 *A. semialata MDG* (12.3 ± 0.5 µmol m^{-2} s^{-1}), C_4 *F. bidentis* (18.7 ± 1.0 µmol m^{-2} s^{-1}), and C_4 *G. gynandra* (23.5 ± 2.0 µmol m^{-2} s^{-1}) were respectively higher than phylogenetic pairs C_3 *A. semialata GMT* (11.3 ± 0.9 µmol m^{-2} s^{-1}), C_3 *F. cronquistii* (13.8 ± 1.4 µmol m^{-2} s^{-1}), and C_3 *T. hassleriana* (14.6 ± 0.5 µmol m^{-2} s^{-1}). Under 2% oxygen, photosynthetic rates increased by 33% in C_3 *A. semialata GMT*, 81% in C_3 *F. cronquistii,* and 86% in C_3 *T. hassleriana*, compared to a more modest increase of 6%, 15% and 16% in their respective C_4 pairs. Nevertheless, the effect of O_2 at 800 µmol m^{-2} s^{-1} PFD on A_{CO2} as well as on quantum yield of CO_2 assimilation (ΦCO_2) was significant across all three genera ($p \leq 0.02$, **Table 3.2**).

Table 3.1: Photosynthetic parameters estimated from steady state light response curves under 21% and 2% O_2 on phylogenetically linked C_3 and C_4 *Alloteropsis*, *Flaveria* and *Cleome* species. Respiration in the light (*Rd*) was calculated by fitting the light response curves with a non-rectangular hyperbola. Values for *800* A_{CO2}, *100* A_{CO2}, $C_{i\,800}$, $C_{i\,100}$, *800* ΦCO_2, and *100* ΦCO_2 were taken at PFD = 800 µmol m^{-2} s^{-1} and PFD = 100 µmol m^{-2} s^{-1}. Means and standard error of the mean are shown (n = 5).

		21% Oxygen		2% Oxygen	
Genus	**Parameter**	**C_3**	**C_4**	**C_3**	**C_4**
Alloteropsis	*800* A_{CO2} (µmol m^{-2} s^{-1})	11.3 ± 0.9	12.3 ± 0.5	15.0 ± 1.2	13.1 ± 0.1
	100 A_{CO2} (µmol m^{-2} s^{-1})	3.2 ± 0.5	4.7 ± 0.5	4.8 ± 0.7	4.7 ± 0.7
	$C_{i\,800}$ (µmol mol^{-1})	235 ± 20	265 ± 15	207 ± 21	245 ± 20
	$C_{i\,100}$ (µmol mol^{-1})	348 ± 9	349 ± 2	334 ± 9	345 ± 2
	800 ΦCO_2	0.017 ± 0.003	0.021 ± 0.002	0.025 ± 0.006	0.022 ± 0.00
	100 ΦCO_2	0.047 ± 0.012	0.075 ± 0.014	0.065 ± 0.005	0.076 ± 0.018
	Rd	0.6 ± 0.1	1.7 ± 0.3	1.5 ± 0.3	1.5 ± 0.1
Flaveria	*800* A_{CO2} (µmol m^{-2} s^{-1})	13.8 ± 1.4	18.7 ± 1.0	25.0 ± 2.9	21.5 ± 1.7
	100 A_{CO2} (µmol m^{-2} s^{-1})	3.9 ± 0.2	4.2 ± 0.3	6.6 ± 0.3	4.7 ± 0.4
	$C_{i\,800}$ (µmol mol^{-1})	246 ± 25	157 ± 8	230 ± 8	182 ± 18
	$C_{i\,100}$ (µmol mol^{-1})	352 ± 6	339 ± 4	351 ± 5	343 ± 9
	800 ΦCO_2	0.022 ± 0.004	0.027 ± 0.00	0.038 ± 0.01	0.030 ± 0.005
	100 ΦCO_2	0.057 ± 0.005	0.057 ± 0.007	0.085 ± 0.01	0.056 ± 0.009
	Rd	0.4 ± 0.4	0.8 ± 0.3	0.6 ± 0.2	0.4 ± 0.2
Cleome	*800* A_{CO2} (µmol m^{-2} s^{-1})	14.6 ± 0.5	23.5 ± 2.0	27.3 ± 4.0	27.4 ± 0.9
	100 A_{CO2} (µmol m^{-2} s^{-1})	4.1 ± 0.2	3.2 ± 0.4	6.2 ± 0.6	4.7 ± 0.5
	$C_{i\,800}$ (µmol mol^{-1})	281 ± 14	190 ± 12	266 ± 21	192 ± 9
	$C_{i\,100}$ (µmol mol^{-1})	363 ± 7	352 ± 3	358 ± 18	344 ± 7
	800 ΦCO_2	0.020 ± 0.001	0.026 ± 0.006	0.033 ± 0.012	0.030 ± 0.003
	100 ΦCO_2	0.048 ± 0.004	0.056 ± 0.011	0.090 ± 0.016	0.061 ± 0.012
	Rd	1.5 ± 1.0	1.2 ± 0.4	2.1 ± 0.7	0.8 ± 0.5

Table 3.2: ANOVA table of light response curve parameters at 100 and 800 µmol m^{-2} s^{-1} PFD for phylogenetically linked C_3 and C_4 *Alloteropsis*, *Flaveria* and *Cleome* species. Photosynthetic pathway, PP. O_2 concentration, [O_2]. Interaction effect, PP:[O_2]. Table shows degrees of freedom; *F*-value; and *p*-value. Significant *p*-values ($a < 0.05$) are shown in bold.

	Alloteropsis			***Flaveria***			***Cleome***		
Parameter	**PP**	**[O_2]**	**PP:[O_2]**	**PP**	**[O_2]**	**PP:[O_2]**	**PP**	**[O_2]**	**PP:[O_2]**
800 A_{CO2}	1,16; 0.35; 0.56	1,16; 7.77; **0.01**	1,16; 3.24; 0.09	1,16; 0.12; 0.73	1,16; 13.48; **0.01**	1,16; 4.83; **0.04**	1,15; 0.01; 0.91	1,15; 6.18; **0.02**	1,15; 0.82; 0.28
100 A_{CO2}	1,16; 1.21; 0.29	1,16; 1.60; 0.22	1,16; 1.56; 0.23	1,16; 7.01; **0.02**	1,16; 25.64; **≤0.001**	1,16; 11.38; **0.01**	1,15; 7.28; **0.02**	1,15; 15,06; **0.01**	1,15; 0.43; 0.52
$C_{i\,800}$	1,16; 3.21; 0.09	1,16; 1.62; 0.22	1,16; 0.05; 0.83	1,16; 17.63; **≤0.001**	1,16; 0.09; 0.76	1,16; 1.63; 0.22	1,16; 31.44; **≤0.001**	1,16; 0.19; 0.66	1,16; 1.33; 0.58
$C_{i\,100}$	1,16; 0.87; 0.36	1,16; 1.96; 0.40	1,16; 0.74; 0.40	1,16; 2.52; 0.13	1,16; 0.11; 0.75	1,16; 0.16; 0.70	1,16; 3.65; 0.07	1,16; 1.01; 0.33	1,16; 0.04; 0.84
800 ΦCO_2	1,16; 0.22; 0.07	1,16; 8.12; **0.01**	1,16; 4.47; **0.05**	1,16; 0.13; 0.72	1,16; 11.90; **0.01**	1,16; 5.95; **0.03**	1,16; 0.19; 0.67	1,16; 6.96; **0.02**	1,16; 2.18; 0.15
100 ΦCO_2	1,16; 11.03; **0.01**	1,16; 2.67; 0.12	1,16; 2.04; 0.17	1,16; 15.56; **0.01**	1,16; 13.93; **0.01**	1,16; 16.53; **≤0.001**	1,16; 4.50; **0.05**	1,16; 21.01; **≤0.001**	1,16; 12.72; **0.01**

At 100 µmol m^{-2} s^{-1} PFD, the effects of photosynthetic pathway, O_2 concentration and their interaction on A_{CO2} varied between genera. In *Alloteropsis,* none of the effects were significant, although C_4 *A. semialata MDG* (4.7 ± 0.5 µmol m^{-2} s^{-1}) showed slightly higher A_{CO2} values than C_3 *A. semialata GMT* (3.2 ± 0.5 µmol m^{-2} s^{-1}) under ambient O_2. In *Flaveria,* values of A_{CO2} were similar under ambient O_2 in C_4 *F. bidentis* (4.2 ± 0.3 µmol m^{-2} s^{-1}), and C_3 *F. cronquistii* (3.9 ± 0.2 µmol m^{-2} s^{-1}), but significantly higher in C_3 *F. cronquistii* under 2% O_2 (4.7 ± 0.4 vs 6.6 ± 0.3 µmol m^{-2} s^{-1}, respectively, **Table 3.2**). As a result, both the main effects of O_2 and photosynthetic pathway as well as their interaction on both A_{CO2} and ΦCO_2 were significant in *Flaveria* ($p \leq 0.02$). In *Cleome*, A_{CO2} under 21% O_2 was lower in C_4 *G. gynandra* (3.2 ± 0.4 µmol m^{-2} s^{-1}) than in C_3 *T. hassleriana* (4.1 ± 0.2 µmol m^{-2} s^{-1}) and both rates increased under 2% O_2 (4.7 ± 0.5 and 6.2 ± 0.6 µmol m^{-2} s^{-1}, respectively), resulting in significant effects of both photosynthetic pathway and O_2 concentration ($p \leq 0.02$, **Table 3.2**).

3.3.2. CO_2 assimilation under fluctuating light differs between genera and is significantly affected by fluctuation frequency, photosynthetic pathway, and oxygen concentration

After characterising steady state light responses, CO_2 assimilation rates were measured in response to three different 1-hour fluctuating light treatments. Each treatment consisted of acclimation at 150 µmol m^{-2} s^{-1} PFD, followed by repetitive stepwise changes between 800 and 100 µmol m^{-2} s^{-1} PFD where each light step lasted 6, 30, or 300 seconds. Data from minutes 50-60 of each treatment (**Figure 3.2**) were used for analysis to exclude the effect of initial induction (for the complete timeseries see **Supplementary figure 3.1**). Since dynamic measurements violate the steady state assumption underlying default rate equations, a dynamic correction was applied using principles of mass balance recently outlined by (Saathoff and Welles, 2021). The fluctuating light response generally consisted of a rise in A_{CO2} towards steady state in the 800 µmol m^{-2} s^{-1} PFD period, and a subsequent decrease during the 100 µmol m^{-2} s^{-1} PFD period. A_{CO2} was strongly increased under 2% O_2 in the C_3 species, but much less so in the C_4 species. More subtle patterns varied by photosynthetic type, fluctuation length, and between genera as described below.

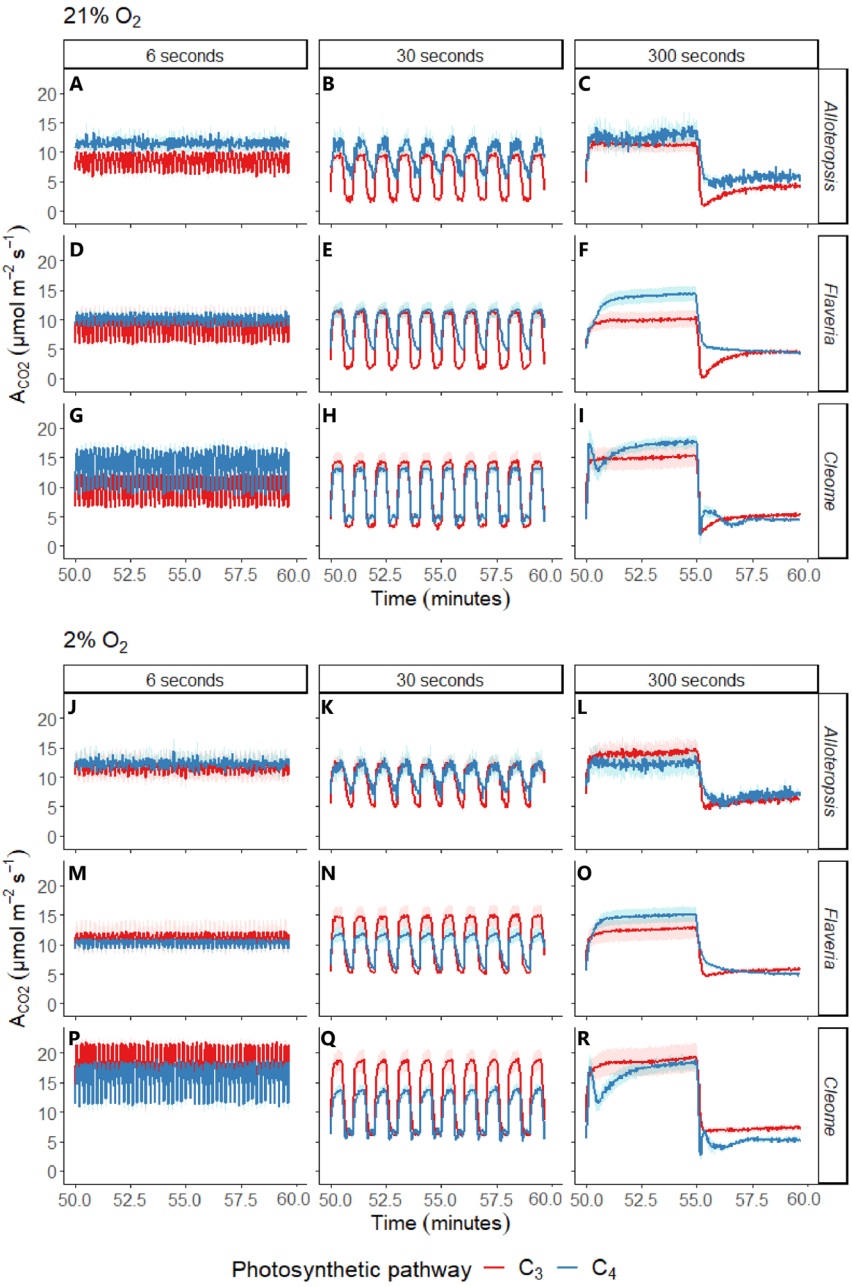

Figure 3.2: Net CO_2 assimilation (A_{CO2}) in phylogenetically linked C_3 and C_4 *Alloteropsis*, *Flaveria* and *Cleome* species under three different fluctuating light regimes at 21% and 2% O_2. Each light regime consisted of alternating 800 and 100 µmol m^{-2} s^{-1} PFD periods, where each light step lasted 6, 30, or 300 seconds before changing. Treatments were started after leaves were acclimated at 150 µmol m^{-2} s^{-1} PFD and lasted 1 hour, data was analysed from minutes 50-60 of each treatment. Ribbons represent standard error of the mean (n=5). The full timeseries is shown in **Supplementary figure 3.1**.

After transitioning from 800 to 100 µmol m^{-2} s^{-1} PFD, photosynthetic assimilation in C_4 *A. semialata MDG* and C_4 *F. bidentis* decreased more gradually compared to the immediate drop followed by a rise towards steady state observed in C_3 *A. semialata GMT,* C_3 *F. cronquistii* and C_3 *T. hassleriana*. This drop in assimilation in the C_3 species, known as the post-illumination

CO_2 burst (PIB), has previously been associated with photorespiration (Forrester et al., 1966, Wynn et al., 1973) and indeed was suppressed in all C_3 species under 2% oxygen (most easily seen in **Figure 3.2 C/F/I** compared to **Figure 3.2 L/O/R)**. The slower decrease of A_{CO2} in C_4 *A. semialata MDG* and C_4 *F. bidentis* was evident under 30 s (**Figure 3.2 B/E**) and 300 s light steps (**Figure 3.2 C/F**) in both oxygen concentrations, whilst under 6 s light steps (**Figure 3.2 A/D**) A_{CO2} at 100 µmol m^{-2} s^{-1} stayed closer to rates obtained during the 800 µmol m^{-2} s^{-1} PFD periods, suggesting a less substantial initial decline. Irrespective of oxygen concentration and unlike the delayed decrease observed in the other C_4 species, in C_4 *G. gynandra* an initial dip in A_{CO2} was observed immediately following the transition to low light (**Figure 3.2 I/R**).

Following the transition from 100 to 800 µmol m^{-2} s^{-1} PFD, induction patterns strongly varied between the three C_4 species, in contrast with the more consistent patterns observed in C_3 species. C_4 *F. bidentis* and C_4 *G. gynandra* had higher A_{CO2} during the 300 s light steps than C_3 *F. bidentis* and C_3 *T. hassleriana* (**Figure 3.2 C/F**), but similar or lower A_{CO2} than their C_3 counterparts during the 30 s light step (**Figure 3.2 B/E**) even under 21% oxygen, suggesting a comparatively greater lag in photosynthetic induction. However, induction of A_{CO2} in C_4 *A. semialata MDG* was very similar to that of C_3 *A. semialata GMT*. In C_4 *G. gynandra* a strong temporary depression in A_{CO2} was observed after an initial sharp increase upon exposure to higher light under the 300 s light step that was not affected by the suppression of photorespiration by low oxygen (see **Figure 3.2 I vs R**).

To compare photosynthetic performance between C_3 and C_4 species whilst accounting for their different steady state photosynthetic capacities, A_{CO2} was expressed as a relative percentage of steady state values obtained from light response curves (shown in **Figure 3.3)**. The corresponding absolute carbon assimilation values are provided in **Supplementary figure 3.2**, and steady state values in **Figure 3.1**). This analysis showed clear, systematic differences between C_3 and C_4 species during the 100 µmol m^{-2} s^{-1} PFD steps, where all C_4 species were able to sustain higher A_{CO2} under 100 µmol m^{-2} s^{-1} relative to steady state than their matching C_3 counterparts under both 21% and 2% oxygen. However, no systematic difference between photosynthetic types was apparent during the 800 µmol m^{-2} s^{-1} PFD steps (**Supplementary figure 3.3)**.

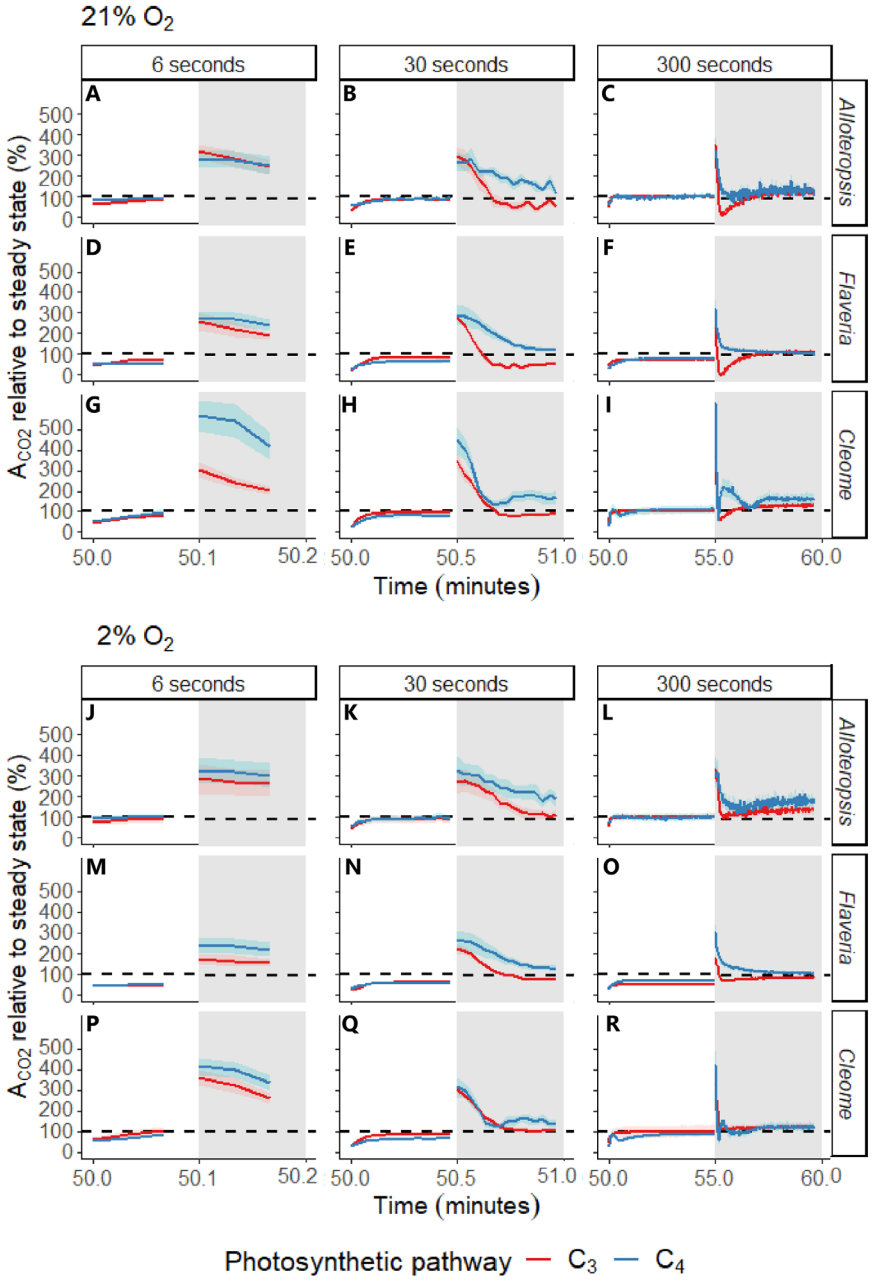

Figure 3.3: Net CO_2 assimilation (A_{CO2}) relative to steady state (%) across the 800 and 100 µmol m^{-2} s^{-1} PFD light steps of differing length starting at the 50 minute mark, in white and grey respectively. Depending on the fluctuating light treatment, subplots are showing one complete fluctuation of 12, 60, or 600 seconds. Values represent A_{CO2} at a given point in the fluctuating light treatment relative to A_{CO2} obtained from steady state light response curves at the light intensity of each period in phylogenetically linked C_3 and C_4 *Alloteropsis*, *Flaveria* and *Cleome* species at 21% and 2% O_2. The dashed line represents 100%, where assimilation would be exactly that of steady state. Ribbons represent standard error of the mean (n=5). The corresponding absolute assimilation values are provided in **Supplementary figure 3.2**.

3.3.3. Stimulation of CO_2 assimilation at low light is most prominent in short light steps and significantly greater in C_4 compared to C_3 species.

To quantify the stimulation of A_{CO2} during the 100 µmol m^{-2} s^{-1} PFD steps of the fluctuations, the average A_{CO2} during the 100 µmol m^{-2} s^{-1} PFD steps was normalized against the steady state rate at the same intensity (**Figure 3.4 D-F**, for a boxplot of the absolute A_{CO2} values see **Supplementary figure 3.3 E-G**). This analysis showed that assimilation was higher than steady state (as seen in the **Figure 3.3** grey half, values greater than 100%) in all species immediately following the transition but declined with duration of the light steps (**Table 3.3**, $p \leq 0.001$ for all). In addition, the relative stimulation compared to steady state values was consistently significantly greater in the C_4 species compared to the C_3 species in the *Flaveria* and *Cleome* pairs (*Flaveria* $p \leq 0.01$; *Cleome* $p \leq 0.001$, **Table 3.3**). Although not significant, a similar trend was observed for the *Alloteropsis* pair at 300 s and 30 s, but not at 6 s light steps.

Table 3.3: ANOVA table of percentage A_{CO2} relative to steady state during the two different light steps of the light fluctuation treatments for phylogenetically linked C_3 and C_4 *Alloteropsis*, *Flaveria* and *Cleome* species. Photosynthetic pathway, PP. Fluctuating length, fl. O_2 concentration, [O_2]. Interaction effects, PP:fl, PP:[O_2], fl:[O_2], and PP:fl:[O_2]. Table shows degrees of freedom, *F*-value, and *p*-value. Significant *p*-values ($a < 0.05$) are shown in bold.

Light period (µmol m^{-2} s^{-1})	Genus	PP	fl	[O_2]	PP:fl	PP:[O_2]	fl:[O_2]	PP:fl:[O_2]
800	*Alloteropsis*	1,52; 0.01; 0.92	1,52; 3.64; 0.06	1,52; 0.01; 0.93	1,52; 0.96; 0.33	1,52; 0.13; 0.72	1,52; 0.19; 0.66	1,52; 0.00; 0.98
	Flaveria	1,52; 0.07; 0.80	1,52; 8.58; **0.01**	1,52; 13.90; **≤0.001**	1,52; 4.23; **0.04**	1,52; 4.65; **0.04**	1,52; 0.04; 0.84	1,52; 0.09; 0.76
	Cleome	1,52; 1.32; 0.25	1,52; 7.96; **0.01**	1,52; 0.53; 0.47	1,52; 0.00; 0.98	1,52; 1.54; 0.22	1,52; 0.72; 0.40	1,52; 0.00; 0.95
100	*Alloteropsis*	1,52; 1.15; 0.29	1,52; 15.30; **≤0.001**	1,52; 1.48; 0.23	1,52; 0.01; 0.90	1,52; 0.07; 0.79	1,52; 0.00; 0.96	1,52; 0.02; 0.89
	Flaveria	1,52; 14.20; **≤0.001**	1,52; 31.18; **≤0.001**	1,52; 0.50; 0.48	1,52; 0.94; 0.33	1,52; 0.03; 0.87	1,52; 0.24; 0.62	1,52; 0.02; 0.89
	Cleome	1,52; 7.65; **0.01**	1,52; 25.08; **≤0.001**	1,52; 0.50; 0.48	1,52; 2.64; 0.11	1,52; 3.06; 0.08	1,52; 0.00; 0.99	1,52; 0.53; 0.46

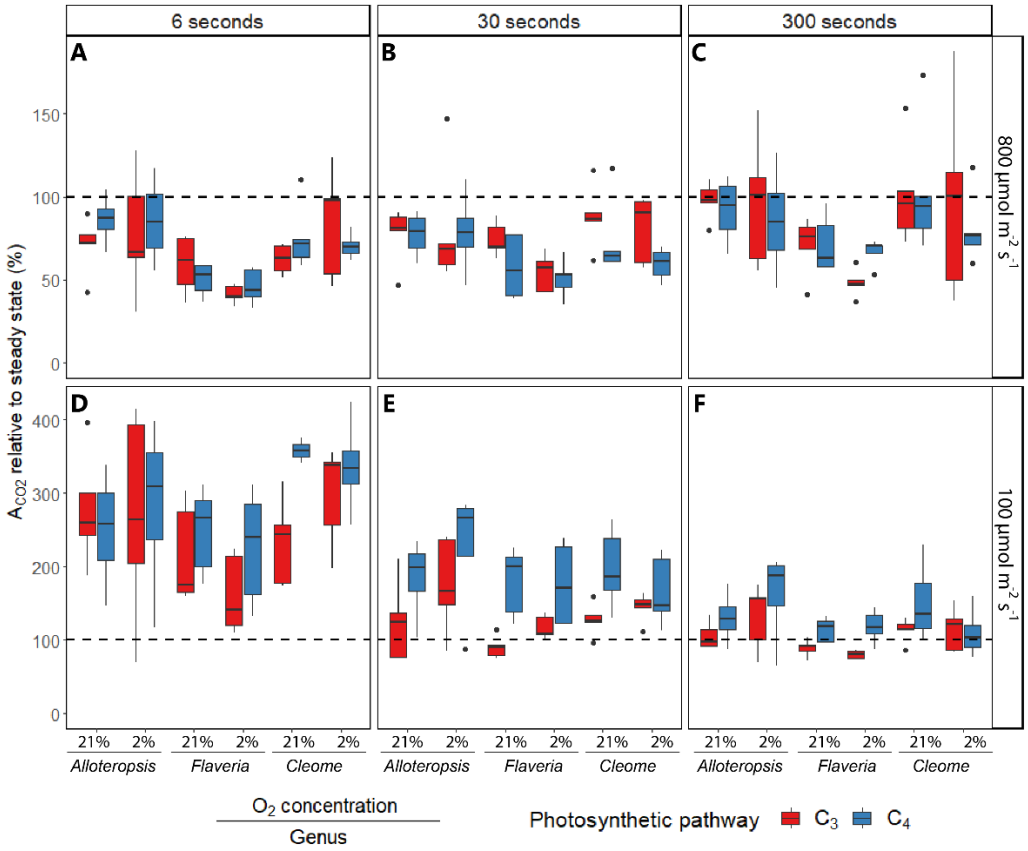

Figure 3.4: Boxplots of net CO_2 assimilation (A_{CO2}) relative to steady state (%) under the 800 and 100 µmol m^{-2} s^{-1} PFD light steps of the fluctuating light regimes. Each regime consisted of alternating 800 and 100 µmol m^{-2} s^{-1} PFD periods, where each light step lasted 6, 30, or 300 seconds. For each period, A_{CO2} across the timeseries for phylogenetically linked C_3 and C_4 *Alloteropsis*, *Flaveria* and *Cleome* species at 21% or 2% O_2 was calculated as a percentage of steady state values obtained from light response curves at the same light intensity and O_2 concentration. The dashed line represents 100%, where assimilation rate would equal steady state. Box edges represent the lower and upper quartiles, the solid line indicates the median, and points represent outliers beyond 1.5 times the interquartile range (n = 5 for each combination of species/oxygen). Three-way ANOVA (**Table 3.3**) was used to test the effect of photosynthetic pathway, fluctuating length, O_2 concentration and their interaction on A_{CO2} relative to steady state in *Alloteropsis, Flaveria*, and *Cleome*. The corresponding absolute assimilation values are shown in **Supplementary figure 3.3.**

Three-way ANOVA (**Table 3.3**) showed A_{CO2} relative to steady state was significantly affected by fluctuation length in all genera ($p \leq 0.001$ for all), as well as by photosynthetic pathway in *Flaveria* and *Cleome* (*Flaveria* $p \leq 0.01$; *Cleome* $p \leq 0.001$). Overall, although all species had greater CO_2 fixation during the 100 µmol m^{-2} s^{-1} PFD periods than under steady state, the effect was time sensitive and therefore more significant during shorter light steps. In addition, C_4 species were able to sustain the higher rates for longer than their C_3 counterparts. The greatest increases in relative assimilation occurred during the 6 s light steps (**Figure 3.4 D**) where C_4 species were on average 329% of steady state A_{CO2} compared to 242% in C_3 species under 21%

oxygen and similarly 290% in C_4 vs 243% in C_3 at 2% oxygen. Under 30 s light steps (**Figure 3.4 E**) the stimulation of A_{CO2} relative to steady state was less pronounced than 6 s, but still substantially higher in C_4 species at 187% compared to C_3 species at 114% of steady state A_{CO2} at 21% O_2, and 190% vs 146% of steady state A_{CO2} at 2% O_2, respectively. The impact of C_4 photosynthesis was most apparent under these two light steps, whereas during the 300 s light steps (**Figure 3.4 F**) the stimulation of A_{CO2} was less evident. Averaged across the 300 s, C_4 species were operating at 132% relative to steady state A_{CO2} compared to C_3 species at 103% under ambient oxygen, and at 130% and 109% of steady state A_{CO2} under 2% O_2, respectively. Interestingly, A_{CO2} relative to steady state was typically higher in C_4 compared to C_3 species under both 21% and 2% oxygen and no significant effect of the interaction between photosynthetic pathway and oxygen concentration was found in any of the genera, suggesting a systematic advantage to C_4 photosynthesis to bridge low light periods which was still apparent when photorespiration was suppressed.

Despite the fact that photorespiration did not account for the difference in A_{CO2} between C_3 and C_4 species during the initial transition to lower light, photorespiratory lagging led to a clear PIB in the C_3 species, which further exacerbated the decline in A_{CO2} immediately following high light in the measurements under 21% O_2. To estimate the impact of the PIB on A_{CO2} in the C_3 species, periods of the 100 μmol m^{-2} s^{-1} PFD light steps where a PIB was evident were compared between 21% and 2% O_2 (10-30 s in the 30 s light steps and 10-70 s in the 300 s light steps). Under 21% O_2 the average A_{CO2} relative to steady state of C_3 species during those periods was 69% and 61% for the 30 and 300 s light steps, compared to 111% and 112% respectively under 2% O_2. In contrast, under both oxygen concentrations the relative assimilation of C_4 species was consistently greater than 100% across both fluctuation lengths, averaging 150% and 158% under 21% O_2, and 161% and 151% under 2% over the same 30 and 300 s periods.

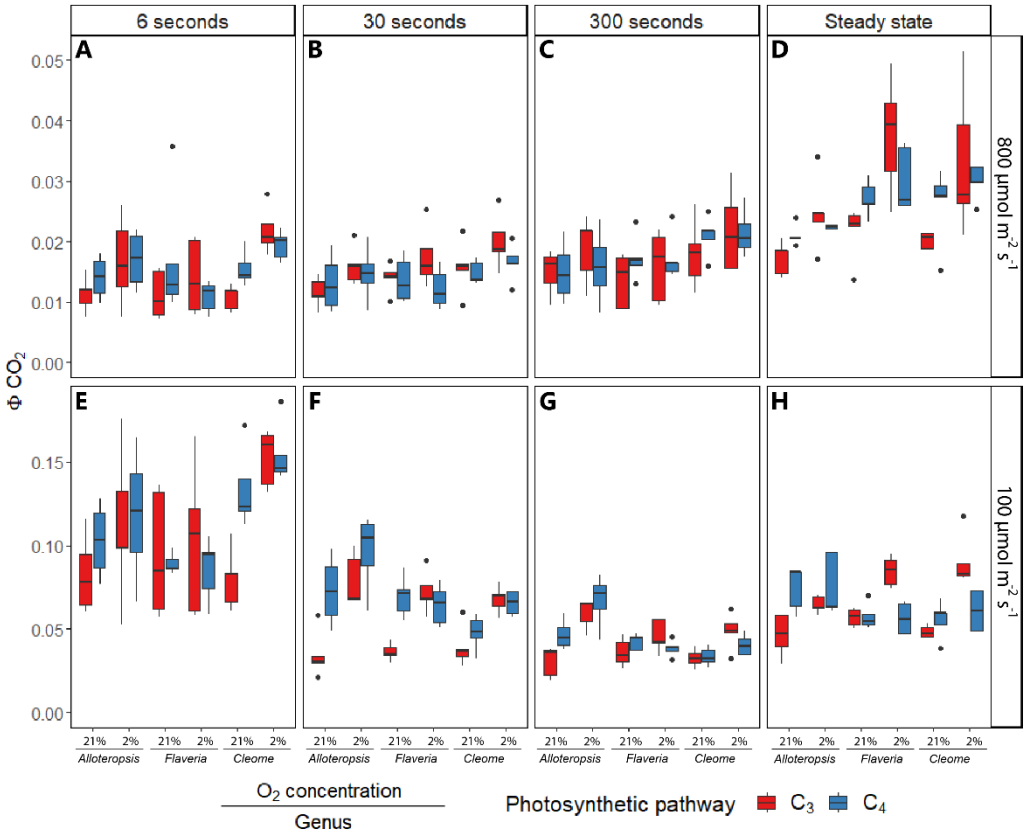

Figure 3.5: Boxplots of the quantum yield of carbon assimilation (ΦCO_2) under the 800 and 100 µmol m^{-2} s^{-1} PFD periods of the fluctuating light regimes or from steady state measurements. Each fluctuating regime consisted of alternating 800 and 100 µmol m^{-2} s^{-1} PFD periods, where each light step lasted 6, 30, or 300 seconds. Box edges represent the lower and upper quartiles, the solid line indicates the median, and points represent outliers beyond 1.5 times the interquartile range (n = 5 for each combination of species/measurement condition). Three-way ANOVA was used to test the effect of photosynthetic pathway, fluctuating length, O_2 concentration and their interaction on ΦCO_2 in *Alloteropsis, Flaveria*, and *Cleome* (results shown in **Table 3.4**).

To estimate to what extent the low light stimulation of CO_2 assimilation was decoupled from photochemical provision of ATP and NADPH, ΦCO_2 was calculated for each light step (**Figure 3.5, Table 3.4**). Based on steady state stoichiometry of electron flow and proton requirements for ATP synthesis and NADPH:ATP energy demands, the theoretical maximum ΦCO_2 has been estimated as 0.111 CO_2/photon for C_3 species (Ehleringer and Pearcy, 1983), as 0.064 CO_2/photon for C_4 NADP-ME and NAD-ME species accounting for estimated BS leakiness (Yin and Struik, 2018), and due to the theorised lower energy requirements of mixed C_4 pathways as 0.075 CO_2/photon for mixed subtype NADP-ME/PEPCK (Ishikawa et al., 2016, Yin and Struik, 2021). Here we consider observations of quantum yields exceeding these theoretical maxima as conservative evidence for decoupling. At 6 s light steps, C_3 *F. cronquistii* and C_3 *A. semialata GMT* stayed well below the theoretical maximum, but the ΦCO_2 values of

C_3 *T. hassleriana* were significantly higher (**Table 3.4**). ΦCO_2 values of C_4 *A. semialata MDG,* C_4 *F. bidentis, and* C_4 *G. gynandra* during the lower light periods of the 6 s and 30 s fluctuations were also significantly higher than the theoretical limit, suggesting that the provision of ATP and reductant was not directly coupled to production from the thylakoid reactions. By comparing the ΦCO_2 values with these theoretical maxima, it is possible to estimate the degree of decoupling in units of fixed CO_2/photon. At 6 s light steps, the theoretical limit was exceeded by 0.043 ± 0.019 CO_2/photon in C_4 *A. semialata MDG*, 0.022 ± 0.008 CO_2/photon in C_4 *F. bidentis,* 0.091 ± 0.008 CO_2/photon in C_4 *G. gynandra* and 0.042 ± 0.008 CO_2/photon in C_3 *T. hassleriana*. At 30 s light steps, these numbers decreased to 0.021 ± 0.011 CO_2/photon in C_4 *A. semialata MDG*; 0.008 ± 0.005 CO_2/photon in C_4 *F. bidentis*; and 0.005 ± 0.003 CO_2/photon in C_4 *G. gynandra*.

Table 3.4: ANOVA table of ΦCO_2 during the two different light steps of the light fluctuation treatments for phylogenetically linked C_3 and C_4 *Alloteropsis*, *Flaveria* and *Cleome* species. Photosynthetic pathway, PP. Fluctuating length, fl. O_2 concentration, [O_2]. Interaction effects, PP:fl, PP:[O_2], fl:[O_2], and PP:fl:[O_2]. Table shows degrees of freedom, *F*-value, and *p*-value. Significant *p*-values ($a < 0.05$) are shown in bold.

Light period (µmol m^{-2} s^{-1})	Genus	PP	fl	[O_2]	PP:fl	PP:[O_2]	fl:[O_2]	PP:fl:[O_2]
800	*Alloteropsis*	1,52; 0.00; 0.97	1,52; 2.00; 0.16	1,52; 7.08; **0.01**	1,52; 0.76; 0.39	1,52; 1.22; 0.27	1,52; 0.20; 0.66	1,52; 0.00; 0.96
	Flaveria	1,52; 0.10; 0.75	1,52; 2.67; 0.11	1,52; 0.02; 0.89	1,52; 1.17; 0.28	1,52; 4.56; **0.03**	1,52; 0.40; 0.53	1,52; 0.77; 0.38
	Cleome	1,52; 0.01; 0.92	1,52; 11.15; **0.01**	1,52; 16.33; **≤0.001**	1,52; 0.53; 0.47	1,52; 4.45; **0.04**	1,52; 2.48; 0.12	1,52; 0.17; 0.68
100	*Alloteropsis*	1,52; 5.70; **0.02**	1,52; 23.37; **≤0.001**	1,52; 14.02; **≤0.001**	1,52; 0.25; 0.62	1,52; 0.94; 0.34	1,52; 0.04; 0.85	1,52; 0.07; 0.79
	Flaveria	1,52; 0.01; 0.94	1,52; 34.60; **≤0.001**	1,52; 1.28; 0.26	1,52; 0.00; 0.99	1,52; 3.26; 0.08	1,52; 1.15; 0.70	1,52; 0.17; 0.68
	Cleome	1,52; 1.04; 0.31	1,52; 38.70; **≤0.001**	1,52; 9.40; **0.02**	1,52; 1.21; **0.04**	1,52; 1.81; 0.28	1,52; 1.75; 0.19	1,52; 0.42; 0.52

3.3.4. Depression of CO_2 assimilation at high light is not significantly affected by photosynthetic pathway

Unlike in the 100 µmol m^{-2} s^{-1} PFD periods there was no clear trend between the C_3 and C_4 response at 800 µmol m^{-2} s^{-1} PFD periods (**Figure 3.4 A-C**, for a boxplot of the corresponding A_{CO2} values see **Supplementary figure 3.3 A-C**).

A_{CO2} values during the 800 µmol m^{-2} s^{-1} PFD light steps were lower than under steady state (below 100% line in **Figure 3.3**). Three-way ANOVA (**Table 3.3**) was used to analyse the effects of light step duration, photosynthetic pathway, oxygen concentration, and their interactions on relative A_{CO2}. None of these were significant for the *Alloteropsis* subspecies. In *Flaveria*, weakly significant interactions between light step duration and photosynthetic pathway ($p = 0.04$), as well as between oxygen concentration and photosynthetic pathway ($p = 0.04$) were observed, indicating a more complex conditional impact of photosynthetic pathway on assimilation rate relative to steady state. In C_4 *F. bidentis* relative A_{CO2} gradually increased with light step duration, whereas in C_3 *F. cronquistii* this increase was only observed between 6 and 30 s but not between 30 and 300 s. Whilst relative A_{CO2} was depressed by 2% oxygen in both *Flaveria* species, the effect was more pronounced in C_3 *F. cronquistii*. In *Cleome*, light step duration significantly impacted relative A_{CO2} ($p = 0.01$) which increased with duration in both C_3 and C_4 species.

Quantum yields during the 800 µmol m^{-2} s^{-1} PFD periods across all fluctuation regimes and oxygen concentrations were lower than steady state across all species (**Figure 3.5 A-D**), indicating reduced efficiency of carbon assimilation. In *Alloteropsis*, oxygen concentration significantly impacted ΦCO_2 ($p = 0.01$, **Table 3.4**), with 2% oxygen being associated with higher values. In *Flaveria* and *Cleome* 2% oxygen was associated with higher quantum yields only in the C_3 species, and lower or similar values in their C_4 counterparts (significant interactions between O_2 and photosynthetic pathway $p \leq 0.05$, **Table 3.4**).

3.4. Discussion

3.4.1. C_4 species are better able to sustain photosynthetic rates than C_3 species after a transition to lower light

The effect of fluctuating light on C_4 relative to C_3 photosynthesis was systematically evaluated in three phylogenetically controlled comparisons using repetitive low and high light steps with three contrasting durations. The results support the hypothesis that C_4 species are better able to sustain photosynthetic rates than C_3 species during the lower light periods of fluctuating light. The theoretical basis for this hypothesis suggests that the large metabolite pools necessary for diffusional transfer between M and BS in C_4 photosynthesis and the reversible reactions linking these metabolic intermediates can work as a capacitor, providing greater flexibility to respond to variations in light intensity (Leegood and von Caemmerer, 1989, Stitt and Zhu, 2014). In

this chapter, although all tested species had generally higher carbon assimilation during the 100 µmol m^{-2} s^{-1} PFD periods relative to steady state, C_4 *A. semialata MDG,* C_4 *F. bidentis*, and C_4 *G. gynandra* had higher relative rates than C_3 *A. semialata GMT*, C_3 *F. bidentis,* and C_3 *T. hassleriana* under the same fluctuating light regime (**Figure 3.4 D-F**). As C_4 species had higher relative assimilation under both 21% and 2% oxygen, the greater stimulation under low light cannot be solely attributed to increased presence of photorespiration in C_3 species during fluctuating light, and the prevalence of this result across species from diverse evolutionary lineages and C_4 subtypes suggests the ability to sustain high photosynthetic rates after a transition to lower light may indeed be linked to other features of the C_4 pathway – such as the large metabolite pools intrinsic to CCM operation (Arrivault et al., 2017, Leegood and Furbank, 1984, Lilley et al., 1977, Stitt et al., 1985).

Metabolic pools also play a role in C_3 species, and post-illumination CO_2 fixation has previously been attributed to altering pools of C_3 intermediates and ATP and redox equivalents that accumulate during higher light fluctuations (Kaiser et al., 2015). In C_3 *A. semialata GMT*, C_3 *F. bidentis,* and C_3 *T. hassleriana*, the higher A_{CO2} values relative to steady state observed during 6 s fluctuations, as well as during the first half of the 30 s fluctuations (**Figure 3.3 BEH & KNQ**) are in line with previous observations of carbon assimilation exceeding steady state rates immediately after sunflecks (Pons and Pearcy, 1992, Sharkey et al., 1986). However, metabolic pools in C_3 species are typically considerably smaller than in C_4 species (Borghi et al., 2022), which may be why C_4 *A. semialata MDG,* C_4 *F. bidentis*, and C_4 *G. gynandra* were able to sustain higher relative rates for longer than their C_3 counterparts (**Figure 3.3**), as evidenced by the higher average rates across longer fluctuations (**Figure 3.4 D-F**). However, the capacity of C_4 species to buffer through transitions to lower light still decreases across time as metabolite pools are depleted (Slattery et al., 2018), and carbon assimilation relative to steady state during those periods was inversely related to the length of the fluctuations. Altogether, the higher and more sustained stimulation of C_4 photosynthetic rates compared to C_3 rates at low light is consistent with prior work (Laisk and Edwards, 1997, Lee et al., 2022, Li et al., 2021) but the impact of light step duration explains why studies using different fluctuating light regimes can yield contrasting estimates for the comparative advantage of C_4 versus C_3 photosynthesis.

Although the comparative benefit of C_4 species was observed under both oxygen conditions, the decrease in low-light A_{CO2} of the C_3 species under 21% O_2 was exacerbated by PIBs due to

photorespiratory lagging. Previous work has shown that under photorespiration-suppressing conditions, C_3 tree seedlings experience greater carbon gain under sunflecks than uniform light due to a less pronounced PIB, which maximises post-illumination CO_2 fixation (Leakey et al., 2002). This is consistent with our observation that under 2% oxygen, there was greater assimilation relative to steady state in the C3 species during the PIB time window than under 21% oxygen, which supports the idea that the suppression of photorespiration may have a specific benefit to dynamic light environments in C_3 species (Way and Pearcy, 2012).

Finally, the quantum yield of photosynthesis provides another indication of the storage capacity of C_4 metabolic pools. In C_4 species ΦCO_2 during the 6 s and 30 s fluctuations was consistently above the theoretical maximum (Ehleringer and Pearcy, 1983, Ishikawa et al., 2016, Morales et al., 2018, Yin and Struik, 2018, Yin and Struik, 2021), indicating that the energetic equivalent to ~0.022-0.091 CO_2/photon under 6 s fluctuations and ~0.005-0.021 CO_2/photon under 30 s fluctuations was being supplied outside of the thylakoid light reactions. The comparison with the maximum theoretical limit rather than with steady state ΦCO_2 was used to protect our conclusions against measurement uncertainty. The results therefore provide a very conservative estimate of the extent of decoupled CO_2 fixation in C_4 species, which may have been sustained by redox equivalents from malate decarboxylation, with demands for ATP and NADH being buffered through reversible reactions linking 3-PGA and TP, or interconversion of 3-PGA and PEP (Arrivault et al., 2017, Bräutigam et al., 2008, Slattery et al., 2018, Stitt and Zhu, 2014, Wang et al., 2014b). Leaf-level and canopy simulations emphasise ΦCO_2 as the largest determinant of photosynthesis in the lower canopy (Bellasio and Farquhar, 2019, Gu et al., 2014) and the stimulation of low light ΦCO_2 as observed here at three contrasting fluctuation frequencies could provide an important mitigation mechanism of the lower photosynthetic efficiency of C_4 plants under low light (Medeiros et al., 2022, Ubierna et al., 2011).

3.4.2. The C_4 response during the transition to higher light could be related to the specific subtype metabolism

The comparative high light performance of C_4 photosynthesis was not uniform across the three genera. Although the use of a single representative example from each C_4 subtype precludes the separation of species and subtype effects, the specific characteristics of the C_4 pathway within each genus provide a possible explanation for the observed differences.

The highest A_{CO2} relative to steady state rates in C_4 species during the 800 μmol m^{-2} s^{-1} PFD periods were found in C_4 *A. semialata MDG* which is suggested to rely on a mixed NADP-

ME/PEPCK C_4 pathway (Ueno and Sentoku, 2006) (**Figure 3.4 A-C**). The lack of effect of light step duration on A_{CO2} during the higher light periods in *Alloteropsis* (**Table 3.3**) could be explained by photosynthetic induction during these fluctuating light regimes being relatively fast (**Figure 3.2 ABC**). In contrast, high light A_{CO2} relative to steady state was significantly lower with shorter fluctuations in both *Cleome* species; whereas in *Flaveria,* C_4 *F. bidentis* relative assimilation was more significantly reduced during shorter fluctuations than in C_3 *F. cronquistii*, indicating the C_4 cycle lagged behind C_3 activation (**Table 3.3**). The effect of fluctuation length on light induction in *Flaveria* and *Cleome* could be due to shorter fluctuations hindering the formation of metabolite pools necessary for optimal CCM operation, which has been suggested to result in impaired suppression of photorespiration and lagging photosynthetic induction during metabolite build-up (Sage and McKown, 2006). Indeed, we previously found that the C_4 species analysed here were slower to induce photosynthesis from darkness relative to their C_3 counterparts (Arce Cubas et al., 2023b). Consistent with the faster induction observed in *Alloteropsis*, theoretical work indicates that not all subtypes are equally reliant on gradients: mixed C_4 pathways like NADP-ME/PEPCK do not need metabolite gradients as large as NADP-ME or NAD-ME subtypes, as mixed subtypes can concurrently use different transfer acids (Wang et al., 2014a). The use of both Mal and Asp shuttles also allows for finer regulation of the ATP:NADPH ratio in response to changes in light, as only Mal transport brings redox equivalents into the BS (Yin and Struik, 2021).

The suggested effect of subtype detailed above can also be observed in previous work. Li et al. (2021) compared a selection of six C_4 species, five of which were NADP-ME and one NAD-ME, with eight C_3 species, concluding that C_4 species utilized fluctuating light less efficiently by comparing obtained carbon assimilation during fluctuations to constant light values due to slower light induction. However, the role of species variation should not be underestimated – Lee et al. (2022) recently reported distinct species-specific induction patterns across six C_4 grass species, which could also explain the results in this chapter, although similar induction patterns were still observable across NADP-ME species. The varying impact of light step duration on A_{CO2} found in this chapter also provides an important consideration for the interpretation of previous work. For example, Lee et al. concluded that their selection of C_4 species assimilated more carbon under fluctuating light relative to steady state in comparison with six C_3 species, seemingly in contrast with the conclusions by Li et al. (2021). However, – although both experiments had low light steps of two minutes, high light steps were two

minutes in the Li et al. (2021) study and four minutes in Lee et al. (2021). Since both studies observed a slower decrease in photosynthetic rates relative to steady state values in C_4 species after the transition to lower light, the additional two minutes of higher light in the Lee et al. study may have reduced the comparative penalty of C_4 induction relative to the benefits of higher assimilation during the lower light periods, explaining the contrasting conclusions. Overall, this suggests C_4 photosynthesis may have an advantage during brief periods of shade that intermit longer periods of sunlight commonly found in the top and middle layers of a leaf canopy (Kaiser et al., 2018). The comparative C4 advantage during ”shade flecks” would allow for greater assimilation during high light periods and maximise post-illumination CO_2 assimilation, despite the fact that the specific induction response may differ between C_4 species. The comparative advantage of C_4 photosynthesis after a transition to low light may be less impactful in shade environments interspersed with sunflecks like forest understories (Pearcy, 1990), where carbon assimilation at low light steady state dominates and the contribution of post-illumination CO_2 assimilation is less substantial.

3.4.3. Fluctuations in light cause CO_2 bursts in C_4 G. gynandra

C_4 *G. gynandra* had distinctive assimilation kinetics after each light transition in the 300 s fluctuations (**Figure 3.2 I&R**). At the start of the 800 µmol m^{-2} s^{-1} PFD period, a rapid increase in $A_{CO2,}$ described in previous work as a CO_2 gulp (Laisk and Edwards, 1997), was immediately followed by a CO_2 burst, with another CO_2 burst upon changing to the 100 µmol m^{-2} s^{-1} PFD period. These bursts were not a product of photorespiration, as unlike the PIB observed after a transition to lower light in C_3 species, in C_4 *G. gynandra* they occurred independent of oxygen concentration.

Previous studies on sunflecks (Laisk and Edwards, 1997) have characterised the post-illumination CO_2 burst as a specific feature of the NAD-ME and PEPCK pathways, and other fluctuating light studies have also reported it primarily for NAD-ME species (Lee et al., 2022). Unlike NADP-ME species, where malate decarboxylation is linked to reducing equivalents from the C_3 cycle, in NAD-ME species the C_3 and C_4 cycles are less tightly coupled – oxaloacetate is first reduced to malate and then decarboxylated in the mitochondria, but the redox balance is uncoupled from the C_3 cycle (Ishikawa et al., 2016). This can result in excess CO_2 being released despite insufficient RuBP regeneration upon a transition to lower light, causing unfixed CO_2 to leak out of the BS and A_{CO2} to drop.

The CO_2 gulp and burst at the start of the 800 µmol m^{-2} s^{-1} PFD period is similar to induction kinetics observed in short dark-light fluctuations in NAD-ME *Amaranthus cruentus* (Laisk and Edwards, 1997). These were attributed to formation of alanine from the decarboxylation of aspartate in low light (or darkness), leading to rapid conversion of alanine to pyruvate followed by phosphorylation to PEP when light is increased (Laisk and Edwards, 1997, Lee et al., 2022). The initial PEP carboxylation following the increase in light exceeds the rate at which PEP pools can be replenished, but subsequently crashes and readjusts while PEP regeneration is re-established. This may account for the observed temporary gulp and subsequent steady increase in A_{CO2}. Furthermore, the centripetal chloroplast positioning found in NAD-ME species (Yoshimura et al., 2004) could increase path length for metabolites and CO_2, and lead to a more pronounced form of the biphasic induction previously observed in NADP-ME species and attributed to C_4 cycle limitations (Lee et al., 2022).

3.5. Conclusions

The presented work compared C_4 to C_3 photosynthesis in response to fluctuating light. By using three independent phylogenetically controlled comparisons and fluctuations with three contrasting light step durations the presented work circumvented issues in previous studies to yield more robust conclusions. The results showed that the stimulation of A_{CO2} in the low light phase was both higher and more sustained in C_4 photosynthesis across all three comparisons, suggesting this could be a common comparative advantage of C_4 photosynthesis. In contrast, observed patterns of A_{CO2} in the high light phase were found to be more variable across genera rather than attributable to photosynthetic pathway, which could potentially be related to the specific C_4 subtype.

3.6. Supplementary material

Supplementary table 3.1: Leaf absorptance values of phylogenetically linked C_3 and C_4 *Alloteropsis*, *Flaveria*, and *Cleome* species from the blue (475 nm) and red (625 nm) wavelengths of the actinic light source used in Chapter 3 experiments (6800-01A Multiphase Flash Fluorometer, LI-COR), measured with an integrating sphere. Means and standard error of the mean are shown (n = 5).

Genus	Species	L_{abs} (475 nm)	L_{abs} (625 nm)
Alloteropsis	C3 *A. semialata GMT*	0.90±0.02	0.88±0.02
	C4 *A. semialata MDG*	0.87±0.02	0.81±0.02
Flaveria	C3 *F. cronquistii*	0.88±0.02	0.85±0.02
	C4 *F. bidentis*	0.94±0.00	0.90±0.00
Cleome	C3 *T. hassleriana*	0.95±0.00	0.92±0.00
	C4 *G. gynandra*	0.93±0.00	0.89±0.00

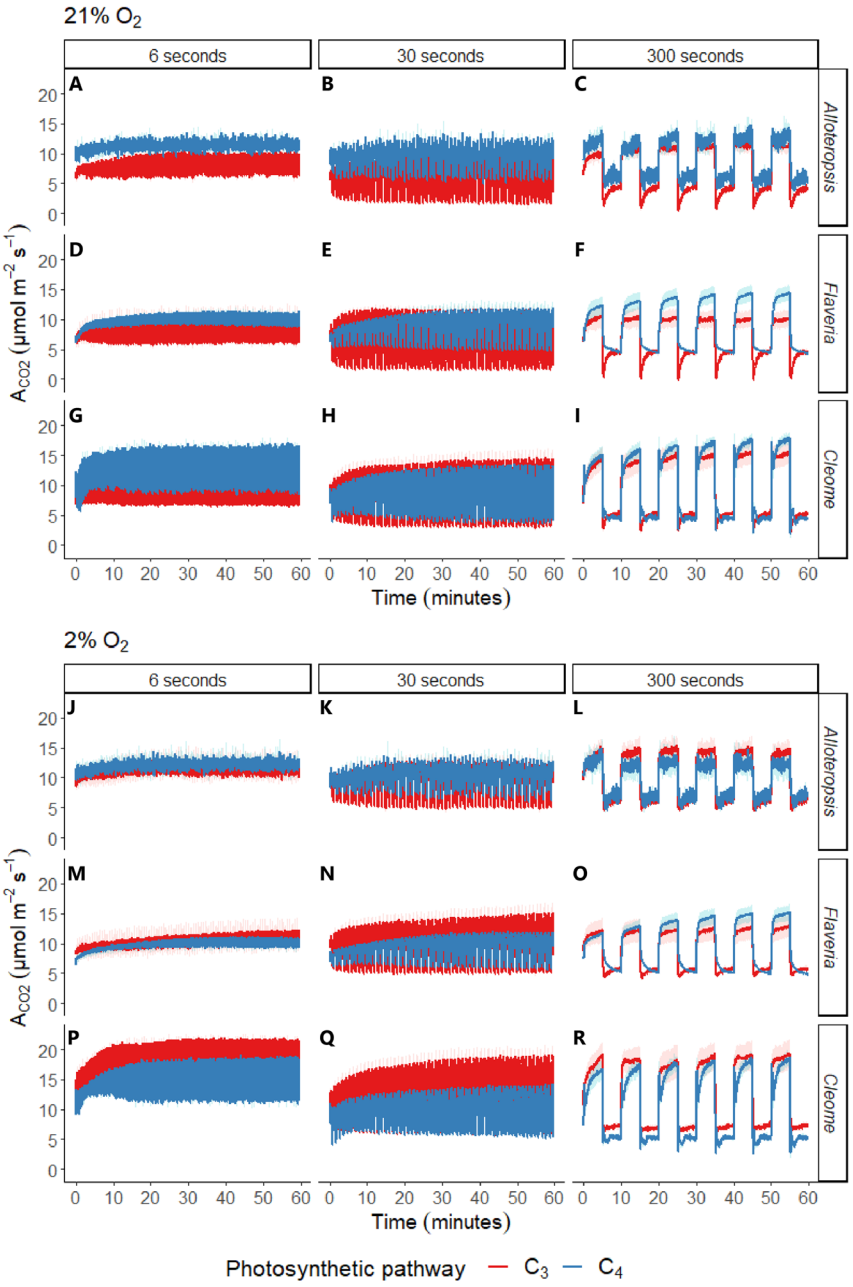

Supplementary figure 3.1: Net CO_2 assimilation (A_{CO2}) in phylogenetically linked C_3 and C_4 *Alloteropsis*, *Flaveria* and *Cleome* species under three different fluctuating light regimes at 21% and 2% O_2. Each light regime consisted of alternating 800 and 100 µmol m^{-2} s^{-1} PFD periods, where each light period lasted 6, 30, or 300 seconds before changing. Treatments were started after leaves were acclimated at 150 µmol m^{-2} s^{-1} PFD and lasted 1 hour, but data in the study was taken from minutes 50-60 of each treatment. Ribbons represent standard error of the mean (n=5).

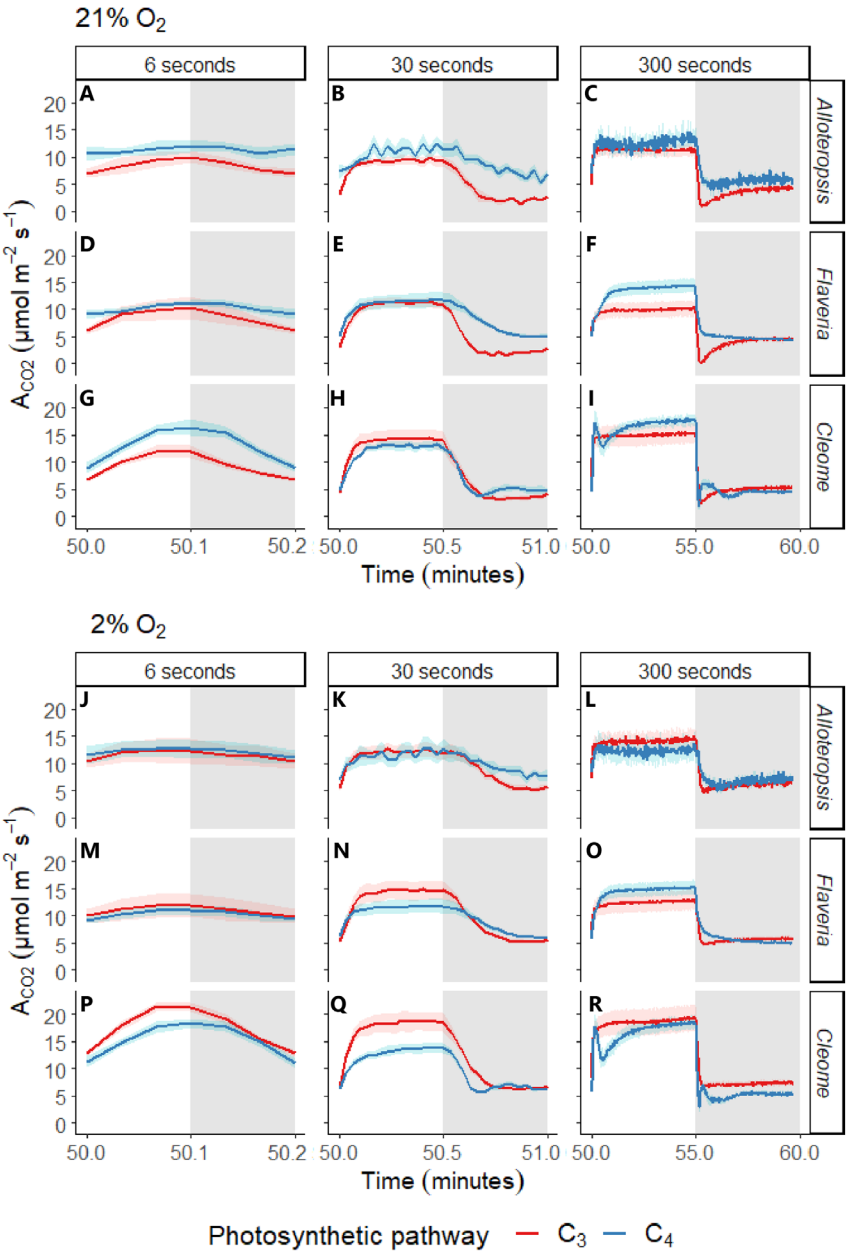

Supplementary figure 3.2: A_{CO2} across a 100 and an 800 µmol m^{-2} s^{-1} PFD period, in white and grey respectively. All data was taken from minute 50 but depending on the fluctuating light treatment, each period was 6, 30, or 300 seconds. Values represent phylogenetically linked C_3 and C_4 *Alloteropsis*, *Flaveria* and *Cleome* species at 21% and 2% O_2. Ribbons represent standard error of the mean (n=5). The corresponding A_{CO2} relative to steady state (%) values are in **Figure 3.3**.

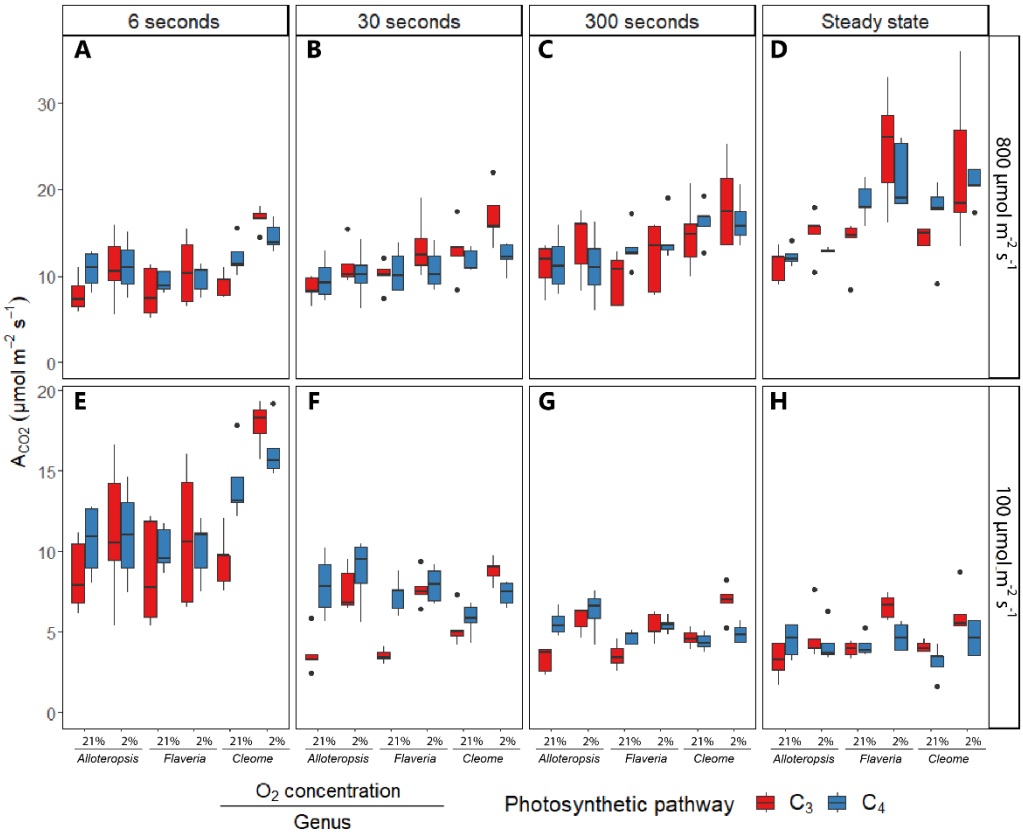

Supplementary figure 3.3: Boxplots of net carbon assimilation (A_{CO2}) under the 800 and 100 µmol m^{-2} s^{-1} PFD periods of the fluctuating light regimes. Each regime consisted of alternating 800 and 100 µmol m^{-2} s^{-1} PFD periods, where each light period lasted 6, 30, or 300 seconds before changing. The plot includes A_{CO2} steady state values taken from the light response curves. The area under the curve (AUC) A_{CO2} of for each period across the timeseries for phylogenetically linked C_3 and C_4 *Alloteropsis*, *Flaveria* and *Cleome* species at 21% or 2% O_2 was calculated from between minutes 50-60 of each fluctuating light treatment and converted to a rate constant for ease of comparison. Box edges represent first and third quartiles, the solid line indicates the median, and points represent outliers beyond 1.5 times the interquartile range (n = 5 for each combination of species/measurement condition).

4. Characterising differences in the NPQ response in C_3 and C_4 species

4.1. Introduction

Leaves in full sunlight regularly absorb more light that can be processed by photochemistry. Non-photochemical quenching (NPQ) refers to a collection of mechanisms wherein excess light energy in the photosystem II (PSII) antennae is dissipated harmlessly as heat, preventing overexcitation and the formation of reactive oxygen species that would damage the photosynthetic machinery (Müller et al., 2001). Although crucial for photoprotection, changes in NPQ are not instantaneous, with the return to the unquenched state in particular lagging behind changes in irradiance and temporarily reducing photosynthetic efficiency (Werner et al., 2001). This has important implications within the dynamic light environments of crop canopies, where model simulations have estimated slow rates of NPQ relaxation to result in a 7.5-30% loss of carbon assimilation (Wang et al., 2020, Zhu et al., 2004). Most excitingly, landmark studies have now provided proof of concept for increasing yield by accelerating the rate of response of NPQ to shade events (De Souza et al., 2022, Kromdijk et al., 2016). It has been suggested that NPQ could also be an area of improvement for plants with C_4 photosynthesis (Sales et al., 2021, Zhu et al., 2004), which include some of the most important crops worldwide (FAO, 2020). However, that potential is limited by our current understanding of NPQ, which is overwhelmingly informed by C_3 species. To find out if NPQ kinetics could be a potential target for improvement in C_4 species, it is necessary to establish the specifics of the C_4 NPQ response (Guidi et al., 2019).

C_4 photosynthesis is a biochemical and physiological adaptation of the ancestral C_3 pathway that has evolved at least 66 times in angiosperms (Kellogg, 2013) and operates a spatial carbon concentration mechanism (CCM) often leading to higher photosynthetic rates and increased water use efficiency (Kiniry et al., 1989, Sage, 2004). Whilst C_3 species directly fix carbon into the Calvin-Benson-Bassham cycle in mesophyll (M) cell chloroplasts, most C_4 species compartmentalise initial carbon fixation and assimilation between morphologically distinct M and bundle sheath (BS) cells, arranged in 'Kranz' anatomy and connected by a biochemical dicarboxylic acid cycle. BS cells are located around the leaf veins and are in turn concentrically surrounded by M cells, where CO_2 is first converted to bicarbonate and fixed by phospho*enol*pyruvate carboxylase (PEPC) into 4-carbon oxalo-acetate molecules that are

reduced to malate or transaminated to aspartate before diffusing into the BS. In the BS, malate or aspartate are decarboxylated, releasing CO_2 around the central carbon fixation enzyme ribulose 1,5-biphosphate carboxylase/oxygenase (Rubisco) (Leegood, 2002). The C_4 CCM achieves CO_2 concentrations around Rubisco that are approximately 10 times higher than C_3 species, which enhances photosynthesis by supporting carboxylation and suppressing Rubisco's alternative oxygenation reaction and subsequent photorespiration pathway, which consumes energy and reducing equivalents, and re-releases CO_2. Different C_4 pathways use different decarboxylating enzymes, often in combination (Calsa and Figueira, 2007, Sales et al., 2018) – predominant decarboxylases include nicotinamide adenine dinucleotide malic enzyme (NAD-ME), nicotinamide adenine dinucleotide phosphate-malic enzyme (NADP-ME), and phosphoenolpyruvate carboxykinase (PEPCK) (Hatch et al., 1975), although the energetics of PEPCK suggest it has to operate as a supplementary pathway (Furbank, 2011). The specifics of the C_4 light reactions have been comparatively less studied than C_4 biochemistry and anatomy (Guidi et al., 2019), but higher PSI/PSII ratios than in C_3 plants have been found in NADP-ME BS (Majeran et al., 2010, Meierhoff and Westhoff, 1993) and NAD-ME M cells (Takabayashi et al., 2005). Linear electron flow (LEF) requires PSII and PSI and produces both ATP and NADPH, whereas cyclic electron flow (CEF) around PSI contributes only to ATP production and increases ΔpH across the thylakoid membrane as electrons are recycled from the PSI acceptor site to plastoquinone (PQ) (Allen, 2003). The regeneration of CCM biochemical intermediates comes with an energetic cost (Ishikawa et al., 2016, Yin and Struik, 2018), and the increased PSI:PSII ratios are often thought to reflect the increase in CEF to contribute towards meeting the increased ATP requirement of C_4 photosynthesis (Munekage, 2016).

During NPQ, the conformational change of PSII-associated antennae that triggers the quenched state can be induced by a number of mechanisms that activate at different timescales and can be resolved based on their relaxation kinetics (Müller et al., 2001, Murchie and Ruban, 2020). Energy dependent quenching (qE) (Wraight and Crofts, 1970) relaxes within seconds to minutes (10-90 seconds) and is activated by the acidification of the lumen, which leads to the protonation of PSII subunit PsbS (Li et al., 2000, Li et al., 2004, Ruban et al., 2012). Low lumen pH also activates xanthophyll cycle enzyme Violaxanthin De-Epoxidase (VDE), which de-epoxidizes violaxanthin to zeaxanthin (Demmig-Adams, 1990), enhancing the magnitude of qE (Horton, 2012). Zeaxanthin formation is also related to a qE-independent component

termed zeaxanthin-dependent quenching (qZ), which relaxes more slowly (10-15 minutes) (Dall'Osto et al., 2005, Demmig-Adams and Adams, 1996, Kress and Jahns, 2017, Nilkens et al., 2010). Finally, sustained, long-term quenching due to damage to PSII core protein D1 (pI) is attributed to photoinhibition (Ruban, 2017), and takes substantially longer to recover as it requires *de novo* synthesis of the D1 protein (Aro et al., 1993, Keren and Krieger-Liszkay, 2011). More recently, the newly-termed qH was identified a photoinhibition-independent sustained quenching process (Malnoë, 2018). Beyond qE, qZ, qH and qI, other mechanisms also contribute to light-induced changes in NPQ even if they do not correspond to enhanced heat dissipation of absorbed energy. Chloroplast movements (qM) can help to adjust photon absorption (Banaś et al., 2012, Cazzaniga et al., 2013) and state transitions (qT) redistribute light-harvesting complex II (LHCII) from PSII to PSI (Ruban and Johnson, 2009). Both processes can therefore affect apparent NPQ but do not involve a genuine quenching process.

Although the exact distinction between C_3 and C_4 NPQ remains unclear, there are hints of functional differences between both photosynthetic pathways affecting the NPQ response, in particular relating to CEF capacity, pigment content, antioxidant capacity, and chloroplast movements (Doulis et al., 1997, Guidi et al., 2019, Huang et al., 2015b, Ogawa et al., 2023, Romanowska et al., 2017, Sage et al., 2014, Strand et al., 2017). Previous work in maize (*Zea maize*) found a rapid decrease in NPQ after a transition from high to low light (Doncaster et al., 1989), and it has been suggested that the higher CEF found in C_4 species could be contributing to photoprotection by increasing ΔpH and stimulating qE, leading to faster relaxation (Huang et al., 2015a, Huang et al., 2015b, Miyake et al., 2005). Two CEF routes have been identified in land plants, one via a chloroplast NADH dehydrogenase-like (NDH) complex (Peltier et al., 2016) and the other via a proton gradient regulation 5 (PGR5)/PGR5-like photosynthetic phenotype 1 (PGRL1) heterodimer (Munekage et al., 2002). Whereas C_3 species predominantly use the PGR5/PGRL1 pathway, which has been reported as involved in ΔpH-dependent NPQ (Munekage et al., 2002, Suorsa et al., 2012, Yamori et al., 2016), the NDH pathway plays a substantial role in C_4 species that cannot be complemented by PGR5/PGRL1 (Nakamura et al., 2013, Ogawa et al., 2023, Peterson et al., 2016, Takabayashi et al., 2005). Both pathway complexes were found to be more abundant in C_4 than in C_3 *Flaveria* species (Nakamura et al., 2013) although the extent to which PGR5/PGRL1 and NDH individually contribute to C_4 NPQ is still uncertain. Additionally, smaller pools of xanthophyll cycle pigments have been found in maize than in C_3 species, which suggests energy dissipation in some C_4 plants is less

reliant on zeaxanthin content and qZ (Romanowska et al., 2017). The specialisation of M and BS cells also comes with different antioxidant capacity – enzymes like ascorbate peroxidase (APX) and superoxide dismutase (SOD) are mainly localised to BS cells (Doulis et al., 1997), potentially minimising the accumulation of ROS and suppressing qI. Non-quenching mechanisms could also vary. qM could be impaired in C_4 species where chloroplast movements are slower, require more intense light than the homologous C_3 response, and are typically limited to M cells while BS chloroplasts remain in centrifugal or centripetal position (Kobayashi et al., 2008, Sage et al., 2014). Finally, the differential ratios of PSI/PSII between the BS and the M in C_4 species could lead to different CEF relative to LEF (Majeran et al., 2010, Meierhoff and Westhoff, 1993, Takabayashi et al., 2005) but also cause differences in qT.

In this chapter, the aim was to characterise the differences in NPQ relaxation between C_3 and C_4 species. To avoid phylogenetic distance confounding comparisons between photosynthetic pathways (Taylor et al., 2010), the initial characterisation was conducted across three phylogenetically linked pairs of C_3 and C_4 species from *Alloteropsis*, *Flaveria* and *Cleome* genera (respectively, C_3 *Alloteropsis semialata GMT* & C_4 *Alloteropsis semialata MDG*, C_3 *Flaveria cronquistii* & C_4 *Flaveria bidentis*; and C_3 *Tarenaya hassleriana* & C_4 *Gynandropsis gynandra*). Leaves were dark adapted, and NPQ measured during a 1-hour 600 µmol m^{-2} s^{-1} photon flux density (PFD) light period followed by 25 minutes of darkness. To test for the role of individual quenching mechanisms within C_3 and C_4 species, the *Flaveria* and *Cleome* pairs were used for a series of experiments where chemical inhibitors, specific light treatments, and mutants were used to manipulate known components of NPQ. The results showed clear, systematic differences in NPQ relaxation between C_3 and C_4 species during light to dark transitions: the 0-2 minute component was significantly larger, whilst the 2-15 minute component was smaller than in C_3 species, which contributed to overall faster relaxation in C_4 species. The qE component was particularly significant in C_4 species. The results also indicated a potential role for CEF, but the exact pathway remained unclear.

4.2. Materials and methods

4.2.1. Plant materials

For NPQ comparisons between photosynthetic pathways, pairs of phylogenetically linked C_3 and C_4 species from *Alloteropsis*, *Flaveria*, and *Cleome* were selected to control for evolutionary distance (species shown in **Table 1.1**, phylogenetic trees can be found in **Figure**

1.1). Considerable evolutionary distance still exists between the three genera, with the C_4 origin occurring independently in each and dating back to ~17 million years (Ma) in *Cleome*, ~2 Ma in *Flaveria*, and even more recently in *Alloteropsis* (Christin et al., 2011, Lundgren et al., 2015). The selected species encompass monocots (*Alloteropsis*) and dicots (*Flaveria*, *Cleome*) and the three major decarboxylating enzymes suggested to be dominant in different C_4 pathways: NADP-ME/PEPCK in C_4 *A. semialata MDG* (Ueno and Sentoku, 2006), NADP-ME in C_4 *F. bidentis* (Gowik et al., 2011), and NAD-ME in C_4 *G. gynandra* (Bräutigam et al., 2010). Due to limited plant material, the *Alloteropsis* species were only used in the initial comparisons.

Further exploration of the effects of state transitions and chloroplast movements on NPQ relaxation was undertaken using *Arabidopsis thaliana* homozygous mutants lacking either serine/threonine kinase STN7 or chloroplast unusual positioning 1 (CHUP1). Mutant lines *stn7-1* (SALK_073254) (Bellafiore et al., 2005), *stn7-2* (SALK_134469), *chup1* (SALK_129128C) (Schmidt von Braun and Schleiff, 2008), and wild type (WT) ecotype Columbia-0 (Col-0) were obtained from NASC (Nottingham Arabidopsis Stock Centre, Nottingham, UK) and verified by PCR.

The role of CEF in C_4 NPQ was also studied in C_4 *F. bidentis* knockdown lines generated by RNA interference (RNAi) of proton gradient regulation-like 1 (PGRL1, *PGRL1*-RNAi) and chloroplast NADH-dehydrogenase-like complex (NDH, *NdhO*-RNAi) (Ogawa et al., 2023) via a collaboration with Yuri Munekage.

4.2.2. Plant growth and propagation

Alloteropsis accessions were vegetatively propagated and tillers grown in a 4:1 mix of Levington Advance M3 compost (Scotts, Ipswich, UK) and vermiculite in 2 L pots, with 25 g of Miracle-Gro All Purpose Continuous Release Osmocote (Scotts Miracle-Gro Company, Marysville, OH, USA) added per 5 L, whilst the *Flaveria* and *Cleome* were grown in 0.25 L pots and the soil mix did not include vermiculite. Since *F. cronquistii* requires vegetative propagation, *F. bidentis* plants were also vegetatively propagated– lateral shoot cuttings were dipped in Doff Hormone Rooting Powder (Doff Portland Ltd., Hucknall, UK) to induce root development. *Cleome* species were grown from seed, and germination was induced with a 30 ºC/20 ºC day/night cycle for *T. hassleriana*, and at 30ºC for *G. gynandra.* Seedlings were subsequently sown in 24-cell trays before being potted. *Alloteropsis* accessions were well-watered and grown in semi-controlled conditions in a glasshouse at the Cambridge University Botanic Garden at 18-25 ºC, 40-60% RH. In addition to incoming irradiance, supplemental

lightning was provided to a minimum of 140-160 µmol m^{-2} s^{-1} PFD over a 16-hour photoperiod. Measurements were taken 2 weeks after propagation. *Flaveria* and *Cleome* species were well-watered and grown in a Conviron walk-in growth room (Conviron Ltd., Winnipeg, MB, CA) at 20 ºC, 60% relative humidity (RH), and 150 µmol m^{-2} s^{-1} PFD over a 16-hour photoperiod. *Flaveria* species were measured after 8-10 weeks of growth, and to coordinate the different *Cleome* developmental rates, *G. gynandra* and *T. hassleriana* at 8-10 and 4-6 weeks respectively.

A. thaliana Col-0, *stn7* and *chup1* were grown from seed in a 4:1 mix of Levington Advance F2 compost and sand in 0.25 L pots. Seeds were stratified at 4 ºC for 3 days and then transferred to a Conviron growth chamber at 20 ºC, 60% RH, and 200 µmol m^{-2} s^{-1} PFD over an 8-hour photoperiod, where plants were hand-watered. Chlorophyll fluorescence measurements on *A. thaliana* were conducted on 7-9 week old plants.

The *PGRL1*-RNAi, *NdhO*-RNAi, and WT C_4 *F. bidentis* plants were grown at Kwansei Gakuin University (Japan) in a 3:2 mix of soil and vermiculate, in a growth chamber at 24 ºC and 250 µmol m^{-2} s^{-1} PFD over a 12-hour photoperiod. *NdhO*-RNAi plants were measured by the Munekage lab after 12-16 weeks and all other plants after 8-10 weeks..

4.2.3. Chlorophyll fluorescence setup and experimental plan

Chlorophyll fluorescence was measured on young, fully expanded leaves using an open gas exchange system (LI-6400XT, LI-COR, Lincoln, NE, USA) with an integrated leaf chamber fluorometer (6400-40 LCF, LI-COR). Chamber conditions were controlled at 410 ppm sample CO_2 concentration, 30-60% relative humidity, 25 ºC block temperature, and flow rate of 300 µmol s^{-1}. Average VPD at the start of treatment, end of light period, and end of dark period was respectively 1.56 ± 0.02, 1.69 ± 0.02, and 1.58 ± 0.02 kPa. Actinic light was provided by the LCF and, except for an all red light treatment, composed of 10% blue (470 nm) and 90% red light (630 nm). The LCF used a 0.25 Hz modulated measuring light and a multiphase flash (Loriaux et al., 2013) to measure chlorophyll fluorescence parameters.

4.2.4. Chlorophyll fluorescence measurements and experimental plan

Leaves were dark-adapted until stomatal conductance and net CO_2 exchange rate reached constant levels (between 30-60 minutes depending on the species). Subsequently, leaves were illuminated with 600 µmol m^{-2} s^{-1} PFD for 1 hour, before returning to darkness for another 25 minutes. To derive chlorophyll fluorescence parameters, saturating flashes were used to measure steady (F and F') and maximal (F_m and F_m') fluorescence in darkness and light.

Saturating flashes were provided five minutes before the lights were switched on, at 3, 5, 10, 15, 25, 35, 45, and 60 minutes of light exposure; and 30 seconds after return to darkness and then every 90 seconds. The maximum quantum efficiency of PSII (F_v/F_m), quantum efficiency of PSII (ΦPSII), and NPQ were derived (Bilger and Björkman, 1990, Genty et al., 1989) from fluorescence measurements.

This protocol was used to explore differences in NPQ between the C_3 and C_4 pairs (**Table 4.1**) The protocol was first used on all C_3 and C_4 phylogenetic pairs for initial comparisons; Subsequently, *Flaveria* and *Cleome* C_3-C_4 pairs were measured again following infiltration with a specific chemical inhibitors of NPQ and using the protocol with 100% red light. Finally, the protocol was also used on specific mutant lines in *A. thaliana* Col-0, (*stn7-1, stn7-2,* and *chup1*) and in C_4 *F. bidentis* (*PGRL1*-RNAi and *NdhO*-RNAi).

Table 4.1: Set of experiments for the characterisation of C_3 and C_4 NPQ differences, including the NPQ component being tested, the mechanism of action of experimental treatment, the plant species the experiment was conducted on, and, if applicable, chemical infiltrator concentrations.

NPQ component	Experiment	Mechanism of action	Plant species
All	NPQ trace across light induction and return to darkness	---	*Alloteropsis, Flaveria,* and *Cleome* C_3 and C_4 pairs
qE + qZ	100 µM Nigericin infiltration	H+/K+ antiporter nigericin collapses the proton gradient across the thylakoid membrane, inhibiting ΔpH-dependent qE and violaxanthin de-epoxidation (Johnson and Ruban, 2010)	*Flaveria* and *Cleome* C_3 and C_4 pairs
qZ	5 mM DTT infiltration	Violaxanthin de-epoxidase inhibitor DTT, blocks zeaxanthin formation (Neubauer, 1993).	*Flaveria* and *Cleome* C_3 and C_4 pairs
qM + qT	Light treatment with 100% red light	Chloroplast movements and state transitions are both induced by blue light (Mullineaux and Allen, 1990, Sakai et al., 2001)	*Flaveria* and *Cleome* C_3 and C_4 pairs
qT	STN7 mutants	STN7 required for state transitions (Bellafiore et al., 2005).	*A. thaliana*
qM	CHUP1 mutants	CHUP1 required for chloroplast movement (Schmidt von Braun and Schleiff, 2008)	*A. thaliana*
CEF-related	250 µM Antimycin A	Ferredoxin-plastoquinone reductase activity inhibitor antimycin A inhibits the PGR5/PGRL1 CEF pathway (DalCorso et al., 2008).	*Flaveria* and *Cleome* C_3 and C_4 pairs
	250 µM Piericidin A	NADH dehydrogenase inhibitor piericidin A (Lümmen, 1998).	*Flaveria and Cleome C_3 and C_4 pairs*
	PGRL1 and NDH mutants	Knockdown lines lacking the PGR5/PGRL1 or NDH CEF pathway (Ogawa et al., 2022)	C_4 *F. bidentis*

4.3. Chemical infiltrations

Leaves of *Flaveria* and *Cleome* species were left in darkness for 30 minutes and vacuum infiltrated in a syringe with a medium (20 mM HEPES/KOH pH 7.0) supplemented with NPQ chemical inhibitors: 100 μM nigericin, 5 mM DTT, 250 μM Antimycin A, or 250 μM Piericidin A (see **Table 4.1** for inhibitor details). Controls were infiltrated with the medium and equivalent volume of chemical inhibitor solvent. Following infiltration, leaves were patted dry and left to dark adapt for an additional 20-30 minutes before measurements commenced.

4.3.1. NPQ analysis

To quantify general differences in NPQ induction and relaxation, the area under the curve (AUC) (Makowski et al., 2019) of the light and post-illumination periods was integrated using the trapezoidal rule (Jawień, 2014). Differences in the relative makeup of NPQ were explored by separating NPQ relaxation into three component phases: 0-2 minutes, 2-15 minutes, and 15-25 minutes. The amount of NPQ contributed by each component was calculated by subtracting NPQ at the start from NPQ at the end of the phase. For ease of comparison, components were expressed as a proportion of NPQ at the end of the light treatment.

To quantify the effect of photoprotective quenching versus mechanisms that also show as NPQ, such as chloroplast movements or state transitions, actual F_0' – which in the dark is assumed to be equal to F' – and calculated F_0' (**Equation 3A**) (Oxborough and Baker, 1997) were used to obtain photochemical quenching in the dark (qP_d, **Equation 3B**) (Ruban, 2017). ΦPSII was also compared to 'ideal' ΦPSII (**Equation 3C**) where qP is assumed to be 1, i.e. when photodamage or alternative PSII-affecting mechanisms are absent.

$$F_0{}'_{calc} = \frac{F_0}{\frac{F_v}{F_m} + \frac{F_0}{F_m{}'}} \quad \textbf{Equation 3A}$$

$$qP_d = \frac{F_m{}' - F_0{}'_{act}}{F_m{}' - F_0{}'_{calc}} \quad \textbf{Equation 3B}$$

$$\Phi PSII_{ideal} = \frac{qP \times \frac{F_v}{F_m}}{1 + (1 - \frac{F_v}{F_m}) \times NPQ} \quad \textbf{Equation 3C}$$

4.3.2. Statistical analysis

All treatments and species sets (phylogenetic pairs or WT and mutants) were run as independent experiments, and statistical analyses were conducted on paired *Alloteropsis, Flaveria* and *Cleome* species, or on *A. thaliana* and C_4 *F. bidentis* mutant lines and WT.

On the initial comparison of three phylogenetic pairs, one-way ANOVA was used to test for differences between photosynthetic pathways in the AUC of NPQ relaxation, and NPQ components. For chemical inhibitor and light compositions treatments, two-way ANOVA was used to test for the effects of photosynthetic pathway, treatment, and their interactions on AUC of NPQ and NPQ components. The effect of genotype in *A. thaliana* and *F. bidentis* mutants on NPQ AUC, NPQ components, and qP_d was tested for with a one-way ANOVA between WT and the mutant phenotypes. In all analyses, assumptions of normality, homogeneity of variance, and sphericity were tested for and satisfied. Mean and standard error of the mean for NPQ, NPQ AUC, total of NPQ component, and qP_d were calculated if appropriate for reporting.

Plots and data analysis were done in R 4.1.1 (R Core Team, 2021) on RStudio 2023.03.1+446 (Posit Team, 2022) using packages tidyverse (Wickham et al., 2019), RcolorBrewer (Neuwirth, 2014), lme4 (Bates et al., 2015), and bayestestR (Makowski et al., 2019).

4.4. Results

4.4.1. NPQ relaxation is faster and more significant in C_4 compared to C_4 species

To characterise differences in C_3 and C_4 NPQ responses, NPQ was measured on leaves exposed to 600 µmol m^{-2} s^{-1} PFD and subsequently returned to darkness (**Figure 4.1**). Although there was limited variation between photosynthetic types for NPQ induction patterns, NPQ relaxation was significantly faster and more substantial in C_4 species in all three phylogenetic comparisons.

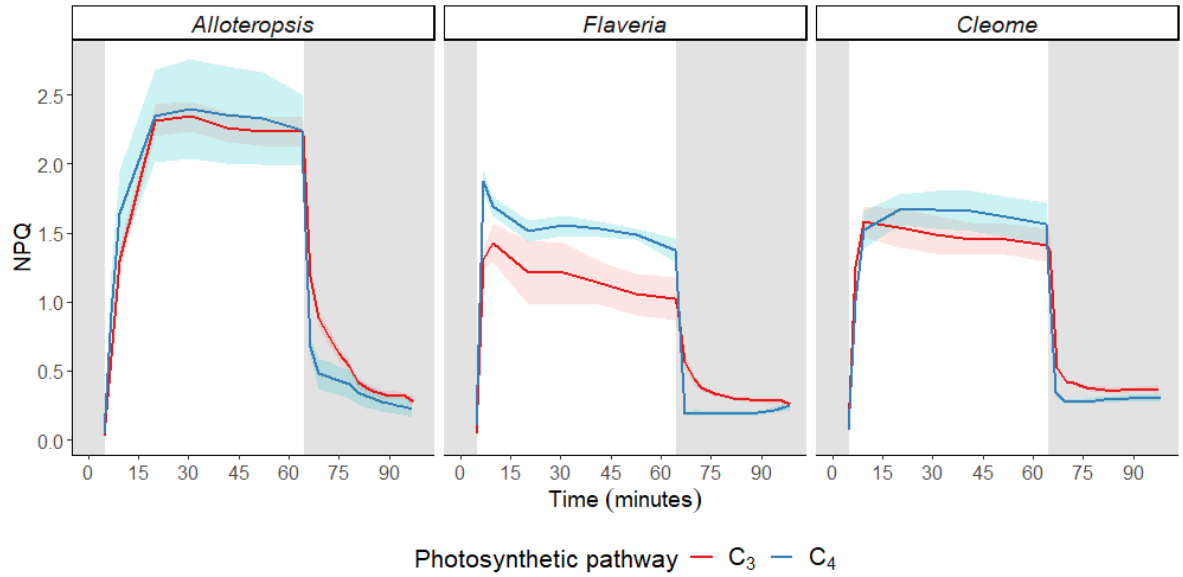

Figure 4.1: NPQ measurements of phylogenetically linked C_3 and C_4 *Alloteropsis, Flaveria* and *Cleome* species during a 1 hour 600 µmol m^{-2} s^{-2} PFD photoperiod followed by 25 minutes of darkness. Ribbons represent standard error of the mean (n = 5).

Table 4.2: ANOVA table of AUC of NPQ during the light period and of the relaxation components in the dark between phylogenetically linked C_3 and C_4 species of the *Alloteropsis*, *Flaveria* and *Cleome* genera. Table shows degrees of freedom; *F*-value; and *p*-value. Significant *p*-values ($a < 0.05$) are shown in bold.

Period of analysis	Compared values	*Alloteropsis*	*Flaveria*	*Cleome*
Light or dark period	AUC of NPQ during light period	1,8; 0.23; 0.64	1,8; 3.79; 0.09	1,8; 0.18; 0.68
	AUC of NPQ relaxation	1,8; 1.32; 0.29	1,8; 16.7; **0.003**	1,8; 6.81; **0.03**
Relaxation components	0-2 minutes	1,8; 23.58; **0.005**	1,8; 36.32; **≤0.001**	1,8; 75.79; **≤0.001**
	2-15 minutes	1,8; 89.36; **≤0.001**	1,8; 230.75; **≤0.001**	1,8; 11.2; **0.015**
	15-25 minutes	1,8; 0.06; 0.81	1,8; 1.32; 0.29	1,8; 5.41; 0.06

After the light to dark transition (**Figure 4.1**) NPQ in C_4 species dropped sharply, in contrast with the slower exponential decline observed in C_3 species. The increased speed of relaxation was particularly evident in C_4 *F. bidentis* and C_4 *G. gynandra*, where further reductions in NPQ were limited after the initial drop. Although C_4 *A. semialata MDG* had more gradual relaxation of NPQ, the initial decline upon switching to darkness was much more substantial than in C_3 *A. semialata GMT.* One-way ANOVA (**Table 4.2**) found the fast decline of NPQ in C_4 species resulted in significantly lower AUC NPQ values during the dark period in the *Flaveria* ($P = 0.03$) and *Cleome* ($P \leq 0.01$) comparisons (**Figure 4.2 A**). In C_4 *F. bidentis* AUC NPQ during dark relaxation was 33% lower than in C_3 *F. cronquistii* and similarly, 21% lower in C_4 *G. gynandra*

than in C_3 *T. hassleriana*. Although not significant ($P = 0.29$), C_4 *A. semialata MDG* also had 21% lower AUC NPQ during dark relaxation than C_3 *A. semialata GMT*. NPQ induction varied across genera, but C_3 and C_4 phylogenetic pairs of the same genus exhibited similar NPQ dynamics in the light and no significant difference in induction AUC NPQ between photosynthetic types was found in any comparison (**Table 4.2**).

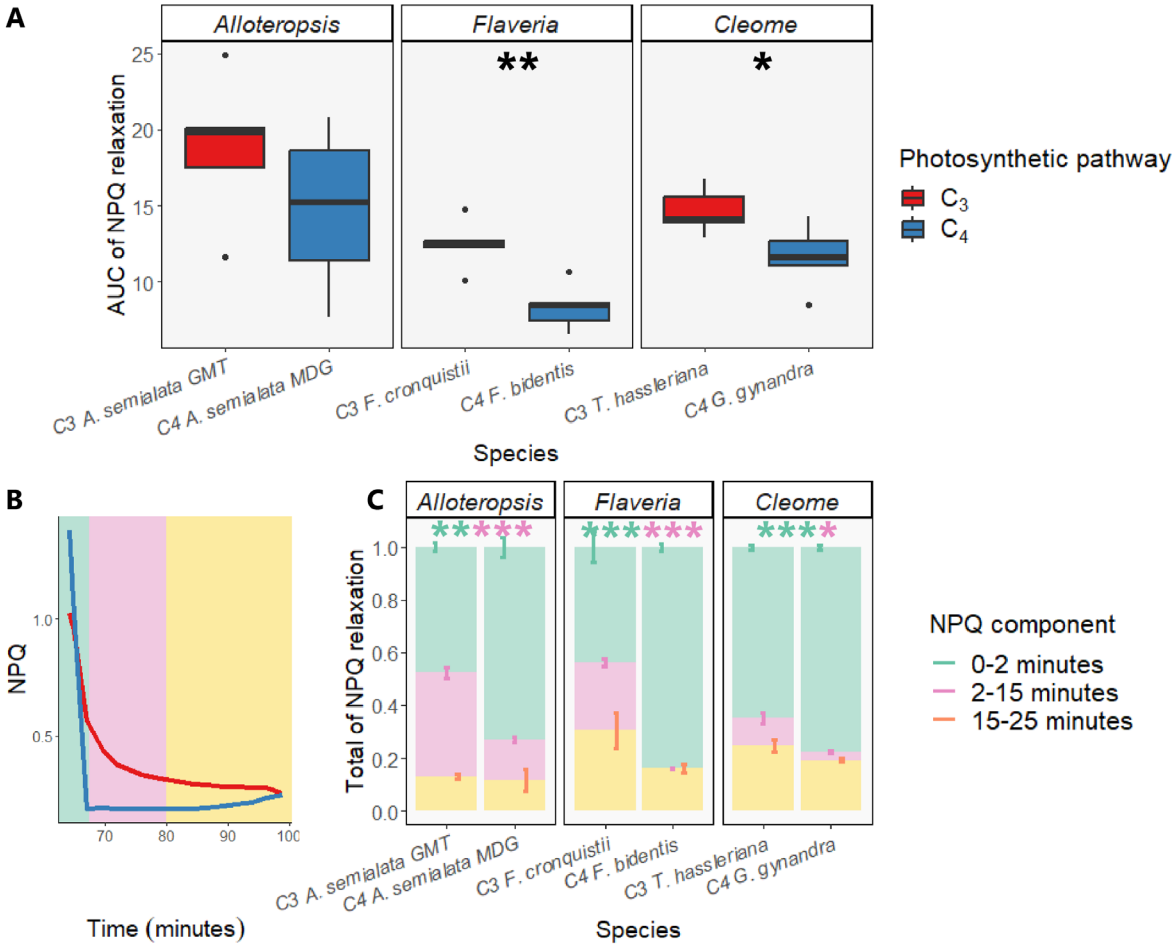

Figure 4.2: Differences in NPQ relaxation between C_3 and C_4 *Alloteropsis, Flaveria* and *Cleome* species. **A)** Differences in AUC of NPQ relaxation between phylogenetic pairs. Box edges represent first and third quartiles, the solid line indicates the median, and points represent outliers beyond 1.5 times the interquartile range. Asterisks represent significant differences in NPQ AUC found by one-way ANOVA between photosynthetic pathways. **B)** Sample NPQ relaxation of C_4 *F. bidentis* and C_3 *F. cronquistii* illustrating the time separation of the NPQ component analysis, **C)** NPQ components based on time of relaxation and expressed as a function of total NPQ. Error bars represent standard error of the mean and asterisks significant differences in the NPQ component of the matching colour found by one-way ANOVA between photosynthetic pathways. * $P \leq 0.05$, ** $P \leq 0.01$, *** $P \leq 0.001$, one-way ANOVAs in **Table 4.2** (n = 5).

As NPQ consists of multiple mechanisms, components were first analysed by separating NPQ relaxation into different timescales of deactivation (**Figure 4.2 B** illustrates the time separation), subsequently expressed as a function of total NPQ. Clear differences in NPQ components were found between C_3 and C_4 species (**Figure 4.2 C**). One-way ANOVA (**Table 4.2**) found that the component that relaxed within a 0-2 minute timeframe was significantly greater in C_4 species in all tested genera compared to their phylogenetic C_3 pairs. The 0-2 minute component in C_4 *A. semialata MDG* was 0.73±0.04 compared to 0.47±0.02 in C_3 *A. semialata GMT* ($P \leq 0.01$), 0.84±0.01 in C_4 *F. bidentis* compared to 0.44±0.06 in C_3 *F. cronquistii* ($P \leq 0.001$), and 0.78±0.01 in C_4 *G. gynandra* versus 0.65±0.01 in C_3 *T. hassleriana* ($P \leq 0.001$). The 2-15 minute in turn represented a significantly smaller fraction in C_4 than in C_3 species. This interval was 0.15±0.007 in C_4 *A. semialata MDG* relative to 0.39±0.02 in C_3 *A. semialata GMT* ($P \leq 0.001$), C_4 *F. bidentis* had 0.0002±0.003 relative to C_3 *F. cronquistii* 0.26±0.01 ($P \leq 0.001$), and C_4 *G. gynandra* had 0.03±0.006 compared to C_3 *T. hassleriana* 0.10±0.02 ($P \leq 0.015$). The results of this NPQ component analysis suggest that even when considering natural variation between genera, there are fundamental differences in the composition of C_3 and C_4 NPQ, with fast relaxation mechanisms that act within a seconds to minutes timeframe constituting a larger component of C_4 NPQ and medium-term relaxation mechanisms playing a larger role in C_3 NPQ.

4.4.2. ΔpH-dependent NPQ mechanisms are more prominent in C_4 than in C_3 species

To further explore the observed differences in the makeup of NPQ between C_3 and C_4 species, *Flaveria* and *Cleome* leaves were infiltrated with chemical inhibitor nigericin to explore the role of the proton gradient on NPQ. The nigericin-induced collapse of the proton gradient (**Figure 4.3**) caused a greater depression of NPQ induction in both C_4 species than in their C_3 counterparts, with C_4 *F. bidentis* showing a reduction of NPQ AUC of 87% in comparison to 63% in C_3 *F. cronquistii*, and of 94% in C_4 *G. gynandra* compared to 78% in C_3 *T. hassleriana*. In line with these observations, two-way ANOVA (**Table 4.3**) found significant interactions between photosynthetic type and nigericin infiltration within *Flaveria* ($P \leq 0.001$) and *Cleome* ($P \leq 0.001$) – C_4 species trended towards lower NPQ values with a collapsed proton gradient, suggesting greater dependence on NPQ mechanisms like qE and qZ that rely on ΔpH.

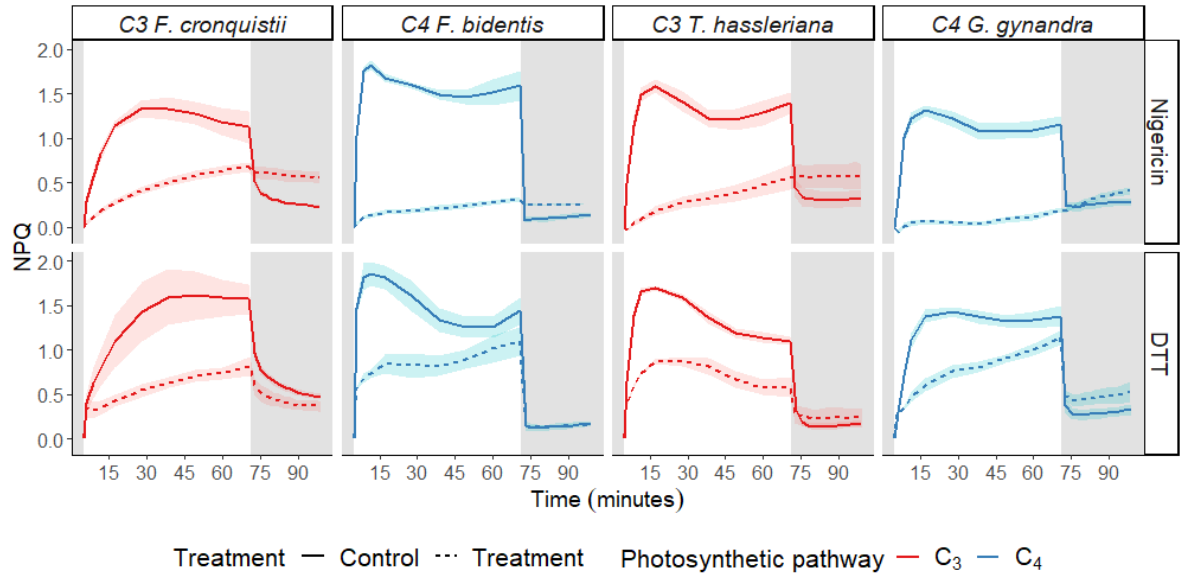

Figure 4.3: NPQ measurements comparing the effect of nigericin and DTT infiltration on phylogenetically linked C_3 and C_4 *Alloteropsis, Flaveria* and *Cleome* species during a 1 hour 600 µmol m^{-2} s^{-2} PFD photoperiod followed by 25 minutes of darkness. Dashed lines represent the chemical infiltration treatment. Ribbons represent standard error of the mean (n = 5), two-way ANOVAs in **Table 4.3**.

Table 4.3: ANOVA table of AUC of NPQ during the light period on the effect of nigericin, DTT, Antimycin A and Piericidin A chemical infiltration treatments, in phylogenetically linked C_3 and C_4 species of the *Flaveria* and *Cleome* genera. Photosynthetic pathway, PP. Treatment, T. Interaction effect, PP:T. Table shows degrees of freedom; *F*-value; and *p*-value. Significant *p*-values ($\alpha < 0.05$) are shown in bold.

	Flaveria			***Cleome***		
Compared values	**PP**	**T**	**PP:T**	**PP**	**T**	**PP:T**
Nigericin AUC of NPQ	1,16; 1.62; 0.22	1,16; 300.05; **≤0.001**	1,16; 29.24; **≤0.001**	1,16; 0.05; 0.83	1,16; 269.16; **≤0.001**	1,16; 26.32; **≤0.001**
DTT AUC of NPQ	1,16; 2.41; 0.14	1,16; 22.89; **≤0.001**	1,16; 0.15; 0.74	1,16; 1.01; 0.33	1,16; 128.01; **≤0.001**	1,16; 1.37; 0.26
Antimycin A AUC of NPQ	1,16; 0.94; 0.35	1,16; 15.29; **0.001**	1,16; 6.84; **0.02**	1,16; 2.86; 0.11	1,16; 14.49; **0.002**	1,16; 7.71; **0.02**
Piericidin A AUC of NPQ	1,16; 6.41; **0.02**	1,16; 0.85; 0.36	1,16; 0.008; 0.93	1,16; 3.75; 0.07	1,16; 0.67; 0.42	1,16; 0.56; 0.46

To then isolate the impact of qZ and the xanthophyll cycle, leaves were infiltrated with VDE inhibitor DTT (**Figure 4.3**) Although all species showed reduced NPQ activation when treated with DTT, in C_3 *F. cronquistii* and C_3 *T. hassleriana* the depression was sustained throughout the photoperiod whereas their respective phylogenetic pairs C_4 *F. bidentis* and C_4 *G. gynandra* trended upwards towards control values. Two-way ANOVA (**Table 4.3**) found DTT infiltration to significantly decrease NPQ ($P \leq 0.001$), but no found no significant effect of species (at least $P \leq 0.14$) or of its interaction with DTT (at least $P \leq 0.26$). This suggests the increased

reduction of NPQ found in nigericin-treated C_4 species is mostly due to differences in qE rather than qZ.

4.4.3. Non-quenching components of NPQ do not affect relaxation kinetics in either photosynthetic type

To evaluate the contribution of state transitions and chloroplast movements, both of which can be induced by blue light (Mullineaux and Allen, 1990, Ohgishi et al., 2004, Sakai et al., 2001), *Flaveria* and *Cleome* leaves were tested under control 90% red and 10% blue light, and 100% red light (**Figure 4.4 A**). Across all species comparisons, no significant effect of treatment nor of its interaction with species was found in NPQ AUC during the light or dark phase (**Table 4.4**). The lack of significant response to a treatment lacking blue light suggests the role of chloroplast movements and state transitions on NPQ at 600 µmol m^{-2} s^{-1} PFD is very limited in C_3 and C_4 *Flaveria* and *Cleome* species. These results were further supported by experiments with *A. thaliana stn7* (**Figure 4.4 B**) and *chup1* (**Figure 4.4 D**) which also suggested a marginal role of state transitions and chloroplast movements in photoprotection, at least in C_3 species. Induction and relaxation of NPQ in these mutant lines were tested against the Col-0 WT control under the 90% red 10% blue light regime, and one-way ANOVA found no significant effect of genotype (**Table 4.5**). As non-quenching mechanisms can hide true photoprotective NPQ, qP_d (Ruban, 2017) was also calculated for all plants to quantify the efficiency of photoprotection (**Figure 4.4 C & E**), but qP_d in Col-0 and all mutant lines yielded very similar results (**Table 4.5**).

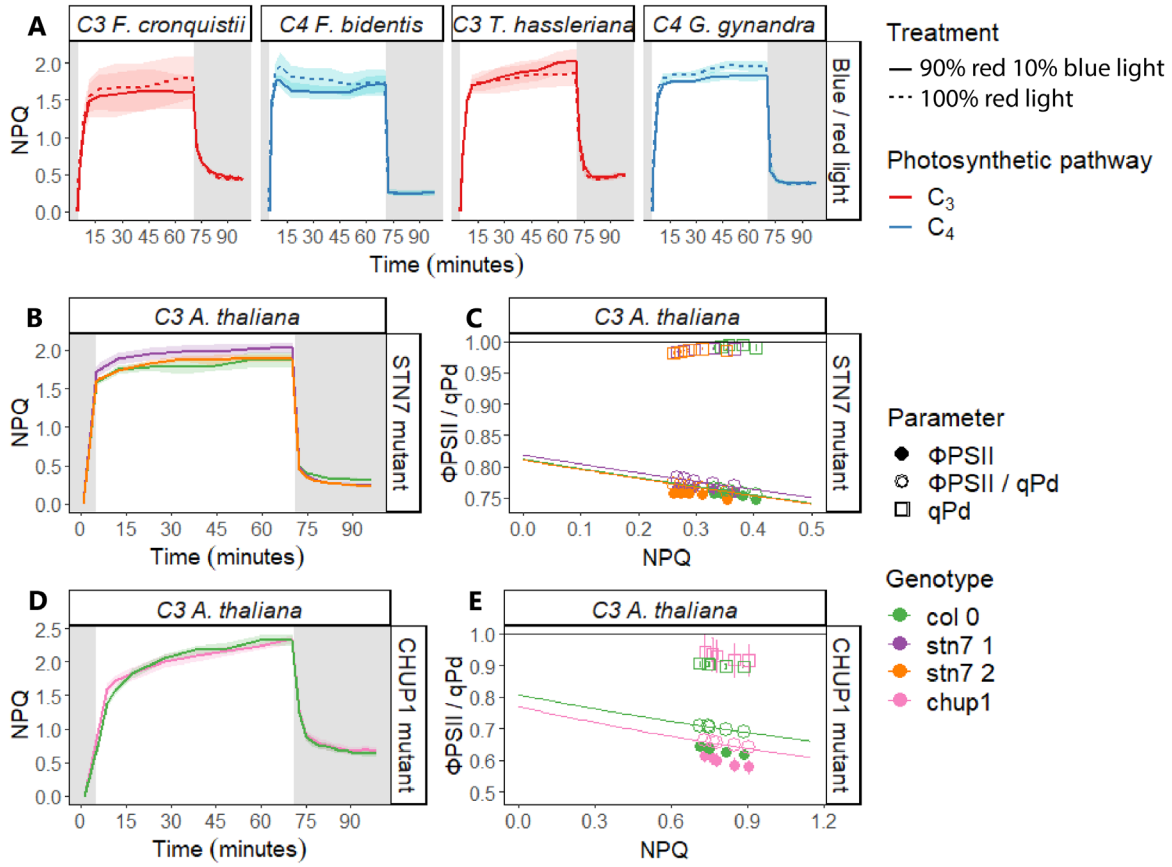

Figure 4.4: Differences in qT and qM across C_3 and C_4 species. **A)** NPQ measurements comparing the effect on NPQ of a negative 100% red light control to the standard light composition of 90% red 10% blue in C_3 and C_4 *Flaveria* and *Cleome*. Dashed lines represent the 100% red light treatment, two-way ANOVAs in **Table 4.4**, ribbons represent standard error of the mean. NPQ measurements of *A. thaliana* Col-0 WT with **B)** *stn7-1* and *stn7-2*, and **D)** *chup1*, with one-way ANOVA in **Table 4.5,** ribbons represent standard error of the mean. **C & E)** Quantifying the efficiency of photoprotection of STN7 and CHUP1 knockout lines as per Ruban et al. 2017. The theoretical yield of PSII (line) was calculated using Equation 3, and photochemical quenching in the dark (squares, from Equation 2) was used as a proxy for photoprotective quenching. Error bars represent standard error of the mean, one-way ANOVAs in **Table 4.4**. (n = 5).

Table 4.4: ANOVA table of AUC of NPQ of 0% blue and 100% red light treatment during the light and NPQ relaxation periods, in phylogenetically linked C_3 and C_4 species of the *Flaveria* and *Cleome* genera. Photosynthetic pathway, PP. Treatment, T. Interaction effect, PP:T. Table shows degrees of freedom; *F*-value; and *p*-value. Significant *p*-values ($a < 0.05$) are shown in bold.

	Flaveria			***Cleome***		
Experiment Compared values	**PP**	**T**	**PP:T**	**PP**	**T**	**PP:T**
Blue / red light AUC of NPQ during light period	1,16; 0.39; 0.54	1,16; 0.30; 0.59	1,16; 0.005; 0.94	1,16; 0.52; 0.92	1,16; 0.16; 0.89	1,16; 0.59; 0.45
Blue / red light AUC of NPQ relaxation	1,16; 37.57; **≤0.001**	1,16; 0.02; 0.89	1,16; 0.38; 0.85	1,16; 16.95; **0.001**	1,16; 0.18; 0.68	1,16; 0.95; 0.35

Table 4.5: ANOVA table of parameters of mutant *A. thaliana* (*stn7-1, stn7-2, chup1*) and *F. bidentis* (*pgrl1, ndho1*). Table shows degrees of freedom; *F*-value; and *p*-value. Significant *p*-values ($\alpha < 0.05$) are shown in bold.

Mutant	Parameters	Genotype effect from ANOVA
A. thaliana stn7-1	AUC of NPQ during light period	1,8; 2.64; 0.14
	AUC of NPQ relaxation	1,8; 3.15; 0.09
	qP_d	1,8; 2.64; 0.14
A. thaliana stn7-2	AUC of NPQ during light period	1,8; 0.24; 0.63
	AUC of NPQ relaxation	1,8; 3.78; 0.08
	qP_d	1,8; 0.24; 0.64
A. thaliana chup1	AUC of NPQ during light period	1,8; 0.013; 0.91
	AUC of NPQ relaxation	1,8; 0.19; 0.67
	qP_d	1,8; 2.54; 0.14
F. bidentis pgrl1	AUC of NPQ during light period	1,4; 30.45; **0.005**
	AUC of NPQ relaxation	1,4; 4.81; 0.09
	0-2 minute	1,4; 17.67; **0.02**
	2-15 minute	1,4; 0.08; 0.80
	15-25 minute	1,4; 52.42; **0.005**
F. bidentis ndho1	AUC of NPQ during light period	1,4; 1.82; 0.25
	AUC of NPQ relaxation	1,4; 11.57; **0.03**
	0-2 minute	1,4; 13.4; **0.05**
	2-15 minute	1,4; 9.19; **0.05**
	15-25 minute	1,4; 12.14; **0.05**

4.4.4. Cyclic Electron Flow could play a role in the fast relaxation of C_4 NPQ

Genetic and chemical approaches were used to test whether higher CEF in C_4 photosynthesis, suggested to fulfil the increased C_4 ATP requirements, also affects qE. The same induction/relaxation protocol was used on C_4 *F. bidentis* knockdown lines (Ogawa et al., 2023) by collaborators in the Munekage lab to evaluate the role of the PGR5/PGRL1 and NDH CEF pathways (**Figure 4.5 A**). NPQ was significantly impaired in *pgrl1* (one-way ANOVA, **Table 4.5**) leading to a reduction in NPQ AUC by 77% relative to WT ($P \leq 0.01$). The *ndho1* lines eventually reached the same NPQ values as the WT but slower induction resulted in a non-significant 25% reduction of NPQ AUC ($P \leq 0.25$). Interestingly, kinetics of *ndho1* NPQ relaxation were somewhat more akin to the exponential decrease observed in C_3 species rather than the instant drop of NPQ in the WT. Component separation of NPQ relaxation for each genotype (**Figure 4.5 B**) showed the 0-2 minute component was a significantly lower fraction of total NPQ in both *pgrl1* (0.43±0.06, $P = 0.02$) and *ndho1* (0.67±0.08, $P \leq 0.05$) than in the WT (0.89±0.02), according to a one-way ANOVA (**Table 4.5**). The *ndho1* (0.27±0.09, $P \leq 0.05$) and *pgrl1* (0.50±0.04, $P \leq 0.01$) also had significantly greater 15-25 minute component of NPQ than the WT (0.13±0.01), and the slower relaxation kinetics of *ndho1* also resulted in a significantly larger proportion of the 2-15 minute component (0.06±0.01, $P \leq 0.05$) than WT (0.01±0.02). The component analysis of the mutants and the shape of induction and relaxation suggested that whilst both PGRL5/PGRL1 and NDH CEF pathways contribute to the 0-2 minute component, in C_4 *F. bidentis* NDH plays a specific role in the initial fast induction and relaxation observed in the WT phenotype.

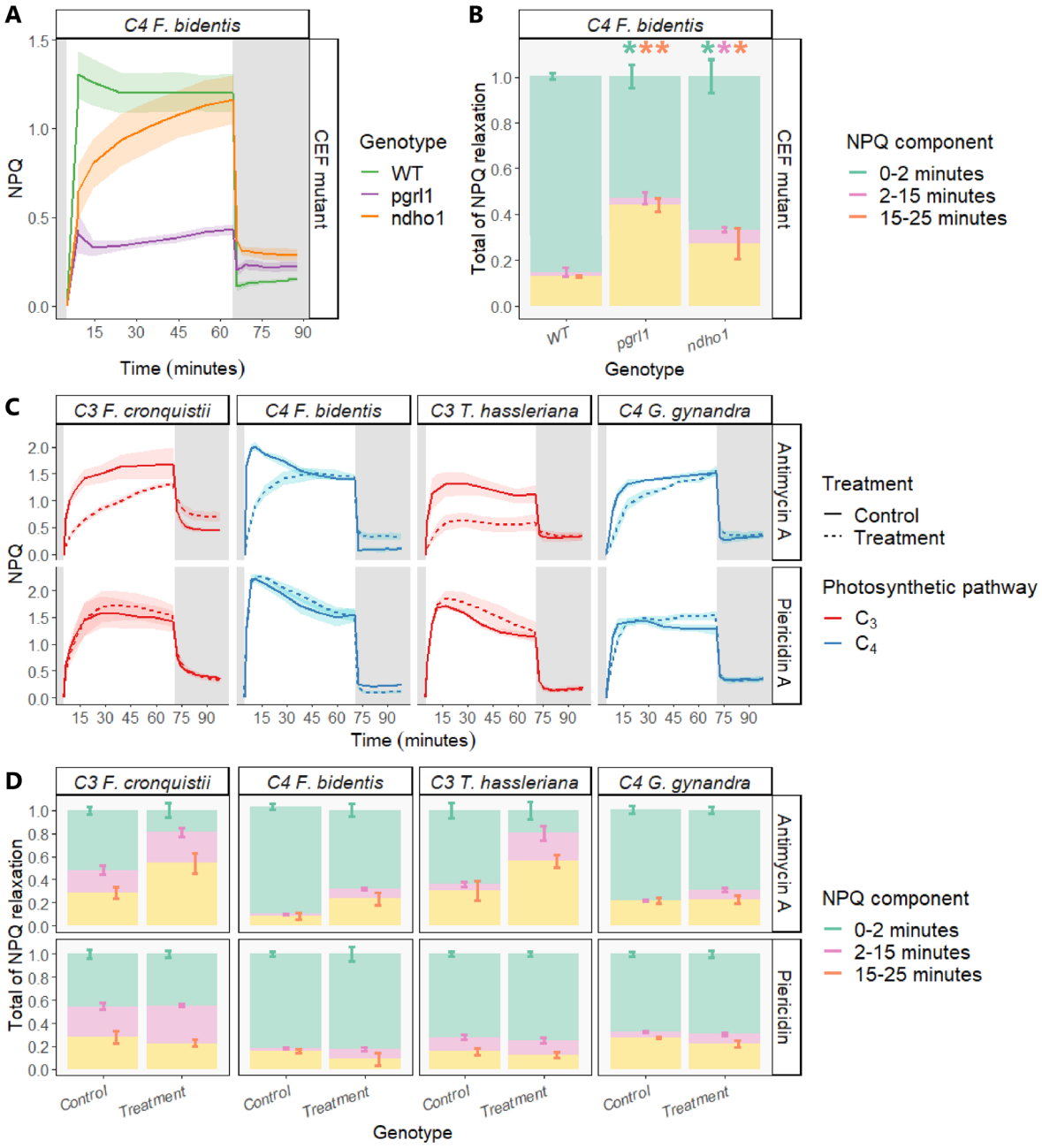

Figure 4.5: Cyclic electron flow and NPQ. From C_4 *F. bidentis* WT and *pgrl1* and *ndho1* lines **A)** NPQ measurements during photoperiod and subsequent return to darkness, one-way ANOVA in **Table 4.5**, ribbon represents standard error of the mean. **B)** NPQ components based on time of relaxation and expressed as a function of total NPQ. Error bars represent standard error of the mean and asterisks significant differences in the NPQ component of the matching colour found by one-way ANOVA (**Table 4.5**) between WT and the respective mutant line. * $P \leq 0.05$, ** $P \leq 0.01$, *** $P \leq 0.001$. From C_3 and C_4 *Flaveria* and *Cleome*, **C)** NPQ measurements comparing the effect of Antimycin A and Piericidin A. Dashed lines represent the chemical infiltration treatment. Ribbons represent standard error of the mean, two-way ANOVAs in **Table 4.3**. **D)** NPQ components based on time of relaxation and expressed as a function of total NPQ. Error bars represent standard error of the mean, two-way ANOVAs in **Table 4.6** (n = 5).

As a complementary test of the role of CEF pathways, *Flaveria* and *Cleome* leaves were also infiltrated with either PGR5/PGRL1 pathway inhibitor Antimycin A, or NDH pathway inhibitor Piericidin A (**Figure 4.5 C**). All leaves treated with Antimycin A had lower NPQ AUC during the light period, with a 41% and 55% reduction observed in C_3 *F. cronquistii* and C_3 *T. hassleriana*, and of 23% and 19% in C_4 *F. bidentis* and C_4 *G. gynandra*. C_3 species experienced a more sustained loss of NPQ compared to C_4 species, where after the first few minutes of induction NPQ rose consistently towards control levels. Two-way ANOVA (**Table 4.3**) found the interaction of photosynthetic pathway and Antimycin A to have a significant effect on NPQ, with infiltrated C_4 leaves being associated with a less marked reduction in NPQ than their C_3 pairs ($P = 0.02$). The components of NPQ relaxation (**Figure 4.5 D**) support the main difference between photosynthetic types occurring in the 0-2 minute component, where there was a significant interaction between Antimycin A and photosynthetic type (at least $P \leq 0.05$), with C_3 species being associated with greater reductions in the 0-2 minute component than their C_4 pairs when infiltrated with Antimycin A, and corresponding increases in the 2-15 minute component (**Table 4.6**). Surprisingly, in stark contrast to the results observed in the *ndho1* lines, Piericidin A did not have a significant effect on NPQ induction for most of the tested species (**Figure 4.5 C**, **Table 4.3**). This extended to NPQ components, where unlike the changes observed in the C_4 *F. bidentis ndho1* lines, there was no significant effect of Piericidin A infiltration (**Table 4.5**). This set of infiltration experiments provide evidence for CEF supporting qE in both C_3 and C_4 species via the PGR5/PGRL1 pathway, although contrasting results from Piericidin A infiltration leave the role of the NDH pathway undecided.

Table 4.6: ANOVA table of NPQ relaxation components during Antimycin A and Piericidin A chemical infiltration, in phylogenetically linked C_3 and C_4 species of the *Flaveria* and *Cleome* genera. Photosynthetic pathway, PP. Treatment, T. Interaction effect, PP:T. Table shows degrees of freedom; *F*-value; and *p*-value. Significant *p*-values ($\alpha < 0.05$) are shown in bold.

		Flaveria			***Cleome***		
Experiment	**Relaxation components**	**PP**	**T**	**PP:T**	**PP**	**T**	**PP:T**
Antimycin A chemical infiltration	0-2 minute	1,16; 92.45; **≤0.001**	1,16; 25.99; **≤0.001**	1,16; 5.46; **0.05**	1,16; 31.50; **≤0.001**	1,16; 20.59; **≤0.001**	1,16; 8.66; **0.01**
	2-15 minute	1,16; 1.17; **≤0.001**	1,16; 53.98; **0.02**	1,16; 0.30; 0.58	1,16; 9.31; **0.008**	1,16; 15.02; **0.001**	1,16; 1.87; 0.19
	15-25 minute	1,16; 19.03; **≤0.001**	1,16; 8.64; **0.009**	1,16; 0.78; 0.39	1,16; 15.47; **0.002**	1,16; 4.92; **0.04**	1,16; 4.59; **0.05**
Piericidin A chemical infiltration	0-2 minute	1,16; 77.23; **≤0.001**	1,16; 1.17; 0.29	1,16; 0.03; 0.85	1,16; 5.68; **0.02**	1,16; 0.31; 0.58	1,16; 0.03; 0.86
	2-15 minute	1,16; 231.89; **≤0.001**	1,16; 2.01; 0.09	1,16; 0.00; 0.99	1,16; 9.23; **0.007**	1,16; 0.18; 0.68	1,16; 0.93; 0.35
	15-25 minute	1,16; 10.67; **0.03**	1,16; 4.1; 0.06	1,16; 0.04; 0.84	1,16; 14.18; **0.001**	1,16; 0.50; 0.48	1,16; 0.19; 0.66

4.5. Discussion

4.5.1. C_4 species have a greater initial reduction in NPQ and thus significantly faster relaxation

Differences in NPQ between C_3 and C_4 species were investigated in phylogenetically controlled comparisons under a 600 µmol m^{-2} s^{-1} PFD photoperiod followed by a transition to darkness. The results revealed that despite similar induction dynamics, C_4 species in all tested genera (*Alloteropsis, Flaveria* and *Cleome*) exhibited significantly faster and overall greater NPQ relaxation than their C_3 pairs (**Figure 4.1 & 4.2 A, Table 4.2**). This result corroborates previous work on maize where a comparatively faster initial relaxation of NPQ relative to C_3 barley (*Hordeum vulgare*) was also observed (Doncaster et al., 1989), even if only superficially explored. Although there exists significant natural variation in NPQ (Cowling et al., 2021, Rungrat et al., 2019, Wang et al., 2020), the consistent differences shown here were observed between closely related C_3 and C_4 pairs with significant evolutionary distance between them, implying the difference in NPQ dissipation is likely to derive from specific features of the photosynthetic pathway.

These results have major implications for our understanding of C_4 species under dynamic light conditions and potential efforts to improve photosynthesis. Previous comparisons of C_3 and C_4 species under fluctuating light conditions found C_4 species had stronger and more sustained CO_2 assimilation than their C_3 counterparts after a transition to lower light (Arce Cubas et al.,

2023a, Lee et al., 2022, Li et al., 2021). Rapid NPQ relaxation could contribute to the higher CO_2 fixation observed in the C_4 species right after a drop in light intensity, as the quantum yield of PSII is less transiently depressed than in C_3 species. In the dynamic light environments of leaf canopies, the elevated qE of C_4 plants could substantially increase photosynthetic efficiency by avoiding the carbon assimilation losses from slow rates of NPQ relaxation during periods of intermittent shade (Kaiser et al., 2018, Wang et al., 2020, Zhu et al., 2004). Beyond the ecological significance, NPQ relaxation is an important target for improvement of photosynthetic efficiency (Sales et al., 2021, Wang et al., 2020, Zhu et al., 2004) and if faster NPQ relaxation is a characteristic of C_4 photosynthesis, the yield increases achieved in C_3 species via increasing the rate of qE and qZ dissipation (De Souza et al., 2022, Kromdijk et al., 2016) might not be replicable to the same extent in C_4 plants. However, some room for improvement might still exist – a recent semi-high-throughput study on maize found variation across lines in maximum values, residual NPQ in the dark, and speed of induction and relaxation (Sahay et al., 2023). Further research into the molecular mechanisms underlying C_4 photoprotection may yet uncover alternative ways to improve NPQ kinetics: Sahay et al. also identified novel candidate genes involved in NPQ kinetics, some of which were shown to have a similar role in *Arabidopsis thaliana*.

4.5.2. An elusive mechanism of action: fast-relaxing component qE makes up a greater proportion of C_4 than C_3 NPQ

The comparatively faster NPQ relaxation found in C_4 plants seemed to be due to a difference in NPQ composition between C_3 and C_4 species. Separation of NPQ into components based on timescales revealed C_4 NPQ had a significantly higher proportion of the 0-2 minute component, whereas the 2-15 minute component was more prevalent in C_3 species (**Figure 4.2 C, Table 4.2**). While C_4 *F. bidentis* and C_4 *G. gynandra* leaves infiltrated with nigericin showed a substantially greater depression in NPQ compared to C_3 *F. cronquistii* and C_3 *T. hassleriana*, DTT infiltration resulted in a similar reduction in both species, suggesting the difference between photosynthetic types is due to qE rather than qZ (**Figure 4.3, Table 4.3**).

qE requires low lumen pH and is aided by the PsbS protein (Nicol and Croce, 2021). CEF has been found to support the formation of ΔpH and thus qE activation (Takahashi et al., 2009). The greater proportion of qE observed in C_4 *F. bidentis* and C_4 *G. gynandra* could be linked to the higher rates of CEF in C_4 plants to meet the energetic requirements of the CCM (Huang et al., 2015a, Huang et al., 2015b, Miyake et al., 2005). CEF is further discussed in the next section, but beyond increased capacity for recycling electrons around PSI, the more significant

presence of the CEF NDH pathway in C_4 species could also contribute to lumen acidification (Strand et al., 2017). Higher rates of PsbS expression have also been found to increase rates of qE induction and relaxation (Hubbart et al., 2012, Li et al., 2002a, Li et al., 2002b, Zia et al., 2011) and although the relative abundance of the protein in C_3 and C_4 species has not been studied, the higher ratio of PSI/PSII found across C_4 species (Majeran et al., 2010, Meierhoff and Westhoff, 1993, Takabayashi et al., 2005) could also result in a higher PsbS/PSII ratio and enhanced NPQ response times.

4.5.3. Cyclic Electron Flow and C_4 species: do pathways make a difference?

C_3 and C_4 species differentially operate the CEF PGR5/PGRL1 and NDH pathways, with the NDH pathway having a more substantial role in C_4 photosynthesis (Munekage et al., 2002, Ogawa et al., 2023, Takabayashi et al., 2005). Although some results indicate this CEF pathway differentiation could contribute to the fast relaxation kinetics observed in C_4 species, contradictory observations between genetic and chemical approaches complicate the interpretation.

The PGR5/PGRL1 pathway is the predominant CEF route in C_3 species (Munekage et al., 2002) and indeed, Antimycin A infiltration had a greater dampening effect on C_3 *F. cronquistii* and C_3 *T. hassleriana* than on C_4 *F. bidentis* and C_4 *G. gynandra* (**Figure 4.5 C, Table 4.3**). Despite these differences, the significant impact of antimycin A infiltration on NPQ induction in all tested species illustrates the role of this CEF route in supporting ΔpH-dependent NPQ in both photosynthetic types (Suorsa et al., 2012, Yamori et al., 2016). Whilst the C_4 *F. bidentis* PGRL1 knockdown line also experienced a significant decrease in NPQ during the photoperiod (**Figure 4.5 A, Table 4.5**), this reduction was of 77% compared to the WT – much higher than the 23% decrease from the control found in Antimycin A-treated C_4 *F. bidentis*. Additionally, the infiltrated C_4 *F. bidentis* had a significantly higher proportion of the 2-15 minute component relative to the control due to slower NPQ relaxation (**Figure 4.5 C & D, Table 4.6**), an effect not present in the knockout line (**Figure 4.5 B, Table 4.5**). These differences in results highlight some of the limitations of each approach. Knockdown lines are specifically deficient in the gene product of interest, but the long-term pleiotropic effects of the deficiency can be substantial and more difficult to predict. Meanwhile, Antimycin A infiltration acts transiently but also inhibits mitochondrial respiration via Complex III (Sweetlove et al., 2002). Since inhibition of respiratory activity has also been shown to decrease the NPQ activation and relaxation response (Cardol et al., 2010), this could offer an alternative explanation for the

slower relaxation observed specifically in Antimycin A-infiltrated plants (**Figure 4.5 D, Table 4.3**). Despite differences across experimental treatments, results suggest that CEF via the PGR5/PGRL1 pathway does play a role in qE in both C_3 and C_4 species.

NDH is more abundant in C_4 than in C_3 species (Nakamura et al., 2013) and the NDH CEF pathway is integral to meeting the higher ATP demands of C_4 photosynthesis (Peterson et al., 2016, Takabayashi et al., 2005). Given its proton-pumping stoichiometry, NDH has been hypothesised to favour "reverse" operation under high ΔpH and a predominantly reduced PQ pool, an expected condition immediately after a reduction in light intensity (Strand et al., 2017). Thus, although the difference in speed of NPQ dissipation between C_3 and C_4 species could simply be due to higher rates of CEF from multiple pathway operation, NDH reversibility could also contribute to faster qE deactivation by rapidly dissipating ΔpH. C_4 *F. bidentis* NDH knockdown lines support a role for the NDH pathway in the faster relaxation of C_4 NPQ: the 0-2 minute component of NPQ was significantly reduced compared to the WT (**Figure 4.5 B, Table 5**), and a slower rate of NPQ dissipation was evident in both a more significant 2-15 minute component and a shape of NPQ relaxation (**Figure 4.5 A**) more reminiscent of the exponential decay seen in C_3 *F. cronquistii* (**Figure 4.5 C**). However, the results of Piericidin A infiltration were dissonant, as the treatment did not significantly affect NPQ induction nor relaxation and its components in C_3 or C_4 *Flaveria* and *Cleome* species (**Figure 4.5 C & D, , Table 4.6**). NDH knockdown lines of C_4 *F. bidentis* experience drastically delayed growth and suppressed CO_2 assimilation, so observed NPQ phenotypes could be caused by long-term physiological impairments. However, Piericidin A infiltration has previously primarily been done on isolated thylakoid membranes (Ikezawa et al., 2002), and whole leaf infiltration might have been less successful due to method, concentration, or resting time. Given Piericidin A is also an inhibitor of mitochondrial respiration, via Complex I (Zhou and Fenical, 2016), the lack of effect of treatment contrasts with the observations under Antimycin A infiltration (**Figure 4.5 C & D**), making a failure to successfully infiltrate with Piericidin A perhaps more likely. Ultimately, although the NDH pathway shows some promise as a contributing mechanism to faster C_4 NPQ relaxation, further studies are required to confirm the role of CEF as an explanation for the observed C_3-C_4 differences in NPQ and settle the NDH contribution to CEF and qE. These experiments would be strongly benefited by an inducible NDH mutant in *C_4 F. bidentis* which could limit the impact of pleiotropic effects such as the diminished growth seen

in the constitutive NDH knockdown lines, and a C_3 *F. cronquistii* NDH knockdown line could provide a point of comparison.

4.5.4. qM and qT play a limited role in NPQ for both C_3 and C_4 species

The light treatment experiments suggests that the qM and qT components, both of which avoid PSII photon absorption rather than actually quench (Cazzaniga et al., 2013, Ruban and Johnson, 2009), did not significantly contribute towards NPQ in either the C_3 or C_4 *Flaveria* and *Cleome* species under 600 µmol m^{-2} s^{-1} PFD light intensity with 10% blue light. Blue light directly triggers chloroplast avoidance responses via photoreceptors (Ohgishi et al., 2004, Sakai et al., 2001) and is more strongly absorbed by PSII. This can lead to a more reduced plastoquinone pool, which is thought to induce STN7 kinase activation and result in state transitions (Mullineaux and Allen, 1990). However, no significant difference in either NPQ induction or relaxation was found in any of the tested species between a negative control of 100% red light, and the standard light composition used across the study of 90% red and 10% blue light (**Figure 4.4 A, Table 4.4**).

The blue-light dependent qM component of NPQ was originally identified in phototropin 2 - deficient (*phot2*) mutants, which lack chloroplast avoidance responses. In these lines, a missing fluorescence decay component correlated with leaf transmittance changes from chloroplast relocation and was absent under red light (Cazzaniga et al., 2013). However, more recently the validity of qM has been called into question, as the blue-light dependent 'component' of NPQ was also found in *phot2* and *chup1* as well as WT, indicating independence from blue light-dependent chloroplast movements (Wilson and Ruban, 2020). In this chapter, no significant difference in either NPQ values (**Figure 4.4 D, Table 4.5**) nor in photoprotective capacity specifically (**Figure 4.4 E, Table 4.5**; Ruban and Murchie, 2012) was found when comparing *A. thaliana* Col-0 WT with *chup1* under the standard 90%:10% red and blue light treatment. Chloroplast movements are significantly more constrained in C_4 than in C_3 species (Sage et al., 2014, Sage and McKown, 2006), and while the chloroplast avoidance response may support C_3 photosynthetic efficiency under high light by allowing for more uniform light penetration into the leaf (Osborne and Raven, 1986) and more efficient CO_2 diffusion between chloroplasts (Evans, 1999), there appears to be no significant difference between C_3 and C_4 qM at the given light intensity.

In a similar vein, *A. thaliana stn7-1* and *stn7-2* did not exhibit significantly different NPQ or qP_d from the Col-0 WT (**Figure 4.4 B & C, Table 4.5**). In combination with the light

composition experiment, this suggests qT does not play a significant role in the difference between C_3 and C_4 NPQ observed in this chapter, but differential operation of state transitions between photosynthetic pathways cannot be discounted. The classical state transition model switches between LHCII association with PSII in state I, to PSI in state II in a change triggered by increases in light intensity and excess PSII excitation so under changing light conditions qT balances photosystem excitation by rebalancing excess energy between PSI and PSII (Ruban and Johnson, 2009). Most of what we know about qT comes from C_3 species, but BS chloroplast have been found to support LHCII-PSI association in C_4 *Flaveria trinervia* (Nakamura et al., 2013), to exist in a permanent state 2 in maize (Rogowski et al., 2018), and models for state 1 and state 2 arrangements across M and BS chloroplasts depending on C_4 subtype have been suggested (Wasilewska-Dębowska et al., 2022), although whether these differences have a significant effect on NPQ still requires further study.

4.6. Conclusion

The above set of experiments compared C_3 and C_4 NPQ responses between phylogenetically linked species and sought to understand differences in NPQ composition through a variety of light, chemical, and genetic treatments. The results showed *Alloteropsis*, *Flaveria*, and *Cleome* C_4 species all had faster rates of NPQ relaxation in comparison with the slower dissipation of NPQ found in their C_3 counterparts. Further experiments on the *Flaveria* and *Cleome* species found a greater proportion of qE in C_4 species, potentially due to differential operation of CEF pathways. Although the complexity of NPQ molecular mechanisms as well as the lack of existing knowledge of C_4 NPQ dynamics mean further study is required to confirm the mechanism of action for C_4 qE, the presented work has major implications for both our understanding of C_4 photosynthesis under dynamic light conditions, and regarding efforts to improve photosynthesis via more efficient regulation of NPQ.

5. Conclusion

5.1. Thesis findings

Plant canopies in the open field are extremely dynamic light environments. Photosynthetic responses often lag behind changes in light intensity, potentially leading to losses in carbon assimilation and making the response to dynamic conditions a valuable target for the improvement of photosynthesis (Long et al., 2022, Taylor and Long, 2017, Wang et al., 2020, Zhu et al., 2004). Although in recent years there has been increased interest in characterising photosynthetic responses to non-steady environments, most of the work has been conducted on C_3 species, and there is a gap in knowledge regarding the effect of the C_4 pathway on dynamic light responses (Guidi et al., 2019, Slattery et al., 2018). This thesis aimed to improve understanding of C_4 photosynthetic performance under dynamic light environments through a comparative analysis against congeneric C_3 species, and to identify potential targets for photosynthetic improvement. These aims were achieved through the following work, conducted on independent phylogenetically controlled comparisons between C_3 and C_4 species from the *Alloteropsis, Flaveria* and *Cleome* genera (**Figure 1.1**):

Chapter 2 compared C_3 and C_4 photosynthetic pathways during light induction to test whether C_4 species are more affected by transient decreases in photosynthetic efficiency than C_3 species. The results confirmed that C_4 species have slower activation of CO_2 assimilation during photosynthetic induction than C_3 species, but the specific mechanism behind the differences varied between genera, highlighting the importance of controlling for evolutionary variation when comparing photosynthetic pathways.

Chapter 3 evaluated the photosynthetic efficiency of C_3 and C_4 photosynthesis under fluctuating light relative to steady state, looking at both transitions to and from low and high light under protocols with repeat fluctuations of different lengths. This chapter demonstrated that when comparing C_4 with C_3 species, elevation of CO_2 assimilation immediately following the transition to low light was higher and more sustained in C_4 plants, whereas the CO_2 assimilation patterns found during the reverse switch to high light varied across species or possibly due to subtype differences. The opposing hypotheses regarding the efficiency of C_4 photosynthesis under fluctuating light found in the literature (Slattery et al., 2018, Stitt and Zhu,

2014) were reconciled by showing that the duration of each light step in the fluctuation light protocol strongly influences experimental outcomes.

Chapter 4 tested whether the NPQ kinetics of C_3 and C_4 photosynthesis had a different proportional makeup of NPQ components by characterising the induction and relaxation responses, and further studying observed differences to identify the underpinning mechanisms. The results revealed that despite similar induction dynamics, C_4 species had significantly faster and overall greater NPQ relaxation than C_3 species due to a greater proportion of qE. The intrinsically faster NPQ relaxation rate in C_4 species suggests that speeding up NPQ relaxation may have less potential as a target for improvement in C_4 than in C_3 species, demonstrating the importance of understanding differences in photosynthetic pathways.

Overall, the thesis used a powerful experimental set up to account for phylogenetic differences when comparing photosynthetic pathways and thereby could characterise differences in photosynthetic efficiency and NPQ responses specifically related to photosynthetic pathway in C_3 and C_4 species during light induction and transitions to lower light. The results suggest that specific features of the C_4 pathway, like the enlarged metabolite pools and enhanced CEF contribution, could be important determinants of the photosynthetic performance under dynamic light. The following sections expand on the results of the chapters summarised above and discuss some of the implications of the overall findings of the thesis and future directions.

5.2. Principal thesis conclusions

5.2.1. C_3 and C_4 photosynthetic induction responses

Photosynthetic efficiency during light induction was measured and compared to steady state responses under both 21% and 2% O_2 in C_3 and C_4 phylogenetic pairs from *Alloteropsis*, *Flaveria*, and *Cleome* species (**Figure 2.4**). The results confirmed that the activation of CO_2 assimilation is generally slower in C_4 photosynthesis (Mott and Woodrow, 2000, Pearcy and Seemann, 1990, Sassenrath-Cole and Pearcy, 1992), as all C_4 species experienced greater lag in CO_2 assimilation at the start of light induction than C_3 species across all comparisons (**Figure 2.5**, **Table 2.3**). However, the underlying mechanism for slower activation was genus specific: in C_4 *F. bidentis*, 2% O_2 increased CO_2 assimilation and reduced the transfer of electrons per fixed CO_2 (**Figure 2.6**, **Table 2.4**), suggesting that the observed lags in induction under ambient conditions could be due to incomplete suppression of photorespiration from slow C_4 cycle activation which may stem from the need to build up metabolic intermediates for CCM

activation (Sage and McKown, 2006). While measurements under 2% O_2 in C_4 *A. semialata MDG* and C_4 *G. gynandra* also reflected diminished electron sinks, CO_2 assimilation did not increase, implying C_3 cycle activation was the main limiting factor rather than CCM operation (Mott and Woodrow, 2000, Sassenrath-Cole and Pearcy, 1992).

A potential supporting role of photorespiration during photosynthetic induction was also suggested by the results in this chapter, as 2% O_2 actually suppressed the activation of CO_2 assimilation in C_3 *T. hassleriana* and both C_3 and C_4 *Alloteropsis* species (**Figure 2.5**, **Table 2.3**). The photorespiratory pathway has also been suggested to help prime the C_4 cycle by providing a carbon source from which to build both C_3 and C_4 metabolite pools (Fu and Walker, 2022, Kromdijk et al., 2014, Medeiros et al., 2022, Stitt and Zhu, 2014, Wang et al., 2014b, Weber and von Caemmerer, 2010). Alternatively, reverse sensitivity to O_2 in C_3 species has been linked to TPU limitations (Sharkey, 1985) – reduced photorespiratory activity could result in suboptimal stromal phosphate levels and a transient exacerbation of TPU limitations. However, prior to this thesis very little data was available for the impact of these phenomena in C_4 species (Zhou et al., 2019). Indeed, the results reported here may be the first to suggest that this mechanism also affects CO_2 assimilation in C_4 species.

5.2.2. C_4 photosynthetic efficiency under fluctuating light

Photosynthetic responses to fluctuating light were measured in C_3 and C_4 phylogenetic pairs of *Alloteropsis*, *Flaveria* and *Cleome* species, under 21% and 2% oxygen. Leaves were subjected to repetitive stepwise changes in light intensity (800 and 100 μmol m^{-2} s^{-1} PFD) with the length of each light step lasting 6, 30,and 300 s (**Figure 3.2**).

Results supported the hypothesis that C_4 species are better able to sustain photosynthetic rates after a transition to lower light than C_3 species – C_4 species achieved significantly higher photosynthetic rates relative to steady state than their C_3 pairs under the same fluctuating light regime, and under both oxygen concentrations, suggesting the difference could not solely be attributed to photorespiration (**Figure 3.3 & 3.4 D-F**, **Table 3.3**). During 6 and 30 s fluctuations, the ΦCO_2 of C_4 species was calculated to be higher than the theoretical maximum (Ehleringer and Pearcy, 1983, Ishikawa et al., 2016, Yin and Struik, 2018), strongly indicating an energy supply outside of the thylakoid light reactions (**Figure 3.5 E-H**, **Table 3.4**). This provides evidence for the hypothesis that large metabolite pools necessary for the transfer of CCM intermediates between M and BS cells and the reversible reactions throughout the pathway can

provide and store ATP and reducing equivalents and support photosynthesis during changes in light intensity (Arrivault et al., 2017, Leegood and von Caemmerer, 1989, Stitt and Zhu, 2014).

The response to the transition to higher light varied across comparisons. Mixed NADP-ME/PEPCK subtype C_4 *A. semialata MDG* showed both the highest rates of assimilation relative to steady state and was not affected by light step duration (**Figure 3.4 A-C**, **Table 3.3**), indicating faster photosynthetic induction. In contrast, carbon assimilation during the high light phase in NAD-ME C_4 *G. gynandra* and NADP-ME C_4 *F. bidentis* was considerably lower with shorter fluctuations. Theoretical work suggests mixed C_4 pathways could be less reliant on the establishment of large metabolite pools due to the ability to concurrently use different transfer acids (Wang et al., 2014a, Yin and Struik, 2021), which is consistent with the observations in this chapter as well as previous work (Lee et al., 2022, Li et al., 2021). The distinctive assimilation kinetics of C_4 *G. gynandra* (most evident in **Figure 3.2 I & R**) had a CO_2 gulp and a burst at the start of the high light period, and another CO_2 burst upon transitioning to lower light, which were independent of photorespiration. These patterns have been observed primarily in other NAD-ME species (Laisk and Edwards, 1997, Lee et al., 2022) and linked to specific regulation of decarboxylation and PEP carboxylation in the NAD-ME pathway (Ishikawa et al., 2016).

Crucially, the capacity of C_4 species to buffer through transitions to lower light and restart high rates under high light decreased with duration of the light steps, presumably as metabolite pools depleted over time (Slattery et al., 2018). The inverse relationship between carbon assimilation relative to steady state and the length of fluctuations reconciles the opposing results found in previous work (Laisk and Edwards, 1997, Lee et al., 2022, Li et al., 2021) – studies with different fluctuating light regimes can yield different estimates of the comparative advantage of C_4 and C_3 photosynthesis depending on the specific length of the low and high light periods of the fluctuating regime.

5.2.3. Differences in the NPQ response of C_3 and C_4 species

NPQ induction and relaxation was characterised in phylogenetically linked C_3 and C_4 species of the *Alloteropsis, Flaveria* and *Cleome* genera (**Figure 4.1**). Further genetic and chemical experiments to attempt to identify the mechanistic source of the differences were conducted on the *Flaveria* and *Cleome* pairs (**Table 4.1**). The results of the initial characterisation showed that all C_4 species had significantly faster and overall greater NPQ relaxation (**Figure 4.2 A**, **Table 4.2**) than their C_3 pairs due to C_4 NPQ having a greater proportion of a fast relaxing (0-

2 minutes) component (**Figure 4.2 C**, **Table 4.2**). Chemical infiltration experiments identified this component as qE (**Figure 4.3**, **Table 4.3**).

The greater proportion of qE observed in C_4 *F. bidentis* and C_4 *G. gynandra* could be linked to the higher rates of CEF found in C_4 species (Huang et al., 2015a, Huang et al., 2015b, Miyake et al., 2005), seeing as CEF-dependent ΔpH has already been shown to contribute to qE formation in C_3 species (Takahashi et al., 2009). Differential operation of CEF pathways could also play a role, as in addition to the PGR5/PGRL1 pathway, in C_4 species the NDH pathway also has a more substantial role (Munekage et al., 2002, Ogawa et al., 2023, Takabayashi et al., 2005), which could either contribute to higher CEF rates or as has been previously suggested (Strand et al., 2017), the reverse operation of NDH could contribute to faster qE deactivation by contributing to ΔpH dissipation. Genetic and chemical approaches (**Figure 5**, **Table 4.3**) demonstrated that the PGR5/PGRL1 played a role in qE formation in both C_3 and C_4 species but yielded contradictory results regarding the role of NDH – in C_4 *F. bidentis* NDH knockdown lines a slower rate of NPQ dissipation was evident as well as a reduced 0-2 minute component, supporting a role for the NDH pathway in the faster relaxation of C_4 NPQ, but infiltration by NDH-inhibitor Piericidin A had no significant effect. Given the limitations present within both approaches, further work is required to confirm the role of specific CEF pathways in C_4 NPQ. The higher qE of C_4 species may also be related to altered expression of PsbS, which has been found to affect qE induction and relaxation (Hubbart et al., 2012, Li et al., 2002a, Li et al., 2002b, Zia et al., 2011), or the proportion of PsbS relative to PSII. Further exploration of this hypothesis would require determination of the relative abundance of the protein in C_3 and C_4 species, which has yet to be studied. Finally, no significant effect of qM nor qT was observed in any species (**Figure 4**, **Table 4.3 & 4.4**), nor in selected mutant lines in *Arabidopsis thaliana*. The apparent lack of effect from chloroplast movements on NPQ found across this chapter in C_3 species is in line with recent work that calls the validity of qM into question (Wilson and Ruban, 2020).

5.3. Discussion and future directions

5.3.1. Importance of sources of variation within experimental design

Controlling for phylogenetic distance is important when comparing C_3 to C_4 photosynthesis due to the large species variation that exists across comparisons (Taylor et al., 2010). Some of the differences between C_3 and C_4 species characterised in this thesis, such as the mechanisms

for increased lag in photosynthetic induction described in Chapter 2, also have potential to strongly vary across genera (McAusland et al., 2016) highlighting the importance of controlling for evolutionary distance. Beyond that, the work described herein also brings attention to the large impact of specific dynamic light protocols and the necessity to consider the starting point of light regimes and the length of fluctuations, when interpreting results of dynamic light responses.

Whilst in Chapter 2 lags in photosynthetic induction across all C_4 species were observed when light treatments started from dark adaption, the lag period was not significant – and at times not even present – in the Chapter 3 results, wherein leaves were repeatedly exposed to step-changes in light intensity. Initial activation likely represents the most significant time lag, and as such considering the starting point of light treatments is crucial when setting up experiments to assess photosynthetic induction, as well as when interpreting results from such experiments. The work presented in Chapter 3 also shows the relevance of fluctuation length – different treatments had previously led to opposite conclusions across different studies (Lee et al., 2022, Li et al., 2021), and given dynamic light research necessarily focuses on temporal responses, length of exposure to either the high or low light period of the particular fluctuating light regime will affect the results. Reporting and considering fluctuation length as part of the interpretation of experimental results is necessary within dynamic light studies, and ideally controls of such variation should be included when studying fluctuating light responses.

5.3.2. Several features of C_4 photosynthesis appear well-adapted to dynamic light conditions

The large metabolite pools intrinsic to C_4 CMM operation are likely to support the enhanced CO_2 assimilation rates observed in C_4 compared to C_3 species during the low light period of fluctuations in Chapter 3. The fast decrease in C_4 NPQ after a decrease in light intensity found in Chapter 3 could also contribute to these higher carbon assimilation rates. Slow relaxation of NPQ has been found to result in significant losses in photosynthetic efficiency (Wang et al., 2020, Werner et al., 2001, Zhu et al., 2004), as until PSII returns to the unquenched state, photosynthesis is operating at a lower efficiency and light energy that is no longer in excess is still being released as heat.

Fast NPQ relaxation and the capacity to buffer through periods of low light could provide C_4 species with a comparative advantage under environments with dynamic conditions. However, C_4 species are known to be absent from some of such environments, like forest understoreys

(Sage and Pearcy, 2000) and indeed some studies in fluctuating light found C_4 carbon assimilation relative to steady state to be lower than in C_3 species under certain light regimes (Li et al., 2021). The advantages provided by C_4 photosynthesis under dynamic light come with nuance – fast NPQ relaxation and the capacity to sustain high carbon assimilation rates after a decrease in light intensity are maximised in fluctuations where the low light period is shorter. A short low light step allows for photosynthetic rates to remain high, whilst maximising utilisation of available light energy compared to C_3 species. Brief periods of shade distributed between longer periods of high light, known as "shade flecks" are commonly found in the top and middle layers of a leaf canopy (Kaiser et al., 2018), which contribute most strongly to overall canopy carbon gain. Many C_4 species produce large canopies which are likely to create similar dynamic light environments, and some of the specific attributes of the C_4 pathway found in this thesis may have contributed to the success of the photosynthetic pathway under such conditions. In contrast, in predominantly shaded environments with occasional sunflecks, the higher rate of carbon assimilation after a light event is diluted across longer periods of lower assimilation, and the benefit of post-high light elevation of CO_2 assimilation has much less impact.

The photosynthetic efficiency of C_4 species relative to steady state during the transition to higher light was hypothesised to vary according to the reliance of the specific C_4 pathway variants on metabolite gradients in Chapter 3. Indeed, the fact that the NADP-ME/PEPCK variant in *Alloteropsis semialata* responded most rapidly seemed to be in line with this idea, since the prominent engagement of PEPCK likely makes BS and M cells more autonomous in their energy supply. However, the use of only three phylogenetic pairs makes it impossible to separate the effects of C_4 pathway variants from species-specific variation– further work on a greater number of C_4 plants with variation in engagement of the three decarboxylation pathways could shed light on whether different C_4 pathways have different photosynthetic efficiencies under fluctuating light.

5.3.3. Exploring metabolite pools in C_4 photosynthesis

Flux profiling of photosynthetic carbon metabolism employing gas chromatography and liquid mass spectrometry (Heise et al., 2014) has already been successfully used to track metabolic changes in C_4 photosynthesis (Arrivault et al., 2016, Arrivault et al., 2017, Medeiros et al., 2022), and could address whether metabolite pool buildup is related to limitations on

photosynthetic induction (Kubásek et al., 2013), and whether during transitions to lower light the C_4 CCM is contributing metabolites to support photosynthesis (Stitt and Zhu, 2014).

Furthermore, analysis of C_4 species that operate different decarboxylation pathways could establish differences in the temporal limitation of the CCM based on their different need for metabolite pool buildup during light induction. This could provide experimental evidence to support modelling analysis which suggests that mixed pathways are less reliant on large metabolite gradients and confer added tolerance to fluctuations in light (Wang et al., 2014a). A theoretical mixed NADP-ME/PEPCK C_4 pathway has been proposed as an ideotype (Yin and Struik, 2021) for improvement of ΦCO_2 both when introducing the C_4 pathway into C_3 species, an effort so far primarily focused on NADP-ME (Ermakova et al., 2020), and also as a strategy for improving photosynthesis in specific C_4 crop species, which could lead to improved performance under fluctuating light. Finally, metabolomics analysis is required to confirm the mechanism underpinning the light induction CO_2 gulp and burst and post-illumination burst observed in NAD-ME species like C_4 *G. gynandra* in Chapter 2. These phenomena have been suggested to relate to PEP carboxylation kinetics and 2-step NAD-ME decarboxylation (Ishikawa et al., 2016, Laisk and Edwards, 1997), but there is little experimental evidence backing this hypothesis. Confirmation of a metabolic bottleneck of NAD-ME C_4 photosynthesis could potentially identify another target for improvement of photosynthetic efficiency under fluctuating light.

5.3.4. Limited potential for improving NPQ relaxation in C_4 species

Crop canopy simulations of C_3 species have shown a substantial loss in carbon assimilation due to slow relaxation of NPQ (Zhu et al., 2004), and increasing the rate of NPQ relaxation is an important target for the improvement of photosynthetic efficiency under dynamic conditions (Long et al., 2022, Wang et al., 2020). Although this approach has proven successful in C_3 species (De Souza et al., 2022, Kromdijk et al., 2016), the results obtained in Chapter 4 suggest that the possible gains in photosynthetic efficiency obtained from speeding up the rate of NPQ relaxation are considerably more limited in C_4 than in C_3 species.

The specific mechanism behind the higher contribution of qE in C_4 species was not identified in this thesis, although higher CEF and the more significant role of the NDH pathway in C_4 photosynthesis are promising avenues for further research (Ogawa et al., 2023, Strand et al., 2017, Takahashi et al., 2009). Further studies into such molecular mechanisms could confirm the role of CEF through parallel *in vivo* quantification of electron flow through PSI. In addition,

use of inducible NDH mutants could limit pleiotropic effects of the constitutive knockdown line in *F. bidentis* used here, while mitigating the potential issues with chemical inhibitors.

Further examining C_4 species with mixed pathways like C_4 *A. semialata MDG* to identify the mechanisms underpinning differences in NPQ would also be of interest, and especially how the results compare to predominantly single-pathway C_4 species. Out of all C_4 species, C_4 *A. semialata MDG* had the highest AUC of NPQ relaxation, as well as the least steep initial drop after the transition to lower light (**Figure 4.1 & 4.2 A**). NADP-ME/PEPCK is also theorised to have lower ATP energy requirements (Ishikawa et al., 2016, Yin and Struik, 2021), therefore also requiring less CEF to balance ATP/NADPH energy budget, which could affect speed of NPQ relaxation via qE formation and dissipation. The more efficient energy requirements of NADP-ME/PEPCK could thus come at the cost of fast NPQ relaxation, and further characterisation of the NPQ response would allow for a more informed recommendation of mixed pathways as an avenue of improvement for C_3 and C_4 species.

References

ACEVEDO-SIACA, L. G., COE, R., WANG, Y., KROMDIJK, J., QUICK, W. P. & LONG, S. P. 2020. Variation in photosynthetic induction between rice accessions and its potential for improving productivity. *New Phytologist,* 227**,** 1097-1108.

ADACHI, S., STATA, M., MARTIN, D. G., CHENG, S., LIU, H., ZHU, X. G. & SAGE, R. F. 2023. The Evolution of C4 Photosynthesis in Flaveria (Asteraceae): Insights from the Flaveria linearis Complex. *Plant Physiology,* 191**,** 233-251.

AINSWORTH, E. A. & LONG, S. P. 2021. 30 years of free-air carbon dioxide enrichment (FACE): What have we learned about future crop productivity and its potential for adaptation? *Global Change Biology,* 27**,** 27-49.

ALLEN, J. F. 2003. Cyclic, pseudocyclic and noncyclic photophosphorylation: new links in the chain. *Trends in Plant Science,* 8**,** 15-9.

ANDERSSON, I. & BACKLUND, A. 2008. Structure and function of Rubisco. *Plant Physiology and Biochemistry,* 46**,** 275-291.

ARCE CUBAS, L., SALES, C. R. G., VATH, R. L., BERNARDO, E. L., BURNETT, A. C. & KROMDIJK, J. 2023a. Lessons from relatives: C_4 photosynthesis enhances CO_2 assimilation during the low-light phase of fluctuations. *Plant Physiology,* 193**,** 1073-1090.

ARCE CUBAS, L., VATH, R. L., BERNARDO, E. L., SALES, C. R. G., BURNETT, A. C. & KROMDIJK, J. 2023b. Activation of CO_2 assimilation during photosynthetic induction is slower in C_4 than in C_3 photosynthesis in three phylogenetically controlled experiments. *Frontiers in Plant Science,* 13.

ARNON, D. I., ALLEN, M. B. & WHATLEY, F. R. 1954. Photosynthesis by Isolated Chloroplasts. *Nature,* 174**,** 394-396.

ARO, E. M., VIRGIN, I. & ANDERSSON, B. 1993. Photoinhibition of Photosystem II. Inactivation, protein damage and turnover. *Biochimica et Biophysica Acta,* 1143**,** 113-34.

ARRIVAULT, S., OBATA, T., SZECÓWKA, M., MENGIN, V., GUENTHER, M., HOEHNE, M., FERNIE, A. R. & STITT, M. 2016. Metabolite pools and carbon flow during C4 photosynthesis in maize: 13CO2 labeling kinetics and cell type fractionation. *Journal of Experimental Botany,* 68**,** 283-298.

ARRIVAULT, S., OBATA, T., SZECÓWKA, M., MENGIN, V., GUENTHER, M., HOEHNE, M., FERNIE, A. R. & STITT, M. 2017. Metabolite pools and carbon flow during C4 photosynthesis in maize: 13CO2 labeling kinetics and cell type fractionation. *Journal of Experimental Botany,* 68**,** 283-298.

AYDINALP, C. & CRESSER, M. S. 2008. The effects of global climate change on agriculture. *American-Eurasian Journal of Agricultural & Environmental Sciences,* 3**,** 672-676.

BANAŚ, A. K., AGGARWAL, C., ŁABUZ, J., SZTATELMAN, O. & GABRYŚ, H. 2012. Blue light signalling in chloroplast movements. *Journal of Experimental Botany,* 63**,** 1559-1574.

BATES, D., MÄCHLER, M., BOLKER, B. & WALKER, S. 2015. Fitting Linear Mixed-Effects Models Using lme4. *Journal of Statistical Software,* 67**,** 1 - 48.

BELLAFIORE, S., BARNECHE, F., PELTIER, G. & ROCHAIX, J. D. 2005. State transitions and light adaptation require chloroplast thylakoid protein kinase STN7. *Nature,* 433**,** 892-5.

BELLASIO, C. & FARQUHAR, G. D. 2019. A leaf-level biochemical model simulating the introduction of C_2 and C_4 photosynthesis in C_3 rice: gains, losses and metabolite fluxes. *New Phytologist,* 223**,** 150-166.

BENSON, A. & CALVIN, M. 1947. The Dark Reductions of Photosynthesis. *Science,* 105**,** 648-649.

BILGER, W. & BJÖRKMAN, O. 1990. Role of the xanthophyll cycle in photoprotection elucidated by measurements of light-induced absorbance changes, fluorescence and photosynthesis in leaves of Hedera canariensis. *Photosynthesis Research,* 25**,** 173-185.

BORGHI, G. L., ARRIVAULT, S., GÜNTHER, M., BARBOSA MEDEIROS, D., DELL'AVERSANA, E., FUSCO, G. M., CARILLO, P., LUDWIG, M., FERNIE, A. R., LUNN, J. E. & STITT, M. 2022. Metabolic profiles in C3, C3-C4 intermediate, C4-like, and C4 species in the genus Flaveria. *Journal of Experimental Botany,* 73**,** 1581-1601.

BRÄUTIGAM, A., HOFFMANN-BENNING, S. & WEBER, A. P. 2008. Comparative proteomics of chloroplast envelopes from C3 and C4 plants reveals specific adaptations of the plastid envelope to C4 photosynthesis and candidate proteins required for maintaining C4 metabolite fluxes. *Plant Physiology,* 148**,** 568-79.

BRÄUTIGAM, A., KAJALA, K., WULLENWEBER, J., SOMMER, M., GAGNEUL, D., WEBER, K. L., CARR, K. M., GOWIK, U., MAß, J., LERCHER, M. J., WESTHOFF, P., HIBBERD, J. M. & WEBER, A. P. M. 2010. An mRNA Blueprint for C4 Photosynthesis Derived from Comparative Transcriptomics of Closely Related C3 and C4 Species *Plant Physiology,* 155**,** 142-156.

BROWN, N. J., PARSLEY, K. & HIBBERD, J. M. 2005. The future of C4 research--maize, Flaveria or Cleome? *Trends in Plant Science,* 10**,** 215-21.

BUCHANAN, B. B. 2016. The carbon (formerly dark) reactions of photosynthesis. *Photosynthesis Research,* 128**,** 215-217.

BUCHANAN, B. B., SCHÜRMANN, P., WOLOSIUK, R. A. & JACQUOT, J.-P. 2002. The ferredoxin/thioredoxin system: from discovery to molecular structures and beyond. *Photosynthesis Research,* 73**,** 215-222.

BUSCH, F. A., SAGE, R. F. & FARQUHAR, G. D. 2018. Plants increase CO2 uptake by assimilating nitrogen via the photorespiratory pathway. *Nature Plants,* 4**,** 46-54.

C4 RICE PROJECT. 2023. *The C4 Rice Project: Driven by the Future Needs of Developing World Agriculture* [Online]. Available: https://c4rice.com/ [Accessed 2023].

CALSA, T. & FIGUEIRA, A. 2007. Serial analysis of gene expression in sugarcane (*Saccharum* spp.) leaves revealed alternative C4 metabolism and putative antisense transcripts. *Plant Molecular Biology,* 63**,** 745-762.

CAPITALISE. 2023. *Working with nature to improve crops* [Online]. Available: https://www.capitalise.eu/ [Accessed 2023].

CARDOL, P., DE PAEPE, R., FRANCK, F., FORTI, G. & FINAZZI, G. 2010. The onset of NPQ and ΔμH+ upon illumination of tobacco plants studied through the influence of mitochondrial electron transport. *Biochimica et Biophysica Acta (BBA) - Bioenergetics,* 1797**,** 177-188.

CARMO-SILVA, A. E. & SALVUCCI, M. E. 2013. The Regulatory Properties of Rubisco Activase Differ among Species and Affect Photosynthetic Induction during Light Transitions *Plant Physiology,* 161**,** 1645-1655.

CAZZANIGA, S., DALL' OSTO, L., KONG, S. G., WADA, M. & BASSI, R. 2013. Interaction between avoidance of photon absorption, excess energy dissipation and zeaxanthin synthesis against photooxidative stress in Arabidopsis. *The Plant Journal,* 76**,** 568-79.

CHRISTIN, P.-A. & OSBORNE, C. P. 2014. The evolutionary ecology of C4 plants. *New Phytologist,* 204**,** 765-781.

CHRISTIN, P.-A., OSBORNE, C. P., SAGE, R. F., ARAKAKI, M. & EDWARDS, E. J. 2011. C4 eudicots are not younger than C4 monocots. *Journal of Experimental Botany,* 62**,** 3171-3181.

COGATO, A., MEGGIO, F., DE ANTONI MIGLIORATI, M. & MARINELLO, F. 2019. Extreme Weather Events in Agriculture: A Systematic Review. *Sustainability,* 11**,** 2547.

COWLING, S. B., TREEINTONG, P., FERGUSON, J., SOLTANI, H., SWARUP, R., MAYES, S. & MURCHIE, E. H. 2021. Out of Africa: characterizing the natural variation in dynamic photosynthetic traits in a diverse population of African rice (Oryza glaberrima). *Journal of Experimental Botany,* 73**,** 3283-3298.

DALCORSO, G., PESARESI, P., MASIERO, S., ASEEVA, E., SCHÜNEMANN, D., FINAZZI, G., JOLIOT, P., BARBATO, R. & LEISTER, D. 2008. A complex containing PGRL1 and PGR5 is involved in the switch between linear and cyclic electron flow in Arabidopsis. *Cell,* 132**,** 273-85.

DALL'OSTO, L., CAFFARRI, S. & BASSI, R. 2005. A mechanism of nonphotochemical energy dissipation, independent from PsbS, revealed by a conformational change in the antenna protein CP26. *Plant Cell,* 17**,** 1217-32.

DE SOUZA, A. P., BURGESS, S. J., DORAN, L., HANSEN, J., MANUKYAN, L., MARYN, N., GOTARKAR, D., LEONELLI, L., NIYOGI, K. K. & LONG, S. P. 2022. Soybean photosynthesis and crop yield are improved by accelerating recovery from photoprotection. *Science,* 377**,** 851-854.

DEMMIG-ADAMS, B. 1990. Carotenoids and photoprotection in plants: A role for the xanthophyll zeaxanthin. *Biochimica et Biophysica Acta (BBA) - Bioenergetics,* 1020**,** 1-24.

DEMMIG-ADAMS, B. & ADAMS, W. W. 1996. Xanthophyll cycle and light stress in nature: uniform response to excess direct sunlight among higher plant species. *Planta,* 198**,** 460-470.

DIETZ, K.-J. 1985. A possible rate-limiting function of chloroplast hexosemonophosphate isomerase in starch synthesis of leaves. *Biochimica et Biophysica Acta (BBA) - General Subjects,* 839**,** 240-248.

DONCASTER, H. D., ADCOCK, M. D. & LEEGOOD, R. C. 1989. Regulation of photosynthesis in leaves of C4 plants following a transition from high to low light. *Biochimica et Biophysica Acta (BBA) - Bioenergetics,* 973**,** 176-184.

DOULIS, A. G., DEBIAN, N., KINGSTON-SMITH, A. H. & FOYER, C. H. 1997. Differential Localization of Antioxidants in Maize Leaves. *Plant Physiology,* 114**,** 1031-1037.

DRIEVER, S. M. & BAKER, N. R. 2011. The water-water cycle in leaves is not a major alternative electron sink for dissipation of excess excitation energy when CO2 assimilation is restricted. *Plant, Cell & Environment,* 34**,** 837-846.

DRINCOVICH, M. F., CASATI, P., ANDREO, C. S., CHESSIN, S. J., FRANCESCHI, V. R., EDWARDS, G. E. & KU, M. S. 1998. Evolution of C4 photosynthesis in flaveria species. Isoforms of NADP-Malic Enzyme. *Plant Physiology,* 117**,** 733-44.

DUNNING, L. T., MORENO-VILLENA, J. J., LUNDGREN, M. R., DIONORA, J., SALAZAR, P., ADAMS, C., NYIRENDA, F., OLOFSSON, J. K., MAPAURA, A., GRUNDY, I. M., KAYOMBO, C. J., DUNNING, L. A., KENTATCHIME, F., ARIYARATHNE, M., YAKANDAWALA, D., BESNARD, G., QUICK, W. P., BRÄUTIGAM, A., OSBORNE, C. P. & CHRISTIN, P.-A. 2019. Key changes in gene expression identified for different stages of C4 evolution in Alloteropsis semialata. *Journal of Experimental Botany,* 70**,** 3255-3268.

EDWARDS, E. J. & STILL, C. J. 2008. Climate, phylogeny and the ecological distribution of C4 grasses. *Ecology Letters,* 11**,** 266-76.

EDWARDS, E. J., STILL, C. J. & DONOGHUE, M. J. 2007. The relevance of phylogeny to studies of global change. *Trends in Ecology & Evolution* 22**,** 243-9.

EHLERINGER, J. & PEARCY, R. W. 1983. Variation in Quantum Yield for CO2 Uptake among C3 and C4 Plants. *Plant Physiology,* 73**,** 555-559.

EHLERINGER, J. R. 1978. Implications of quantum yield differences on the distributions of C_3 and C_4 grasses. *Oecologia,* 31**,** 255-267.

ELLIS, R. P. 1974. The Significance of the Occurrence of Both Kranz and non-Kranz Leaf Anatomy in the Grass species *Alloteropsis semialata*. *South African Journal of Science,* 70**,** 169-173.

ERMAKOVA, M., DANILA, F. R., FURBANK, R. T. & VON CAEMMERER, S. 2020. On the road to C_4 rice: advances and perspectives. *The Plant Journal,* 101**,** 940-950.

ERMAKOVA, M., WOODFORD, R., TAYLOR, Z., FURBANK, R. T., BELIDE, S. & VON CAEMMERER, S. 2023. Faster induction of photosynthesis increases biomass and grain yield in glasshouse-grown transgenic Sorghum bicolor overexpressing Rieske FeS. *Plant Biotechnology Journal,* 21**,** 1206-1216.

EVANS, J. R. 1999. Leaf anatomy enables more equal access to light and CO2 between chloroplasts. *The New Phytologist,* 143**,** 93-104.

EVANS, L. T. 1997. Adapting and improving crops: the endless task. *Philosophical Transactions of the Royal Society B: Biological Sciences,* 352**,** 901-906.

EVANS, L. T. & DUNSTONE, R. L. 1970. Some Physiological Aspects of Evolution in Wheat. *Australian Journal of Biological Sciences,* 23**,** 725-742.

FAO. 2009. Global agriculture towards 2050.

FAO 2020. Production, Trade and Prices of Commodities. *World Food and Agriculture - Statistical Yearbook 2020.* Rome, Italy: FAO.

FAO 2021. Food Security and Nutrition Around The World. *The State of Food Security and Nutrition in the World 2021.* Rome, Italy.

FEODOROVA, T. A., VOZNESENSKAYA, E. V., EDWARDS, G. E. & ROALSON, E. H. 2010. Biogeographic Patterns of Diversification and the Origins of C_4 in *Cleome* (Cleomaceae). *Systematic Botany,* 35**,** 811-826, 16.

FORRESTER, M. L., KROTKOV, G. & NELSON, C. D. 1966. Effect of oxygen on photosynthesis, photorespiration and respiration in detached leaves. I. Soybean. *Plant Physiology,* 41**,** 422-7.

FRYER, M. J., ANDREWS, J. R., OXBOROUGH, K., BLOWERS, D. A. & BAKER, N. R. 1998. Relationship between CO2 Assimilation, Photosynthetic Electron Transport, and Active O2 Metabolism in Leaves of Maize in the Field during Periods of Low Temperature. *Plant Physiology,* 116**,** 571-580.

FU, X. & WALKER, B. J. 2022. Dynamic response of photorespiration in fluctuating light environments. *Journal of Experimental Botany*.

FURBANK, R. T. 2011. Evolution of the C4 photosynthetic mechanism: are there really three C4 acid decarboxylation types? *Journal of Experimental Botany,* 62**,** 3103-3108.

GENTY, B., BRIANTAIS, J.-M. & BAKER, N. R. 1989. The relationship between the quantum yield of photosynthetic electron transport and quenching of chlorophyll fluorescence. *Biochimica et Biophysica Acta (BBA) - General Subjects,* 990**,** 87-92.

GOWIK, U., BRÄUTIGAM, A., WEBER, K. L., WEBER, A. P. M. & WESTHOFF, P. 2011. Evolution of C4 Photosynthesis in the Genus *Flaveria*: How Many and Which Genes Does It Take to Make C4? *The Plant Cell,* 23**,** 2087-2105.

GU, J., YIN, X., STOMPH, T.-J. & STRUIK, P. C. 2014. Can exploiting natural genetic variation in leaf photosynthesis contribute to increasing rice productivity? A simulation analysis. *Plant, Cell & Environment,* 37**,** 22-34.

GUIDI, L., LO PICCOLO, E. & LANDI, M. 2019. Chlorophyll Fluorescence, Photoinhibition and Abiotic Stress: Does it Make Any Difference the Fact to Be a C3 or C4 Species? *Frontiers in Plant Science,* 10**,** 174.

HABIB-UR-RAHMAN, M., AHMAD, A., RAZA, A., HASNAIN, M. U., ALHARBY, H. F., ALZAHRANI, Y. M., BAMAGOOS, A. A., HAKEEM, K. R., AHMAD, S., NASIM, W., ALI, S., MANSOUR, F. & EL SABAGH, A. 2022. Impact of climate change on agricultural production; Issues, challenges, and opportunities in Asia. *Frontiers in Plant Science,* 13**,** 925548.

HATCH, M., KAGAWA, T. & CRAIG, S. 1975. Subdivision of C4-Pathway Species Based on Differing C4 Acid Decarboxylating Systems and Ultrastructural Features. *Functional Plant Biology,* 2**,** 111-128.

HEINEKE, D. & SCHEIBE, R. Photosynthesis: The Calvin Cycle. *Encyclopedia of Life Sciences.*

HEISE, R., ARRIVAULT, S., SZECOWKA, M., TOHGE, T., NUNES-NESI, A., STITT, M., NIKOLOSKI, Z. & FERNIE, A. R. 2014. Flux profiling of photosynthetic carbon metabolism in intact plants. *Nature Protocols,* 9**,** 1803-24.

HIBBERD, J. M., SHEEHY, J. E. & LANGDALE, J. A. 2008. Using C4 photosynthesis to increase the yield of rice—rationale and feasibility. *Current Opinion in Plant Biology,* 11**,** 228-231.

HOANG, N. V., SOGBOHOSSOU, E. O. D., XIONG, W., SIMPSON, C. J. C., SINGH, P., WALDEN, N., VAN DEN BERGH, E., BECKER, F. F. M., LI, Z., ZHU, X. G., BRAUTIGAM, A., WEBER, A. P. M., VAN HAARST, J. C., SCHIJLEN, E., HENDRE, P. S., VAN DEYNZE, A., ACHIGAN-DAKO, E. G., HIBBERD, J. M. & SCHRANZ, M. E. 2023. The Gynandropsis gynandra genome provides insights into whole-genome duplications and the evolution of C4 photosynthesis in Cleomaceae. *Plant Cell,* 35**,** 1334-1359.

HORTON, J. L. & NEUFELD, H. S. 1998. Photosynthetic responses of Microstegium vimineum (Trin.) A. Camus, a shade-tolerant, C4 grass, to variable light environments. *Oecologia,* 114**,** 11-19.

HORTON, P. 2012. Optimization of light harvesting and photoprotection: molecular mechanisms and physiological consequences. *Philosophical Transactions of the Royal Society B: Biological Sciences,* 367**,** 3455-3465.

HUANG, W., HONG, H. & ZHANG, S. 2015a. Photorespiration plays an important role in the regulation of photosynthetic electron flow under fluctuating light in tobacco plants grown under full sunlight. *Frontiers in Plant Science,* 6.

HUANG, W., YANG, Y. J., HU, H. & ZHANG, S. B. 2015b. Different roles of cyclic electron flow around photosystem I under sub-saturating and saturating light intensities in tobacco leaves. *Frontiers in Plant Science,* 6**,** 923.

HUBBART, S., AJIGBOYE, O. O., HORTON, P. & MURCHIE, E. H. 2012. The photoprotective protein PsbS exerts control over CO(2) assimilation rate in fluctuating light in rice. *The Plant Journal,* 71**,** 402-12.

IBRAHIM, D. G., BURKE, T., RIPLEY, B. S. & OSBORNE, C. P. 2009. A molecular phylogeny of the genus *Alloteropsis* (Panicoideae, Poaceae) suggests an evolutionary reversion from C4 to C3 photosynthesis. *Annals of Botany,* 103**,** 127-136.

IKEZAWA, N., IFUKU, K., ENDO, T. & SATO, F. 2002. Inhibition of Photosystem II of Spinach by the Respiration Inhibitors Piericidin A and Thenoyltrifluoroacetone. *Bioscience, Biotechnology, and Biochemistry,* 66**,** 1925-1929.

ILTIS, H. H. & COCHRANE, T. S. 2007. Studies in the Cleomaceae V: A New Genus and Ten New Combinations for the *Flora of North America*. *Novon: A Journal for Botanical Nomenclature,* 17**,** 447-451, 5.

IPCC 2022. Food security. *In:* CHANGE, I. P. O. C. (ed.) *Climate Change and Land: IPCC Special Report on Climate Change, Desertification, Land Degradation, Sustainable Land Management, Food Security, and Greenhouse Gas Fluxes in Terrestrial Ecosystems.* Cambridge: Cambridge University Press.

ISHIKAWA, N., TAKABAYASHI, A., SATO, F. & ENDO, T. 2016. Accumulation of the components of cyclic electron flow around photosystem I in C_4 plants, with respect to the requirements for ATP. *Photosynthesis Research,* 129**,** 261-277.

JAWIEŃ, W. 2014. Searching for an optimal AUC estimation method: a never-ending task? *Journal of Pharmacokinetics and Pharmacodynamics,* 41**,** 655-673.

JOHNSON, M. P. 2016. Photosynthesis. *Essays in Biochemistry,* 60**,** 255-273.

JOHNSON, M. P. & RUBAN, A. V. 2010. Arabidopsis plants lacking PsbS protein possess photoprotective energy dissipation. *The Plant Journal,* 61**,** 283-289.

KAISER, E., MORALES, A. & HARBINSON, J. 2018. Fluctuating Light Takes Crop Photosynthesis on a Rollercoaster Ride. *Plant Physiology,* 176**,** 977-989.

KAISER, E., MORALES, A., HARBINSON, J., KROMDIJK, J., HEUVELINK, E. & MARCELIS, L. F. M. 2015. Dynamic photosynthesis in different environmental conditions. *Journal of Experimental Botany,* 66**,** 2415-2426.

KELLOGG, E. A. 2013. C4 photosynthesis. *Current Biology,* 23**,** R594-R599.

KEREN, N. & KRIEGER-LISZKAY, A. 2011. Photoinhibition: molecular mechanisms and physiological significance. *Physiologia Plantarum,* 142**,** 1-5.

KIMBALL, B. A. 1983. Carbon Dioxide and Agricultural Yield: An Assemblage and Analysis of 430 Prior Observations1. *Agronomy Journal,* 75**,** 779-788.

KINIRY, J. R., JONES, C. A., O'TOOLE, J. C., BLANCHET, R., CABELGUENNE, M. & SPANEL, D. A. 1989. Radiation-use efficiency in biomass accumulation prior to grain-filling for five grain-crop species. *Field Crops Research,* 20**,** 51-64.

KOBAYASHI, H., YAMADA, M., TANIGUCHI, M., KAWASAKI, M., SUGIYAMA, T. & MIYAKE, H. 2008. Differential Positioning of C4 Mesophyll and Bundle Sheath Chloroplasts: Recovery of Chloroplast Positioning Requires the Actomyosin System. *Plant and Cell Physiology,* 50**,** 129-140.

KOK, B. 1949. On the interrelation of respiration and photosynthesis in green plants. *Biochimica et Biophysica Acta,* 3**,** 625-631.

KOPITTKE, P. M., MENZIES, N. W., WANG, P., MCKENNA, B. A. & LOMBI, E. 2019. Soil and the intensification of agriculture for global food security. *Environment International,* 132**,** 105078.

KORNHUBER, K., LESK, C., SCHLEUSSNER, C. F., JÄGERMEYR, J., PFLEIDERER, P. & HORTON, R. M. 2023. Risks of synchronized low yields are underestimated in climate and crop model projections. *Nature Communications,* 14**,** 3528.

KOZAKI, A. & TAKEBA, G. 1996. Photorespiration protects C3 plants from photooxidation. *Nature,* 384**,** 557-560.

KRALL, J. P. & EDWARDS, G. E. 1990. Quantum yields of photosystem II electron transport and carbon dioxide fixation in C4 plants. *Australian Journal of Plant Physiology,* 17**,** 579-588.

KRALL, J. P. & PEARCY, R. W. 1993. Concurrent Measurements of Oxygen and Carbon Dioxide Exchange during Lightflecks in Maize (Zea mays L.). *Plant Physiology,* 103**,** 823-828.

KRESS, E. & JAHNS, P. 2017. The Dynamics of Energy Dissipation and Xanthophyll Conversion in Arabidopsis Indicate an Indirect Photoprotective Role of Zeaxanthin in Slowly Inducible and Relaxing Components of Non-photochemical Quenching of Excitation Energy. *Frontiers in Plant Science,* 8**,** 2094.

KRIEGER-LISZKAY, A. 2005. Singlet oxygen production in photosynthesis. *Journal of Experimental Botany,* 56**,** 337-46.

KROMDIJK, J., GŁOWACKA, K., LEONELLI, L., GABILLY, S. T., IWAI, M., NIYOGI, K. K. & LONG, S. P. 2016. Improving photosynthesis and crop productivity by accelerating recovery from photoprotection. *Science,* 354**,** 857-861.

KROMDIJK, J., GRIFFITHS, H. & SCHEPERS, H. E. 2010. Can the progressive increase of C_4 bundle sheath leakiness at low PFD be explained by incomplete suppression of photorespiration? *Plant, Cell & Environment,* 33**,** 1935-48.

KROMDIJK, J. & LONG, S. P. 2016. One crop breeding cycle from starvation? How engineering crop photosynthesis for rising CO_2 and temperature could be one important route to alleviation. *Proceedings of the Royal Society B: Biological Sciences,* 283**,** 20152578.

KROMDIJK, J., SCHEPERS, H. E., ALBANITO, F., FITTON, N., CARROLL, F., JONES, M. B., FINNAN, J., LANIGAN, G. J. & GRIFFITHS, H. 2008. Bundle Sheath Leakiness and Light Limitation during C4 Leaf and Canopy CO2 Uptake *Plant Physiology,* 148**,** 2144-2155.

KROMDIJK, J., UBIERNA, N., COUSINS, A. B. & GRIFFITHS, H. 2014. Bundle-sheath leakiness in C4 photosynthesis: a careful balancing act between CO2 concentration and assimilation. *Journal of Experimental Botany,* 65**,** 3443-57.

KU, M. S., WU, J., DAI, Z., SCOTT, R. A., CHU, C. & EDWARDS, G. E. 1991. Photosynthetic and photorespiratory characteristics of *Flaveria* species. *Plant Physiology,* 96**,** 518-28.

KUBÁSEK, J., URBAN, O. & ŠANTRŮČEK, J. 2013. C4 plants use fluctuating light less efficiently than do C3 plants: a study of growth, photosynthesis and carbon isotope discrimination. *Physiologia Plantarum,* 149**,** 528-539.

KUZNETSOVA, A., BROCKHOFF, P. B. & CHRISTENSEN, R. H. B. 2017. lmerTest Package: Tests in Linear Mixed Effects Models. *Journal of Statistical Software,* 82**,** 1 - 26.

LAISK, A. & EDWARDS, G. E. 1997. Post-illumination CO_2 Exchange and Light-induced CO_2 Bursts during C_4 Photosynthesis. *Functional Plant Biology,* 24**,** 517-528.

LAWSON, T., KRAMER, D. M. & RAINES, C. A. 2012. Improving yield by exploiting mechanisms underlying natural variation of photosynthesis. *Current Opinion in Biotechnology,* 23**,** 215-220.

LEAKEY, A. D. B., PRESS, M. C., SCHOLES, J. D. & WATLING, J. R. 2002. Relative enhancement of photosynthesis and growth at elevated CO_2 is greater under sunflecks than uniform irradiance in a tropical rain forest tree seedling. *Plant, Cell & Environment,* 25**,** 1701-1714.

LEE, M. S., BOYD, R. A. & ORT, D. R. 2022. The photosynthetic response of C3 and C4 bioenergy grass species to fluctuating light. *GCB Bioenergy,* 14**,** 37-53.

LEEGOOD, R. C. 2002. C4 photosynthesis: principles of CO2 concentration and prospects for its introduction into C3 plants. *Journal of Experimental Botany,* 53**,** 581-590.

LEEGOOD, R. C. & FURBANK, R. T. 1984. Carbon metabolism and gas exchange in leaves of *Zea mays* L. *Planta,* 162**,** 450-456.

LEEGOOD, R. C. & VON CAEMMERER, S. 1989. Some relationships between contents of photosynthetic intermediates and the rate of photosynthetic carbon assimilation in leaves of *Zea mays L. Planta,* 178**,** 258-266.

LI-COR, I. 1988. *1800-12 Integrating Sphere Instruction Manual.*

LI, X. P., BJÖRKMAN, O., SHIH, C., GROSSMAN, A. R., ROSENQUIST, M., JANSSON, S. & NIYOGI, K. K. 2000. A pigment-binding protein essential for regulation of photosynthetic light harvesting. *Nature,* 403**,** 391-5.

LI, X. P., GILMORE, A. M., CAFFARRI, S., BASSI, R., GOLAN, T., KRAMER, D. & NIYOGI, K. K. 2004. Regulation of photosynthetic light harvesting involves intrathylakoid lumen pH sensing by the PsbS protein. *Journal of Biological Chemistry,* 279**,** 22866-74.

LI, X. P., GILMORE, A. M. & NIYOGI, K. K. 2002a. Molecular and global time-resolved analysis of a psbS gene dosage effect on pH- and xanthophyll cycle-dependent nonphotochemical quenching in photosystem II. *Journal of Biological Chemistry,* 277**,** 33590-7.

LI, X. P., MULLER-MOULE, P., GILMORE, A. M. & NIYOGI, K. K. 2002b. PsbS-dependent enhancement of feedback de-excitation protects photosystem II from photoinhibition. *Proceedings of the National Academy of Sciences,* 99**,** 15222-15227.

LI, Y.-T., LUO, J., LIU, P. & ZHANG, Z.-S. 2021. C4 species utilize fluctuating light less efficiently than C3 species. *Plant Physiology,* 187**,** 1288-1291.

LILLEY, R. M., CHON, C. J., MOSBACH, A. & HELDT, H. W. 1977. The distribution of metabolites between spinach chloroplasts and medium during photosynthesis in vitro. *Biochimica et Biophysica Acta (BBA) - Bioenergetics,* 460**,** 259-272.

LONG, S. P. 1999. 7 - Environmental Responses. *In:* SAGE, R. F. & MONSON, R. K. (eds.) *C4 Plant Biology.* San Diego: Academic Press.

LONG, S. P., TAYLOR, S. H., BURGESS, S. J., CARMO-SILVA, E., LAWSON, T., SOUZA, A. P. D., LEONELLI, L. & WANG, Y. 2022. Into the Shadows and Back into Sunlight: Photosynthesis in Fluctuating Light. *Annual Review of Plant Biology,* 73**,** 617-648.

LONG, S. P., ZHU, X.-G., NAIDU, S. L. & ORT, D. R. 2006. Can improvement in photosynthesis increase crop yields? *Plant, Cell and Environment,* 29**,** 315-330.

LORIAUX, S. D., AVENSON, T. J., WELLES, J. M., MCDERMITT, D. K., ECKLES, R. D., RIENSCHE, B. & GENTY, B. 2013. Closing in on maximum yield of chlorophyll fluorescence using a single multiphase flash of sub-saturating intensity. *Plant, Cell & Environment,* 36**,** 1755-1770.

LUDWIG, L. J. & CANVIN, D. T. 1971. The Rate of Photorespiration during Photosynthesis and the Relationship of the Substrate of Light Respiration to the Products of Photosynthesis in Sunflower Leaves. *Plant Physiology,* 48**,** 712-9.

LÜMMEN, P. 1998. Complex I inhibitors as insecticides and acaricides1Dedicated to the memory of Dr. Gerhard Salbeck.1. *Biochimica et Biophysica Acta (BBA) - Bioenergetics,* 1364**,** 287-296.

LUNDGREN, M. R., BESNARD, G., RIPLEY, B. S., LEHMANN, C. E. R., CHATELET, D. S., KYNAST, R. G., NAMAGANDA, M., VORONTSOVA, M. S., HALL, R. C., ELIA, J., OSBORNE, C. P. & CHRISTIN, P.-A. 2015. Photosynthetic innovation broadens the niche within a single species. *Ecology Letters,* 18**,** 1021-1029.

LUNDGREN, M. R., CHRISTIN, P.-A., ESCOBAR, E. G., RIPLEY, B. S., BESNARD, G., LONG, C. M., HATTERSLEY, P. W., ELLIS, R. P., LEEGOOD, R. C. & OSBORNE, C. P. 2016. Evolutionary implications of C3-C4 intermediates in the grassAlloteropsis semialata. *Plant, Cell & Environment,* 39**,** 1874-1885.

MACDONALD, G. K., BENNETT, E. M., POTTER, P. A. & RAMANKUTTY, N. 2011. Agronomic phosphorus imbalances across the world's croplands. *Proceedings of the National Academy of Sciences,* 108**,** 3086-3091.

MAJERAN, W., FRISO, G., PONNALA, L., CONNOLLY, B., HUANG, M., REIDEL, E., ZHANG, C., ASAKURA, Y., BHUIYAN, N. H., SUN, Q., TURGEON, R. & VAN WIJK, K. J. 2010. Structural and metabolic transitions of C4 leaf development and differentiation defined by microscopy and quantitative proteomics in maize. *Plant Cell,* 22**,** 3509-42.

MAKOWSKI, D., BEN-SHACHAR, M. S. & LÜDECKE, D. 2019. bayestestR: Describing Effects and their Uncertainty, Existence and Significance within the Bayesian Framework. *Journal of Open Source Software,* 4**,** 1541.

MALNOË, A. 2018. Photoinhibition or photoprotection of photosynthesis? Update on the (newly termed) sustained quenching component qH. *Environmental and Experimental Botany,* 154**,** 123-133.

MARSHALL, D. M., MUHAIDAT, R., BROWN, N. J., LIU, Z., STANLEY, S., GRIFFITHS, H., SAGE, R. F. & HIBBERD, J. M. 2007. Cleome, a genus closely related to Arabidopsis, contains species spanning a developmental progression from C_3 to C_4 photosynthesis. *The Plant Journal,* 51**,** 886-96.

MCAUSLAND, L. & MURCHIE, E. H. 2020. Start me up; harnessing natural variation in photosynthetic induction to improve crop yields. *New Phytologist,* 227**,** 989-991.

MCAUSLAND, L., VIALET-CHABRAND, S., DAVEY, P., BAKER, N. R., BRENDEL, O. & LAWSON, T. 2016. Effects of kinetics of light-induced stomatal responses on photosynthesis and water-use efficiency. *New Phytologist,* 211**,** 1209-1220.

MCCLAIN, A. M. & SHARKEY, T. D. 2019. Triose phosphate utilization and beyond: from photosynthesis to end product synthesis. *Journal of Experimental Botany,* 70**,** 1755-1766.

MEDEIROS, D. B., ISHIHARA, H., GUENTHER, M., ROSADO DE SOUZA, L., FERNIE, A. R., STITT, M. & ARRIVAULT, S. 2022. 13CO2 labeling kinetics in maize reveal impaired efficiency of C4 photosynthesis under low irradiance. *Plant Physiology,* 190**,** 280-304.

MEIERHOFF, K. & WESTHOFF, P. 1993. Differential biogenesis of photosystem II in mesophyll and bundle-sheath cells of monocotyledonous NADP-malic enzyme-type C4 plants: the non-stoichiometric abundance of the subunits of photosystem II in the bundle-sheath chloroplasts and the translational activity of the plastome-encoded genes. *Planta,* 191**,** 23-33.

MIYAKE, C., MIYATA, M., SHINZAKI, Y. & TOMIZAWA, K.-I. 2005. CO2 Response of Cyclic Electron Flow around PSI (CEF-PSI) in Tobacco Leaves—Relative Electron fluxes through PSI and PSII Determine the Magnitude of Non-photochemical Quenching (NPQ) of Chl Fluorescence. *Plant and Cell Physiology,* 46**,** 629-637.

MORALES, A., KAISER, E., YIN, X., HARBINSON, J., MOLENAAR, J., DRIEVER, S. M. & STRUIK, P. C. 2018. Dynamic modelling of limitations on improving leaf CO2 assimilation under fluctuating irradiance. *Plant, Cell & Environment,* 41**,** 589-604.

MOTT, K. A. & WOODROW, I. E. 2000. Modelling the role of Rubisco activase in limiting non-steady-state photosynthesis. *Journal of Experimental Botany,* 51**,** 399-406.

MUELLER, N. D., GERBER, J. S., JOHNSTON, M., RAY, D. K., RAMANKUTTY, N. & FOLEY, J. A. 2012. Closing yield gaps through nutrient and water management. *Nature,* 490**,** 254-257.

MÜLLER, P., LI, X. P. & NIYOGI, K. K. 2001. Non-photochemical quenching. A response to excess light energy. *Plant Physiology,* 125**,** 1558-66.

MULLINEAUX, C. W. & ALLEN, J. F. 1990. State 1-State 2 transitions in the cyanobacterium Synechococcus 6301 are controlled by the redox state of electron carriers between Photosystems I and II. *Photosynthesis Research,* 23**,** 297-311.

MUNEKAGE, Y. 2016. Light harvesting and chloroplast electron transport in NADP-malic enzyme type C4 plants. *Current Opinion in Plant Biology,* 31**,** 9-15.

MUNEKAGE, Y., HOJO, M., MEURER, J., ENDO, T., TASAKA, M. & SHIKANAI, T. 2002. PGR5 is involved in cyclic electron flow around photosystem I and is essential for photoprotection in Arabidopsis. *Cell,* 110**,** 361-71.

MURCHIE, E. H., KEFAUVER, S., ARAUS, J. L., MULLER, O., RASCHER, U., FLOOD, P. J. & LAWSON, T. 2018. Measuring the dynamic photosynthome. *Annals of Botany,* 122**,** 207-220.

MURCHIE, E. H. & RUBAN, A. V. 2020. Dynamic non-photochemical quenching in plants: from molecular mechanism to productivity. *The Plant Journal,* 101**,** 885-896.

NAKAMURA, N., IWANO, M., HAVAUX, M., YOKOTA, A. & MUNEKAGE, Y. N. 2013. Promotion of cyclic electron transport around photosystem I during the evolution of NADP-malic enzyme-type C_4 photosynthesis in the genus *Flaveria*. *New Phytologist,* 199**,** 832-842.

NELSON, N. & BEN-SHEM, A. 2004. The complex architecture of oxygenic photosynthesis. *Nature Reviews Molecular Cell Biology,* 5**,** 971-982.

NEUBAUER, C. 1993. Multiple Effects of Dithiothreitol on Nonphotochemical Fluorescence Quenching in Intact Chloroplasts (Influence on Violaxanthin De-epoxidase and Ascorbate Peroxidase Activity). *Plant Physiology,* 103**,** 575-583.

NEUWIRTH, E. 2014. RColorBrewer: ColorBrewer Palettes.

NICOL, L. & CROCE, R. 2021. The PsbS protein and low pH are necessary and sufficient to induce quenching in the light-harvesting complex of plants LHCII. *Scientific Reports,* 11**,** 7415.

NILKENS, M., KRESS, E., LAMBREV, P., MILOSLAVINA, Y., MÜLLER, M., HOLZWARTH, A. R. & JAHNS, P. 2010. Identification of a slowly inducible zeaxanthin-dependent component of non-photochemical quenching of chlorophyll fluorescence generated under steady-state conditions in Arabidopsis. *Biochimica et Biophysica Acta,* 1797**,** 466-75.

NIU, Y., LAZÁR, D., HOLZWARTH, A. R., KRAMER, D. M., MATSUBARA, S., FIORANI, F., POORTER, H., SCHREY, S. D. & NEDBAL, L. 2022. A plant's capacity to cope with fluctuating light depends on the frequency characteristics of non-photochemical quenching and cyclic electron transport. Cold Spring Harbor Laboratory.

OBERHUBER, W. & EDWARDS, G. E. 1993. Temperature Dependence of the Linkage of Quantum Yield of Photosystem II to CO2 Fixation in C4 and C3 Plants. *Plant Physiology,* 101**,** 507-512.

OGAWA, T., KOBAYASHI, K., TANIGUCHI, Y. Y., SHIKANAI, T., NAKAMURA, N., YOKOTA, A. & MUNEKAGE, Y. N. 2022. Two cyclic electron flows around photosystem I differentially participate in C_4 photosynthesis. *bioRxiv***,** 2022.09.23.509273.

OGAWA, T., KOBAYASHI, K., TANIGUCHI, Y. Y., SHIKANAI, T., NAKAMURA, N., YOKOTA, A. & MUNEKAGE, Y. N. 2023. Two cyclic electron flows around photosystem I differentially participate in C4 photosynthesis. *Plant Physiology,* 191**,** 2288-2300.

OGLE, K. 2003. Implications of interveinal distance for quantum yield in C4 grasses: a modeling and meta-analysis. *Oecologia,* 136**,** 532-542.

OHGISHI, M., SAJI, K., OKADA, K. & SAKAI, T. 2004. Functional analysis of each blue light receptor, cry1, cry2, phot1, and phot2, by using combinatorial multiple mutants in Arabidopsis. *Proceedings of the National Academy of Sciences,* 101**,** 2223-8.

OSBORNE, B. A. & RAVEN, J. A. 1986. LIGHT ABSORPTION BY PLANTS AND ITS IMPLICATIONS FOR PHOTOSYNTHESIS. *Biological Reviews,* 61**,** 1-60.

OXBOROUGH, K. & BAKER, N. R. 1997. Resolving chlorophyll a fluorescence images of photosynthetic efficiency into photochemical and non-photochemical components – calculation of qP and Fv-/Fm-; without measuring Fo. *Photosynthesis Research,* 54**,** 135-142.

OZEKI, K., MIYAZAWA, Y. & SUGIURA, D. 2022. Rapid stomatal closure contributes to higher water use efficiency in major C_4 compared to C_3 Poaceae crops. *Plant Physiology,* 189**,** 188-203.

PARMA, D. F., VAZ, M., FALQUETTO, P., SILVA, J. C., CLARINDO, W. R., WESTHOFF, P., VAN VELZEN, R., SCHLÜTER, U., ARAÚJO, W. L., SCHRANZ, M. E., WEBER, A. P. M. & NUNES-NESI, A. 2022. New Insights Into the Evolution of C_4 Photosynthesis Offered by the *Tarenaya* Cluster of Cleomaceae. *Frontiers in Plant Science,* 12**,** 756505.

PEARCY, R. W. 1990. Sunflecks and Photosynthesis in Plant Canopies. *Annual Review of Plant Physiology and Plant Molecular Biology,* 41**,** 421-453.

PEARCY, R. W., GROSS, L. J. & HE, D. 1997. An improved dynamic model of photosynthesis for estimation of carbon gain in sunfleck light regimes. *Plant, Cell & Environment,* 20**,** 411-424.

PEARCY, R. W. & SEEMANN, J. R. 1990. Photosynthetic Induction State of Leaves in a Soybean Canopy in Relation to Light Regulation of Ribulose-1-5-Bisphosphate Carboxylase and Stomatal Conductance. *Plant Physiology,* 94**,** 628-633.

PELTIER, G., ARO, E. M. & SHIKANAI, T. 2016. NDH-1 and NDH-2 Plastoquinone Reductases in Oxygenic Photosynthesis. *Annual Review of Plant Biology,* 67**,** 55-80.

PENUELAS, J., COELLO, F. & SARDANS, J. 2023. A better use of fertilizers is needed for global food security and environmental sustainability. *Agriculture & Food Security,* 12**,** 5.

PETERSON, R. B., SCHULTES, N. P., MCHALE, N. A. & ZELITCH, I. 2016. Evidence for a Role for NAD(P)H Dehydrogenase in Concentration of CO2 in the Bundle Sheath Cell of Zea mays. *Plant Physiology,* 171**,** 125-38.

PICK, T. R., BRÄUTIGAM, A., SCHULZ, M. A., OBATA, T., FERNIE, A. R. & WEBER, A. P. M. 2013. *PLGG1*, a plastidic glycolate glycerate transporter, is required for photorespiration and defines a unique class of metabolite transporters. *Proceedings of the National Academy of Sciences,* 110**,** 3185-3190.

PIGNON, C. P., LEAKEY, A. D. B., LONG, S. P. & KROMDIJK, J. 2021. Drivers of Natural Variation in Water-Use Efficiency Under Fluctuating Light Are Promising Targets for Improvement in Sorghum. *Frontiers in Plant Science,* 12**,** 627432.

PINGALI, P. L. 2012. Green Revolution: Impacts, limits, and the path ahead. *Proceedings of the National Academy of Sciences,* 109**,** 12302-12308.

PONS, T. L. & PEARCY, R. W. 1992. Photosynthesis in flashing light in soybean leaves grown in different conditions. II. Lightfleck utilization efficiency. *Plant, Cell and Environment,* 15**,** 577-584.

POSIT TEAM 2022. RStudio: Integrated Development Environment for R. Boston, MA: Posit Software, PBC.

R CORE TEAM 2021. R: A Language and Environment for Statistical Computing. Vienna, Austria: R Foundation for Statistical Computing.

RAY, D. K., MUELLER, N. D., WEST, P. C. & FOLEY, J. A. 2013. Yield Trends Are Insufficient to Double Global Crop Production by 2050. *Public Library of Science ONE,* 8**,** e66428.

RIPE. 2023. *Realizing Increased Photosynthetic Efficiency for sustainable increases in crop yield* [Online]. Available: https://ripe.illinois.edu/ [Accessed 2023].

ROGOWSKI, P., WASILEWSKA-DĘBOWSKA, W., URBAN, A. & ROMANOWSKA, E. 2018. Maize bundle sheath chloroplasts - a unique model of permanent State 2. *Environmental and Experimental Botany,* 155**,** 321-331.

ROMANOWSKA, E., BUCZYŃSKA, A., WASILEWSKA, W., KRUPNIK, T., DROŻAK, A., ROGOWSKI, P., PARYS, E. & ZIENKIEWICZ, M. 2017. Differences in photosynthetic responses of NADP-ME type C4 species to high light. *Planta,* 245**,** 641-657.

RUBAN, A. V. 2017. Quantifying the efficiency of photoprotection. *Philosophical Transactions of the Royal Society B: Biological Sciences,* 372.

RUBAN, A. V. & JOHNSON, M. P. 2009. Dynamics of higher plant photosystem cross-section associated with state transitions. *Photosynthesis Research,* 99**,** 173-83.

RUBAN, A. V., JOHNSON, M. P. & DUFFY, C. D. P. 2012. The photoprotective molecular switch in the photosystem II antenna. *Biochimica et Biophysica Acta (BBA) - Bioenergetics,* 1817**,** 167-181.

RUNGRAT, T., ALMONTE, A. A., CHENG, R., GOLLAN, P. J., STUART, T., ARO, E. M., BOREVITZ, J. O., POGSON, B. & WILSON, P. B. 2019. A Genome-Wide Association Study of Non-Photochemical Quenching in response to local seasonal climates in Arabidopsis thaliana. *Plant Direct,* 3**,** e00138.

SAATHOFF, A. J. & WELLES, J. 2021. Gas exchange measurements in the unsteady state. *Plant, Cell & Environment,* 44**,** 3509-3523.

SAGE, R. F. 2000. C_3 versus C_4 photosynthesis in rice: ecophysiological perspectives. *In:* SHEEHY, J. E., MITCHELL, P. L. & HARDY, B. (eds.) *Studies in Plant Science.* Elsevier.

SAGE, R. F. 2004. The evolution of C4 photosynthesis. *New Phytologist,* 161**,** 341-370.

SAGE, R. F., KHOSHRAVESH, R. & SAGE, T. L. 2014. From proto-Kranz to C4 Kranz: building the bridge to C4 photosynthesis. *Journal of Experimental Botany,* 65**,** 3341-3356.

SAGE, R. F. & MCKOWN, A. D. 2006. Is C4 photosynthesis less phenotypically plastic than C3 photosynthesis? *Journal of Experimental Botany,* 57**,** 303-317.

SAGE, R. F. & PEARCY, R. W. 2000. The Physiological Ecology of C4 Photosynthesis. *In:* LEEGOOD, R. C., SHARKEY, T. D. & VON CAEMMERER, S. (eds.) *Photosynthesis: Physiology and Metabolism.* Dordrecht: Springer Netherlands.

SAGE, R. F., SAGE, T. L. & KOCACINAR, F. 2012. Photorespiration and the evolution of C4 photosynthesis. *Annual Review of Plant Biology,* 63**,** 19-47.

SAGE, T. L., BUSCH, F. A., JOHNSON, D. C., FRIESEN, P. C., STINSON, C. R., STATA, M., SULTMANIS, S., RAHMAN, B. A., RAWSTHORNE, S. & SAGE, R. F. 2013. Initial Events during the Evolution of C4 Photosynthesis in C3 Species of Flaveria. *Plant Physiology,* 163**,** 1266-1276.

SAGUN, J. V., BADGER, M. R., CHOW, W. S. & GHANNOUM, O. 2021. Mehler reaction plays a role in C_3 and C_4 photosynthesis under shade and low CO_2. *Photosynthesis Research,* 149**,** 171-185.

SAHAY, S., GRZYBOWSKI, M., SCHNABLE, J. C. & GŁOWACKA, K. 2023. Genetic control of photoprotection and photosystem II operating efficiency in plants. *New Phytologist,* 239**,** 1068-1082.

SAKAI, T., KAGAWA, T., KASAHARA, M., SWARTZ, T. E., CHRISTIE, J. M., BRIGGS, W. R., WADA, M. & OKADA, K. 2001. Arabidopsis nph1 and npl1: blue light receptors that mediate both phototropism and chloroplast relocation. *Proceedings of the National Academy of Sciences,* 98**,** 6969-74.

SALES, C. R. G., RIBEIRO, R. V., HAYASHI, A. H., MARCHIORI, P. E. R., SILVA, K. I., MARTINS, M. O., SILVEIRA, J. A. G., SILVEIRA, N. M. & MACHADO, E. C. 2018. Flexibility of C4 decarboxylation and photosynthetic plasticity in sugarcane plants under shading. *Environmental and Experimental Botany,* 149**,** 34-42.

SALES, C. R. G., WANG, Y., EVERS, J. B. & KROMDIJK, J. 2021. Improving C4 photosynthesis to increase productivity under optimal and suboptimal conditions. *Journal of Experimental Botany,* 72**,** 5942-5960.

SASSENRATH-COLE, G. F. & PEARCY, R. W. 1992. The Role of Ribulose-1,5-Bisphosphate Regeneration in the Induction Requirement of Photosynthetic CO_2 Exchange under Transient Light Conditions. *Plant Physiology,* 99**,** 227-34.

SATTERTHWAITE, D., MCGRANAHAN, G. & TACOLI, C. 2010. Urbanization and its implications for food and farming. *Philosophical Transactions of the Royal Society B: Biological Sciences,* 365**,** 2809–2820.

SCHLÜTER, U. & WEBER, A. P. M. 2020. Regulation and Evolution of C_4 Photosynthesis. *Annual Review of Plant Biology,* 71**,** 183-215.

SCHMIDT VON BRAUN, S. & SCHLEIFF, E. 2008. The chloroplast outer membrane protein CHUP1 interacts with actin and profilin. *Planta,* 227**,** 1151-9.

SHARKEY, T. D. 1985. O_2-insensitive photosynthesis in C_3 plants: its occurrence and a possible explanation. *Plant Physiology,* 78**,** 71-5.

SHARKEY, T. D., SEEMANN, J. R. & PEARCY, R. W. 1986. Contribution of Metabolites of Photosynthesis to Postillumination CO2 Assimilation in Response to Lightflects. *Plant Physiology,* 82**,** 1063-1068.

SIMKIN, A. J., LÓPEZ-CALCAGNO, P. E. & RAINES, C. A. 2019. Feeding the world: improving photosynthetic efficiency for sustainable crop production. *Journal of Experimental Botany,* 70**,** 1119-1140.

SINGH, P., STEVENSON, S. R., DICKINSON, P. J., REYNA-LLORENS, I., TRIPATHI, A., REEVES, G., SCHREIER, T. B. & HIBBERD, J. M. 2023. C_4 gene induction during de-etiolation evolved through changes in cis to allow integration with ancestral C_4 gene regulatory networks. *Science Advances,* 9**,** eade9756.

SLATTERY, R. A., WALKER, B. J., WEBER, A. P. M. & ORT, D. R. 2018. The Impacts of Fluctuating Light on Crop Performance. *Plant Physiology,* 176**,** 990-1003.

STILL, C. J., BERRY, J. A., COLLATZ, G. J. & DEFRIES, R. S. 2003. Global distribution of C3 and C4 vegetation: Carbon cycle implications. *Global Biogeochemical Cycles,* 17**,** 6-1-6-14.

STINZIANO, J. R., ROBACK, C., SARGENT, D., MURPHY, B. K., HUDSON, P. J. & MUIR, C. D. 2021. Principles of resilient coding for plant ecophysiologists. *AoB PLANTS,* 13.

STITT, M., WIRTZ, W., GERHARDT, R., HELDT, H. W., SPENCER, C., WALKER, D. & FOYER, C. 1985. A comparative study of metabolite levels in plant leaf material in the dark. *Planta,* 166**,** 354-64.

STITT, M. & ZHU, X.-G. 2014. The large pools of metabolites involved in intercellular metabolite shuttles in C4 photosynthesis provide enormous flexibility and robustness in a fluctuating light environment. *Plant, Cell & Environment,* 37**,** 1985-1988.

STRAND, D. D., FISHER, N. & KRAMER, D. M. 2017. The higher plant plastid NAD(P)H dehydrogenase-like complex (NDH) is a high efficiency proton pump that increases ATP production by cyclic electron flow. *Journal of Biological Chemistry,* 292**,** 11850-11860.

SUDDERTH, E. A., ESPINOSA-GARCÍA, F. J. & HOLBROOK, N. M. 2009. Geographic distributions and physiological characteristics of co-existing Flaveria species in south-central Mexico. *Flora - Morphology, Distribution, Functional Ecology of Plants,* 204**,** 89-98.

SUORSA, M., JÄRVI, S., GRIECO, M., NURMI, M., PIETRZYKOWSKA, M., RANTALA, M., KANGASJÄRVI, S., PAAKKARINEN, V., TIKKANEN, M., JANSSON, S. & ARO, E. M. 2012. PROTON GRADIENT REGULATION5 is essential for proper acclimation of Arabidopsis photosystem I to naturally and artificially fluctuating light conditions. *Plant Cell,* 24**,** 2934-48.

SUTHERLAND, D. M. 1987. Genera Graminum. Grasses of the World. *Brittonia,* 39**,** 508-508.

SVENSSON, P., BLÄSING, O. E. & WESTHOFF, P. 2003. Evolution of C4 phosphoenolpyruvate carboxylase. *Archives of Biochemistry and Biophysics,* 414**,** 180-188.

SWEETLOVE, L. J., HEAZLEWOOD, J. L., HERALD, V., HOLTZAPFFEL, R., DAY, D. A., LEAVER, C. J. & MILLAR, A. H. 2002. The impact of oxidative stress on Arabidopsis mitochondria. *The Plant Journal,* 32**,** 891-904.

TAKABAYASHI, A., KISHINE, M., ASADA, K., ENDO, T. & SATO, F. 2005. Differential use of two cyclic electron flows around photosystem I for driving CO_2-concentration mechanism in C_4 photosynthesis. *Proceedings of the National Academy of Sciences,* 102**,** 16898-16903.

TAKAHASHI, S. & BADGER, M. R. 2011. Photoprotection in plants: a new light on photosystem II damage. *Trends in Plant Science,* 16**,** 53-60.

TAKAHASHI, S., MILWARD, S. E., FAN, D. Y., CHOW, W. S. & BADGER, M. R. 2009. How does cyclic electron flow alleviate photoinhibition in Arabidopsis? *Plant Physiology,* 149**,** 1560-7.

TANG, Y.-H., WASHITANI, I., TSUCHIYA, T. & IWAKI, H. 1988. Fluctuation of photosynthetic photon flux density within a Miscanthus sinensis canopy. *Ecological Research,* 3**,** 253-266.

TAYLOR, S. H., HULME, S. P., REES, M., RIPLEY, B. S., IAN WOODWARD, F. & OSBORNE, C. P. 2010. Ecophysiological traits in C_3 and C_4 grasses: a phylogenetically controlled screening experiment. *New Phytologist,* 185**,** 780-791.

TAYLOR, S. H. & LONG, S. P. 2017. Slow induction of photosynthesis on shade to sun transitions in wheat may cost at least 21% of productivity. *Philosophical Transactions of the Royal Society B: Biological Sciences,* 372**,** 20160543.

TILMAN, D., BALZER, C., HILL, J. & BEFORT, B. L. 2011. Global food demand and the sustainable intensification of agriculture. *Proceedings of the National Academy of Sciences,* 108**,** 20260-20264.

UBIERNA, N., SUN, W. & COUSINS, A. B. 2011. The efficiency of C4 photosynthesis under low light conditions: assumptions and calculations with CO2 isotope discrimination. *Journal of Experimental Botany,* 62**,** 3119-3134.

UENO, O. & SENTOKU, N. 2006. Comparison of leaf structure and photosynthetic characteristics of C3 and C4 *Alloteropsis semialata* subspecies. *Plant, Cell & Environment,* 29**,** 257-268.

USDA. 2023. *National Agriculture Economic Research Service, feed outlook January 2020* [Online]. Available: https://www.nass.usda.gov/Publications/ [Accessed].

USUDA, H. 1985. Changes in Levels of Intermediates of the C_4 Cycle and Reductive Pentose Phosphate Pathway during Induction of Photosynthesis in Maize Leaves. *Plant Physiology,* 78**,** 859-64.

VAN DER VELDE, M., FOLBERTH, C., BALKOVIČ, J., CIAIS, P., FRITZ, S., JANSSENS, I. A., OBERSTEINER, M., SEE, L., SKALSKÝ, R., XIONG, W. & PEÑUELAS, J. 2014. African crop yield reductions due to increasingly unbalanced Nitrogen and Phosphorus consumption. *Global Change Biology,* 20**,** 1278-1288.

WANG, C., GUO, L., LI, Y. & WANG, Z. 2012. Systematic Comparison of C3 and C4 Plants Based on Metabolic Network Analysis. *BMC Systems Biology,* 6**,** S9.

WANG, Y., BRÄUTIGAM, A., WEBER, A. P. M. & ZHU, X.-G. 2014a. Three distinct biochemical subtypes of C4 photosynthesis? A modelling analysis. *Journal of Experimental Botany,* 65**,** 3567-3578.

WANG, Y., BURGESS, S. J., BECKER, E. M. & LONG, S. P. 2020. Photosynthesis in the fleeting shadows: an overlooked opportunity for increasing crop productivity? *The Plant Journal,* 101**,** 874-884.

WANG, Y., LONG, S. P. & ZHU, X. G. 2014b. Elements required for an efficient NADP-malic enzyme type C4 photosynthesis. *Plant Physiology,* 164**,** 2231-46.

WANG, Y., STUTZ, S. S., BERNACCHI, C. J., BOYD, R. A., ORT, D. R. & LONG, S. P. 2022. Increased bundle-sheath leakiness of CO2 during photosynthetic induction shows a lack of coordination between the C4 and C4 cycles. *New Phytologist,* 236**,** 1661-1675.

WASILEWSKA-DĘBOWSKA, W., ZIENKIEWICZ, M. & DROZAK, A. 2022. How Light Reactions of Photosynthesis in C4 Plants Are Optimized and Protected under High Light Conditions. *International Journal of Molecular Sciences,* 23.

WAY, D. A., KATUL, G. G., MANZONI, S. & VICO, G. 2014. Increasing water use efficiency along the C_3 to C_4 evolutionary pathway: a stomatal optimization perspective. *Journal of Experimental Botany,* 65**,** 3683-3693.

WAY, D. A. & PEARCY, R. W. 2012. Sunflecks in trees and forests: from photosynthetic physiology to global change biology. *Tree Physiology,* 32**,** 1066-1081.

WEBER, A. P. & VON CAEMMERER, S. 2010. Plastid transport and metabolism of C3 and C4 plants--comparative analysis and possible biotechnological exploitation. *Current Opinion in Plant Biology,* 13**,** 257-65.

WERNER, C., RYEL, R. J., CORREIA, O. & BEYSCHLAG, W. 2001. Effects of photoinhibition on whole-plant carbon gain assessed with a photosynthesis model. *Plant, Cell & Environment,* 24**,** 27-40.

WICKHAM, H., AVERICK, M., BRYAN, J., CHANG, W., MCGOWAN, L., FRANÇOIS, R., GROLEMUND, G., HAYES, A., HENRY, L., HESTER, J., KUHN, M., PEDERSEN, T., MILLER, E., BACHE, S., MÜLLER, K., OOMS, J., ROBINSON, D., SEIDEL, D., SPINU, V., TAKAHASHI, K., VAUGHAN, D., WILKE, C., WOO, K. & YUTANI, H. 2019. Welcome to the Tidyverse. *Journal of Open Source Software,* 4**,** 1686.

WILSON, S. & RUBAN, A. V. 2020. Rethinking the Influence of Chloroplast Movements on Non-photochemical Quenching and Photoprotection1. *Plant Physiology,* 183**,** 1213-1223.

WINTER, K., SCHMITT, M. R. & EDWARDS, G. E. 1982. Microstegium vimineum, a shade adapted C4 grass. *Plant Science Letters,* 24**,** 311-318.

WRAIGHT, C. A. & CROFTS, A. R. 1970. Energy-dependent quenching of chlorophyll alpha fluorescence in isolated chloroplasts. *European Journal of Biochemistry,* 17**,** 319-27.

WYNN, T., BROWN, H., CAMPBELL, W. H. & BLACK, C. C., JR. 1973. Dark Release of $^{14}CO_2$ from Higher Plant Leaves. *Plant Physiology,* 52**,** 288-291.

YAMORI, W., MAKINO, A. & SHIKANAI, T. 2016. A physiological role of cyclic electron transport around photosystem I in sustaining photosynthesis under fluctuating light in rice. *Scientific Reports,* 6**,** 20147.

YAMORI, W., MASUMOTO, C., FUKAYAMA, H. & MAKINO, A. 2012. Rubisco activase is a key regulator of non-steady-state photosynthesis at any leaf temperature and, to a lesser extent, of steady-state photosynthesis at high temperature. *The Plant Journal,* 71**,** 871-880.

YAMORI, W. & SHIKANAI, T. 2016. Physiological Functions of Cyclic Electron Transport Around Photosystem I in Sustaining Photosynthesis and Plant Growth. *Annual Review of Plant Biology,* 67**,** 81-106.

YIN, X. & STRUIK, P. C. 2018. The energy budget in C4 photosynthesis: insights from a cell-type-specific electron transport model. *New Phytologist,* 218**,** 986-998.

YIN, X. & STRUIK, P. C. 2021. Exploiting differences in the energy budget among C_4 subtypes to improve crop productivity. *New Phytologist,* 229**,** 2400-2409.

YOSHIMURA, Y., KUBOTA, F. & UENO, O. 2004. Structural and biochemical bases of photorespiration in C4 plants: quantification of organelles and glycine decarboxylase. *Planta,* 220**,** 307-317.

YOUNG, S. N. R., SACK, L., SPORCK-KOEHLER, M. J. & LUNDGREN, M. R. 2020. Why is C4 photosynthesis so rare in trees? *Journal of Experimental Botany,* 71**,** 4629-4638.

ZELITCH, I., SCHULTES, N. P., PETERSON, R. B., BROWN, P. & BRUTNELL, T. P. 2009. High glycolate oxidase activity is required for survival of maize in normal air. *Plant Physiology,* 149**,** 195-204.

ZHOU, H., AKÇAY, E. & HELLIKER, B. R. 2019. Estimating C_4 photosynthesis parameters by fitting intensive A/C_i curves. *Photosynthesis Research,* 141**,** 181-194.

ZHOU, X. & FENICAL, W. 2016. The unique chemistry and biology of the piericidins. *The Journal of Antibiotics,* 69**,** 582-593.

ZHU, X.-G., LONG, S. P. & ORT, D. R. 2010. Improving Photosynthetic Efficiency for Greater Yield. *Annual Review of Plant Biology,* 61**,** 235-261.

ZHU, X. G., ORT, D. R., WHITMARSH, J. & LONG, S. P. 2004. The slow reversibility of photosystem II thermal energy dissipation on transfer from high to low light may cause large losses in carbon gain by crop canopies: a theoretical analysis. *Journal of Experimental Botany,* 55**,** 1167-75.

ZIA, A., JOHNSON, M. P. & RUBAN, A. V. 2011. Acclimation- and mutation-induced enhancement of PsbS levels affects the kinetics of non-photochemical quenching in Arabidopsis thaliana. *Planta,* 233**,** 1253-64.